

Exxon Valdez Oil Spill
Long-Term Herring Research and Monitoring Program Final Report

Herring Condition Monitoring

Exxon Valdez Oil Spill Trustee Council Project 16120111-L
Final Report

Kristen B. Gorman
Thomas C. Kline
Megan E. Roberts
W. Scott Pegau

Prince William Sound Science Center
300 Breakwater Ave
P.O. Box 705
Cordova, Alaska 99574

Fletcher F. Sewall
Ron A. Heintz

NOAA Alaska Fisheries Science Center
Auke Bay Laboratories, Ted Stevens Marine Research Institute
17109 Pt. Lena Loop Road
Juneau, Alaska 99801

May 2018

The *Exxon Valdez* Oil Spill Trustee Council administers all programs and activities free from discrimination based on race, color, national origin, age, sex, religion, marital status, pregnancy, parenthood, or disability. The Council administers all programs and activities in compliance with Title VI of the Civil Rights Act of 1964, Section 504 of the Rehabilitation Act of 1973, Title II of the Americans with Disabilities Act of 1990, the Age Discrimination Act of 1975, and Title IX of the Education Amendments of 1972. If you believe you have been discriminated against in any program, activity, or facility, or if you desire further information, please write to: EVOS Trustee Council, 4230 University Drive, Suite 220, Anchorage, Alaska 99508-4650; or dfg.evos.science@alaska.gov; or O.E.O., U.S. Department of the Interior, Washington, D.C. 20240.

Exxon Valdez Oil Spill
Long-Term Herring Research and Monitoring Program Final Report

Herring Condition Monitoring

Exxon Valdez Oil Spill Trustee Council Project 16120111-L
Final Report

Kristen B. Gorman
Thomas C. Kline
Megan E. Roberts
W. Scott Pegau

Prince William Sound Science Center
300 Breakwater Ave
P.O. Box 705
Cordova, Alaska 99574

Fletcher F. Sewall
Ron A. Heintz

NOAA Alaska Fisheries Science Center
Auke Bay Laboratories, Ted Stevens Marine Research Institute
17109 Pt. Lena Loop Road
Juneau, Alaska 99801

May 2018

Herring Condition Monitoring

Exxon Valdez Oil Spill Trustee Council Project 16120111-L Final Report

Study History: This funding was for a five-year study of juvenile Pacific herring (*Clupea pallasii*) overwinter energetics in Prince William Sound, Alaska, following the study design by Drs. Tom Kline and Ron Heintz. Support for data collection and analysis was provided by *Exxon Valdez* Oil Spill Trustee Council (EVOSTC). The project reported here is a five-year continuation of a project that began as part of the Prince William Sound Herring Survey coordinated by Prince William Sound Science Center. Earlier work included pilot studies between 2007-2008 and 2009-2011, specifically 090811 Herring Forage Contingency, 10100132-C Prince William Sound Herring Survey: Pacific Herring Energetic Recruitment Factors, 10100132-D Prince William Sound Herring Survey: Predictors of Winter Performance, 10100806 Are Herring Energetics Limiting? Other EVOSTC-funded studies relevant to this research include 14120111-M [Prince William Sound Herring Program - A High Temporal and Spatial Resolution Study](#). Data from this project have been published in a manuscript (Gorman et al. 2018) and presented in Appendix A.

Abstract: To date, the Pacific herring (*Clupea pallasii*) population of Prince William Sound, Alaska remains an injured resource from the *Exxon Valdez* oil spill. Survival of juvenile (age-0) herring through their first winter is considered a potential limiting factor regarding strong recruitment to the spawning population. Our goal was to examine juvenile herring winter energy budgets and infer mortality risks of Prince William Sound herring. We used several techniques to measure energy budgets: whole body energy density calculated from dry/wet and carbon/nitrogen stable isotope data, whole body energy density calculated from bomb calorimetry, percent lipid as measure of energy storage, ribonucleic acid/ deoxyribonucleic acid ratios as a measure growth, and diet composition. We found a strong relationship between whole body energy density derived from calorimetry and isotope techniques. Small herring present in fall were rare by spring due to size-dependent winter mortality or growth. Juvenile herring in 2012 had above-average November energy stores and growth effort over the 7-year period studied. This year (2012) had the lowest annual average water temperatures in the study period, suggesting that temperature influenced juvenile herring condition and growth. Herring diets in 2011 were the best in terms of quantity (mass) and quality (energy density), but did not appear to result in high lipid levels or growth. Analyses indicated that in northern and western regions of Prince William Sound, juvenile herring with more depleted $\delta^{13}\text{C}$ values in November, which reflect a Gulf of Alaska carbon source, were more energy dense. Important seasonal aspects of Prince William Sound circulation contribute to variation in early and late winter juvenile herring energy density.

Key words: *Clupea pallasii*, energetics, Gulf of Alaska, overwinter, Pacific herring, Prince William Sound, recruitment, ribonucleic acid/ deoxyribonucleic acid ratio, stable isotope, survival, teleconnections, whole body energy density.

Project Data: Data collected includes research cruise, date, location, capture method, species (primarily *Clupea pallasii*), standard length, fork length, age from length and scales, gross and

net wet and dry weights, dry/wet ratio, % water, Carbon (C) and Nitrogen (N) signal, C and N concentration, $\delta^{13}\text{C}$, $\delta^{13}\text{C}'$ and $\delta^{15}\text{N}$ signature, C and N mass, C/N atom ratio, Whole Body Energy Density (WBED) wet, WBED dry, energy whole fish, lipid mass, % lipid wet, % lipid dry, bomb calorimetry energy dry, bomb calorimetry energy density, deltaE, scale image name, date scale measured, scale annuli width, % lipid, ribonucleic acid/ deoxyribonucleic acid ratio, diet composition. Data are available from Kristen Gorman, kgorman@pwssc.org, PWSSC, Box 705 Cordova, Alaska 99574 or Fletcher Sewall, fletcher.sewall@noaa.gov, NOAA, 17109 Pt. Lena Loop Road, Juneau, Alaska 99801.

Electronic data are in .csv files stored in the Herring Research and Monitoring Ocean Workspace and will be made available through the Alaska Ocean Observing System Gulf of Alaska data portal:

Gorman 2012-2016 (https://workspace.aos.org/project/282629/folder/33867/pwssc-final-energetics-data_2005-2016)

Heintz 2009-2012 (https://researchworkspace.com/project/282615/folder/282621/growth-&-energy-data_final,-2009-2012);

Heintz 2012-2016 (https://researchworkspace.com/project/282629/folder/310989/growth-and-diet-data_final,-2012-2016).

The data may also be found through the DataONE earth and environmental data archive at <https://search.dataone.org/#data> and by selecting the Gulf of Alaska Data Portal under the Member Node filter.

Citation:

Gorman, K.B., T.C. Kline, M.E. Roberts, F.F. Sewall, R.A. Heintz and W.S. Pegau. 2018. Herring Condition Monitoring. *Exxon Valdez Oil Spill Long-Term Herring Research and Monitoring Program Final Report (Exxon Valdez Oil Spill Trustee Council Project 16120111-L)*, Exxon Valdez Oil Spill Trustee Council, Anchorage, Alaska.

TABLE OF CONTENTS

Executive Summary	1
Introduction.....	3
Methods.....	4
Field sampling.....	4
Laboratory Methods	5
Stable isotope and bomb calorimetry	5
Energy storage, growth, diet mass and composition	6
Statistical Analyses	6
Analysis 1 – Stable isotope and bomb calorimetry estimates of energy density.....	6
Analysis 2 – November/March WBED time series.....	7
Analysis 3 – Relationships between % lipid and RNA/DNA to fork length.....	7
Analysis 4 – Temporal and spatial comparisons of energy stores and growth.....	7
Analysis 5 – Herring diet composition.....	7
Analyses 6 and 7 – November WBED	8
Analyses 8 and 9 - March WBED	8
Results.....	9
Analysis 1 – Stable isotope and bomb calorimetry estimates of energy density	9
Analysis 2 – November/March WBED Time Series	10
Analysis 3 – Relationships between % lipid and RNA/DNA to fork length	11
Analysis 4 – Temporal and spatial comparisons of energy stores and growth	15
Analysis 5 – Herring diet composition.....	18
Analyses 6 and 7 – November WBED.....	20
Analyses 8 and 9 - March WBED.....	23
Discussion.....	31
Conclusions.....	33
Acknowledgements.....	34
Literature Cited	35

INDEX OF TABLES

Table 1. Candidate model sets for describing variation in November and March whole body energy density of juvenile Pacific herring in Prince William Sound, Alaska.	26
Table 2. Candidate models describing variation in whole body energy density of juvenile herring in Prince William Sound, Alaska. Models presented are those determined to be most parsimonious, as well all models receiving $\Delta AICc$ values ≤ 2	27
Table 3. Parameter estimates and likelihoods from candidate models for describing variation in whole body energy density of juvenile herring in Prince William Sound, Alaska. Parameter estimates ($\pm 95\%$ CI) are weighted averages, and CIs were calculated as $1.96 \times$ standard errors that are based on unconditional variances. Parameter likelihoods are Akaike weight (w) values summed across all models that include the variable.	28

INDEX OF FIGURES

Figure 1. Prince William Sound study area showing location of nursery bays sampled for juvenile herring. November sampling locations are noted by circles, March sampling locations are noted by triangles. Hydrological regions included Central (green), North (white), West (orange), and East (yellow). Hinchinbrook Entrance and Montague Strait are noted as HE and MS, respectively.	5
Figure 2. Variation in November and March whole body energy density derived from stable isotope data in relation to whole body energy density derived from bomb calorimetry.	10
Figure 3. November and March time series of WBED among juvenile herring collected from Prince William Sound. Sample sizes are noted at the bottom of each bar. Error bars are 95% confidence intervals.	11
Figure 4. Lipid content (% wet tissue mass) as a function of fork length (mm) with GAM fit (dashed lines show 95% CI) for juvenile herring collected in Prince William Sound in November 2009 – 2015 ($n = 708$).	12
Figure 5. Lipid content (% wet tissue mass) as a function of fork length with piecewise regression line (bar at bottom shows breakpoint and 95% CI) for juvenile herring collected in Prince William Sound in November 2009 – 2015 ($n = 708$).	13
Figure 6. RNA/DNA as a function of fork length with GAM fit (dashed lines show 95% CI) for juvenile herring collected in Prince William Sound in November 2009 – 2015 ($n = 745$)...	14
Figure 7. RNA/DNA as a function of fork length with piecewise regression line (bars at bottom show breakpoints and 95% CIs) for juvenile herring collected in Prince William Sound in November 2009 – 2015 ($n = 745$).	15

Figure 8. Residuals from the piecewise regression of lipid (left panel) and RNA/DNA (right panel) versus length of juvenile herring collected in Prince William Sound in November 2009 – 2015. Means and 95 % confidence intervals shown..... 16

Figure 9. Average annual water temperature in PWS in 2009 – 2015, as measured at NOAA Cordova tide station, ~6 ft. below mean lower low water. (Data downloaded 8/8/16 from: <https://tidesandcurrents.noaa.gov/stationhome.html?id=9454050>.)..... 16

Figure 10. Residuals from the piecewise regression of lipid versus fork length of juvenile herring collected in Prince William Sound in November 2009 – 2015. Means and 95 % confidence intervals shown. 17

Figure 11. Residuals from the piecewise regression of RNA/DNA versus fork length of juvenile herring collected in Prince William Sound in November 2009 – 2015. Means and 95 % confidence intervals shown. 18

Figure 12. Stomach contents mass as a percentage of body mass, relative to lipid content (% wet tissue mass) for juvenile herring collected from Prince William Sound in March of 2010 – 2016 ($n = 393$). Dashed line represents minimum 1.5% lipid required for survival in laboratory conditions (J. Vollenweider unpublished data). 19

Figure 13. Stomach contents mass as a percentage of body mass for juvenile herring collected from Prince William Sound in November of 2009 – 2015 ($n = 745$). 19

Figure 14. Diet energy density for juvenile herring collected from Prince William Sound in November of 2011 – 2015 ($n = 303$). 20

Figure 15. Diet proportion (% of total mass consumed) of prey identified in stomach contents of juvenile herring collected from Prince William Sound in November of 2011 – 2015..... 20

Figure 16. Variation in November whole body energy density in relation to $\delta^{13}\text{C}'$, hydrologic region, and year. Regressions are based on weighted parameter estimates across all models for the average size herring and range of $\delta^{13}\text{C}'$ values in the November dataset. 22

Figure 17. Variation in November whole body energy density in relation to $\delta^{15}\text{N}$, hydrologic region, and year. Regressions are based on weighted parameter estimates across all models for the average size herring and range of $\delta^{15}\text{N}$ values in the November dataset. 23

Figure 18. Variation in March whole body energy density in relation to $\delta^{13}\text{C}'$, hydrologic region, and year. Regressions are based on weighted parameter estimates across all models for the average size herring and range of $\delta^{13}\text{C}'$ values in the March dataset. 24

Figure 19. Variation in March whole body energy density in relation to $\delta^{15}\text{N}$, hydrologic region, and year. Regressions are based on weighted parameter estimates across all models for the average size herring and range of $\delta^{15}\text{N}$ values in the March dataset..... 25

Supplemental Material Figure 1..... 38

Supplemental Material Figure 2..... 38

Supplemental Material Figure 3..... 39

Supplemental Material Figure 4..... 39

Appendix A..... 40

EXECUTIVE SUMMARY

To date, the Pacific herring (*Clupea pallasii*, hereafter herring) population of Prince William Sound (PWS), Alaska remains an injured resource from the *Exxon Valdez* oil spill (hereafter the spill). The population biomass has remained at ~20,000 mt since 1998 and continues below a level that would allow a commercial catch. Survival of juvenile (age-0) herring through their first winter is considered a potential limiting factor regarding strong recruitment to the spawning population, and has therefore been the focus of past and ongoing research. The project reported here, juvenile Herring Condition Monitoring (HCM), which was funded by the *Exxon Valdez* Oil Spill Trustee Council between 2012 and 2016, is a five-year continuation of a project that began as part of the Prince William Sound Herring Survey (pilot studies between 2007-2008 and 2009-2011). The project follows the study design by Drs. Tom Kline (Prince William Sound Science Center) and Ron Heintz (NOAA Auke Bay Labs). The initial objectives of the study were to:

1. Monitor juvenile herring condition by sampling in November (2012-2016).
2. Monitor juvenile herring condition by sampling in March (2012-2016).
3. Apply observations from objectives 1 and 2 to continue refining an overwintering mortality model with the addition of physiological indicators.
4. Assess competition interactions with fishes using stable isotope analysis.

The juvenile HCM project successfully monitored juvenile herring condition in November and March during the years this study was funded through the *Exxon Valdez* Oil Spill Trustee Council (EVOSTC) as part of the Herring Research and Monitoring program (2012 – 2016). Further, additional physiological indicators were successfully measured including herring lipid content as an index of stored energy, ribonucleic acid/ deoxyribonucleic acid (RNA/DNA) ratio as a growth index, and diet composition analysis. In response to comments by the EVOSTC Science Panel regarding additional analysis of environmental correlates of variation in whole body energy density (WBED), we present here new a synthesis of the data examining stable carbon and nitrogen ($\delta^{13}\text{C}$, $\delta^{15}\text{N}$) values, which are biogeochemical proxies of trophic foraging, as predictors of age-0 herring energy density and linkages with deep water transport throughout PWS derived from the Gulf of Alaska. The survival-modeling component of this project is ongoing and is not reported here. During the course of this project (Kline: 2012-2013, Pegau: 2013-2014, Gorman: 2014-2016), one of the lead investigators was replaced, which caused a delay in sample processing and final analysis. Further, work in 2011-2012 on a separate project examining high temporal resolution in energy dynamics among juvenile herring (EVOSTC project number) suggests that some of the basic assumptions of the survival model do not hold true, complicating the modeling process. The objective regarding competitive interactions with other species was not continued beyond the first two years of the study with the change in lead investigators. Overall, this study has been important for advancing our understanding of juvenile herring winter energy budgets and mortality risks in PWS.

The research has shown several energetic techniques to be reliably measured in juvenile herring including WBED calculated from dry/wet and C/N stable isotope data, in addition to WBED calculated from bomb calorimetry, % lipid as measure of energy storage, RNA/DNA ratios as a

measure growth, and diet composition. We found a very strong relationship between WBED energy density derived from calorimetry and isotope techniques. Small herring present in fall were rare by spring due to size-dependent winter mortality or growth. Significant growth was unlikely because November RNA/DNA approached the minimum levels needed for routine metabolism. Juvenile herring must reach a critical size threshold before they can begin storing fat for winter. By March, many juvenile herring approached the minimum lipid levels required for survival in lab captivity. Small, lean herring depleted their energy stores in late winter and took on greater predation risk by foraging to avert starvation, as indicated by their stomach content. Juvenile herring in 2012 had above-average November energy stores and growth effort over the 7-year period studied including previous studies. In 2012, the lowest annual average water temperatures were recorded during the length of the study period, suggesting that temperature influenced juvenile herring condition and growth. Herring diets in 2011, which was part of the earlier time series, were the best in terms of quantity (mass) and quality (energy density), but did not appear to result in high lipid levels or growth. Other factors such as temperature may interact with or override diet effects on fall herring condition and growth.

During fall, factors such as juvenile herring structural size, hydrological region of PWS, year, and the interaction between $\delta^{13}\text{C}'$ (lipid-corrected $\delta^{13}\text{C}$ values) or $\delta^{15}\text{N}$ isotope signature and hydrological region were all important predictors of juvenile herring WBED. In particular, analyses indicated that in northern and western regions of PWS juvenile herring with more depleted $\delta^{13}\text{C}'$ values, which reflect a Gulf of Alaska carbon source as opposed to more enriched signatures reflecting local PWS carbon production, resulted in more energy dense fish. This result suggests that intrusion of water derived from the Gulf of Alaska enhanced the condition of age-0 herring, particularly in the northern and western regions of PWS in the fall, which is consistent with regional circulation. During spring, factors such as juvenile herring structural size, year, and the interaction between $\delta^{13}\text{C}'$ or $\delta^{15}\text{N}$ isotope signature and year were all important predictors of juvenile herring energy density. Because results differed for fall and spring seasons regarding the interaction between stable isotope signatures and region or year, it suggests important seasonal aspects of circulation contribute to variation in juvenile herring energy density, and likely the probability that young fish survive and recruit as spawning adults. Winter-feeding may enrich herring without considerable energy gain, removing any relationship between WBED and $\delta^{13}\text{C}'$ isotope signature in the spring.

INTRODUCTION

To date, the Pacific herring (*Clupea pallasii*, hereafter herring) population of Prince William Sound (PWS), Alaska remains an injured resource from the *Exxon Valdez* oil spill (hereafter the spill). The population biomass has remained at ~20,000 mt since 1998 and continues below a level that would allow a commercial catch (Muradian 2015). Survival of juvenile (age-0) herring through their first winter is considered a potential limiting factor regarding strong recruitment to the spawning population, and has therefore been the focus of past and ongoing research (e.g., Norcross et al. 2001). The project reported here, juvenile Herring Condition Monitoring (HCM), which was funded by the *Exxon Valdez* Oil Spill Trustee Council (EVOSTC) between 2012 and 2016, is a five-year continuation of a project that began as part of the Prince William Sound Herring Survey (pilot studies between 2007-2008 and 2009-2011).

Herring are a key component of the marine food web that characterizes the PWS region of the Gulf of Alaska given the species important role in energy transfer from lower to higher trophic levels. Herring are known to rely on an array of zooplankton that can vary not only by ontogeny, but also throughout the annual cycle within developmental stages (Norcross et al. 2001). In turn, herring, including various life stages from spawn to adults, often constitute a major proportion of the diet consumed by higher trophic level predators such as other fishes, seabirds and marine mammals (e.g., Jodice et al. 2006, Womble and Sigler 2006, Sturdevant et al. 2012) indicating a role for the species in the maintenance of marine predator populations.

In addition to their ecological importance, herring populations in PWS historically supported reduction, bait and roe fisheries and were therefore a critical aspect of the local economies that sustain the region's remote communities. However, herring populations were severely reduced following the grounding of the oil tanker, *Exxon Valdez*, on Bligh Reef in March of 1989 and the subsequent spill that covered over 2000 km of regional coastline. By 1993, PWS herring stocks were below minimum thresholds for the fishery (Thorne and Thomas 2008). The fishery re-opened briefly during the late 1990's, and remained closed since 2000.

Several hypotheses have been offered as to why PWS herring initially declined, in addition to why the population has not yet fully recovered since the late 1980's. Regarding the latter, research efforts have focused on factors that influence herring recruitment such as altered oceanographic conditions (both physical and biological), disease, juvenile over-winter energetics that influence survival, and increased predation or competition. The purpose of the juvenile HCM project was to specifically examine the hypothesis that over-winter energetic condition of age-0 herring is an important driver of survival variation that contributes to herring recruitment. Herring are known to be highly seasonally variable in their energetic composition (Vollenweider et al. 2011). In fact, consistent observations from early studies indicated a decline in whole body energy density (WBED) of age-0 herring between November and March at sites throughout PWS, in addition to observations of low winter survival (Norcross et al. 2001). In support of examining links between juvenile herring energetics and survival, fasting experiments by Paul and Paul (1998) suggested that herring die once WBED reaches a threshold of 2.8 - 3.6 (mean = 3.2) kJ/g (wet mass). Despite this early work, physical (ocean-climate) and biological (bottom-up) drivers of variation in WBED and subsequent links with early life stage survival in wild populations have not been well understood.

Our overall goal was to provide a more complete investigation into juvenile herring winter energy budgets and assessment of mortality risks. This study's initial objectives were to:

1. Monitor juvenile herring condition by sampling in November (2012-2016).
2. Monitor juvenile herring condition by sampling in March (2012-2016).
3. Apply observations from objectives 1 and 2 to continue refining an overwintering mortality model with the addition of physiological indicators.
4. Assess competition interactions with fishes using stable isotope analysis.

METHODS

Field sampling

Juvenile herring (age-0) were collected from a total of 19 nursery bays in PWS during research cruises in November (fall) and March (spring), or by contracted commercial herring fisherman in March, of each year between 2007-2016 using cast and gill nets, or trawl gear. Fish were caught at night with field operations generally occurring around the new moon. Deck lights were used to attract herring that were collected by castnet and gillnet along-side the research vessel. Trawl samples were collected using a midwater trawl where groups of fish were targeted during acoustic surveys of each bay. Nursery bays sampled during the Sound Ecosystem Assessment program (e.g., Cooney et al. 2001a, Norcross et al. 2001) were again sampled (i.e., Simpson, Eaglek, Whale and Zaikof Bays) in addition to many others including Cordova Harbor, Windy Bay, Double Bay, Port Gravina, Port Fidalgo, Valdez Arm, Jackson Hole (Glacier Island), Unakwik, West Twin Bay (Perry Island), Northwest Bay (Knight Island), Main Bay, Paddy Bay, Lower Herring Bay, Port Chalmers, and Port Etches (Fig. 1). Not all bays were sampled each year. Upon capture, fish were saved and frozen in groups of 25-50 per sampling location for laboratory processing at Prince William Sound Science Center (PWSSC) in Cordova, Alaska.

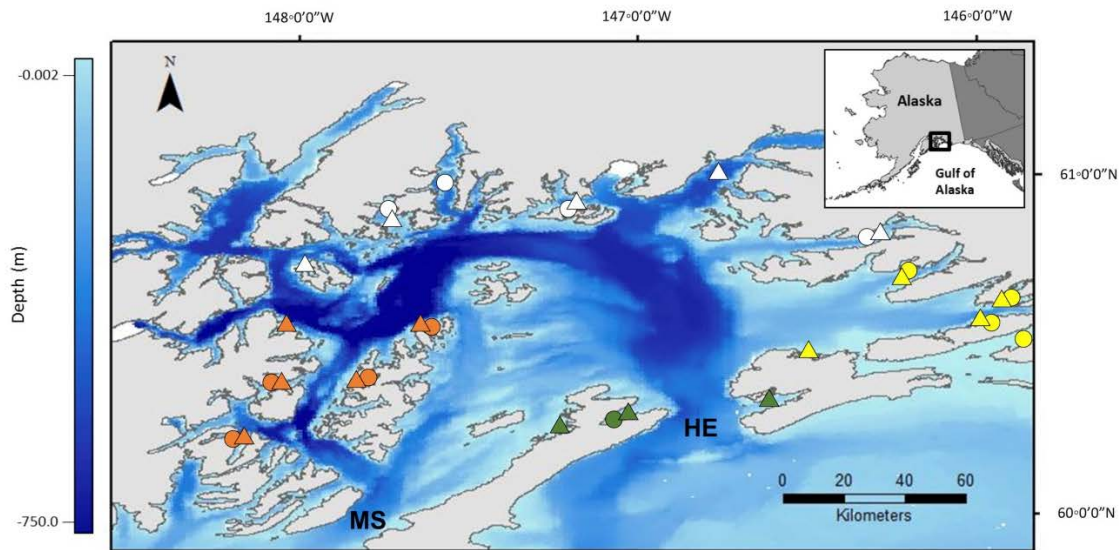


FIGURE 1. PRINCE WILLIAM SOUND STUDY AREA SHOWING LOCATION OF NURSERY BAYS SAMPLED FOR JUVENILE HERRING. NOVEMBER SAMPLING LOCATIONS ARE NOTED BY CIRCLES, MARCH SAMPLING LOCATIONS ARE NOTED BY TRIANGLES. HYDROLOGICAL REGIONS INCLUDED CENTRAL (GREEN), NORTH (WHITE), WEST (ORANGE), AND EAST (YELLOW). HINCHINBROOK ENTRANCE AND MONTAGUE STRAIT ARE NOTED AS HE AND MS, RESPECTIVELY.

Laboratory Methods

Stable isotope and bomb calorimetry

In the laboratory, frozen juvenile herring were thawed and wet mass (mg) obtained using an analytical balance (Mettler Toledo). Fork and standard lengths of each fish were measured to the nearest (mm). Otoliths were excised and saved for other analyses. Fish were oven-dried and the final whole body dry mass recorded (mg?). Dried herring were ground to a fine powder using a ball mill (RETSCH). Approximately 0.1-0.2 mg from each powdered herring was loaded into a tin capsule. Loaded capsules were sent to the Alaska Stable Isotope Facility at the University of Alaska Fairbanks where C and N mass spectrometric analyses were performed. Resultant data for herring included %C, %N, $^{13}\text{C}/^{12}\text{C}$, and $^{15}\text{N}/^{14}\text{N}$ with the latter two data reported using delta notation, $\delta^{13}\text{C}$ and $\delta^{15}\text{N}$, respectively, and were calculated using the following equation: $\delta^{13}\text{C}$ or $\delta^{15}\text{N} = ([R_{\text{sample}}/R_{\text{standard}}]-1) \times 1000$, where R_{sample} is the ratio of the heavy to light isotope for either $^{13}\text{C}/^{12}\text{C}$ or $^{15}\text{N}/^{14}\text{N}$, and R_{standard} is the heavy to light isotope ratios for international standards (Vienna PeeDee Belemnite for carbon, and atmospheric N_2 (Air) for nitrogen). Percent C and N data were used to ascertain C/N atom ratios. The ratio of dry to wet mass and C/N atom ratio data were used to determine WBED based on relationships derived from (Paul et al. 2001) and refined by (Kline 2013) using the following equation: $\text{WBED (kJ/g wet mass)} = -2.90242 + 32.585 \times (\text{dry/wet mass ratio}) + 0.103514 \times \text{C/N atom ratio}$. Raw $\delta^{13}\text{C}$ data were mathematically corrected for lipid content using the method of McConnaughey and McRoy (1979). Lipid-corrected values of $\delta^{13}\text{C}$ are hereafter reported as $\delta^{13}\text{C}'$.

A semi-micro calorimeter (Parr Instrument Company) was used to perform bomb calorimetry on a subset (~10%) of dried herring samples analyzed for C and N stable isotopes in order to ground-truth energy density estimates from dry/wet and C/N ratios. It was expected that estimates of WBED derived from dry/wet and C/N ratios would tightly correlate with energy density estimates derived from bomb calorimetry as has been previously demonstrated (Kline and Campbell 2010).

Energy storage, growth, diet mass and composition

Frozen herring were sent to Auke Bay Labs at National Oceanic and Atmospheric Administration in Juneau for length and weight measurement, diet assessment, and chemical analysis. Lipid content (percentage of wet tissue mass) of herring was used as a measure of stored energy. Following removal of muscle plugs and stomach contents, individual age-0 herring were homogenized with mortar and pestle. Homogenates were then analyzed for lipid mass as a percentage of wet tissue mass (% lipid) following procedures described in Vollenweider et al. (2011). Briefly, lipid extraction was performed following a modified Folch method (Folch et al. 1957) using a Dionex 200 Accelerated Solvent Extractor, followed by drying and weighing lipid extracts. National Institute for Standards and Technology (NIST) reference materials were used for quality control to verify lipid analysis.

Ribonucleic acid (RNA)/deoxyribonucleic acid (DNA) ratios were used as an indicator of the relative growth of individual fish, with higher RNA/DNA reflecting greater protein synthesis rates (Buckley 1984). The RNA and DNA contents of 10 – 15 mg plugs of dorsal white muscle tissue, less than 1% of fish body mass, were determined with a fluorometric dye-binding assay using methodology of Caldarone et al. (2001) as adapted by Sreenivasan (2011). The RNA/DNA ratio of muscle tissue has been used to indicate juvenile herring growth (Bernreuther et al. 2013), and while there is variation in conversions of RNA/DNA to specific growth rates based on different lab studies, it reflects relative growth rates (Sreenivasan 2011). Ratios of RNA and DNA in known quantities of standard materials, calf liver 18s + 28s ribosomal RNA and calf thymus DNA (Sigma), were used for quality control to verify RNA/DNA analysis.

To assess influences of diet mass on herring growth and energy stores, and as an indicator of foraging activity, stomachs of frozen individual herring were excised, and stomach contents removed and weighed prior to chemical analysis of herring. To assess influences of diet composition, individual prey items were enumerated and identified to the lowest practical taxon. Prey biomass and energy density were estimated following the method of Foy and Norcross (1999) to enable comparisons of findings. Due to degradation from digestion and handling, total mass and energy contents of prey were estimated by multiplying counts of individuals for each taxon by values for their undigested mass and energy density from (Coyle et al. 1990, Foy and Norcross 1999). Following removal of contents, empty stomachs were returned to fish carcasses for tissue homogenization and lipid analysis.

Statistical Analyses

Analysis 1 – Stable isotope and bomb calorimetry estimates of energy density

Least-squares general linear models (LM) were used to account for variation in WBED derived from stable isotope data in relation to WBED derived from bomb calorimetry for both November

($n = 258$) and March ($n = 253$) datasets. Two candidate models were considered including an equal-means (null) model, and a model with WBED derived from calorimetry for each dataset.

Analysis 2 – November/March WBED time series

Monthly mean values for WBED were calculated for all years of the study with associated 95% confidence intervals to assess statistical differences between groups.

Analysis 3 – Relationships between % lipid and RNA/DNA to fork length

Exploratory analysis with generalized additive models (GAM) suggested nonlinear relationships of herring lipid and RNA/DNA with fork length. This agreed with reports of nonlinear size-dependent lipid storage for other juvenile fishes in seasonal environments (Post and Parkinson 2001, Stallings et al. 2010), and supported the expectation that energy allocation between growth and lipid storage would change with increasing herring length. Relationships of herring % lipid and RNA/DNA to fork length were therefore described by fitting piecewise, 2-segment linear regressions. A statistical software package in R ('segmented' by Muggeo 2015) employing least-squares regression was used to identify the line breaks that indicated the size of herring where the relationships changed.

Analysis 4 – Temporal and spatial comparisons of energy stores and growth

Comparisons of energy stores and growth of herring from different years and bays used residuals from the piecewise regressions to remove the effects of size. Direct comparisons of energy storage or growth among bays and years would be compromised by the confounding effects of size bias in the sampling gear, with cast nets capturing smaller fish (November mean fork length \pm SE: 73.1 ± 0.7 mm, $N = 302$) than gillnets (87.4 ± 0.7 mm, $N = 343$).

Analysis 5 – Herring diet composition

Comparing herring diets across years required several steps. Diet comparisons were simplified by grouping prey taxa into nine categories: Amphipoda, Calanoida large, Calanoida small, Cirripedia, Euphausiacea, Gastropoda, Harpacticoida, Larvacea, and Other (unidentifiable taxa). To calculate the percentage of prey in herring diets by mass, individual herring diet mass observations were pooled within years, and the estimated mass of prey by taxon was divided by total mass of all taxa consumed. To compare diet energy densities, estimated prey energy contents by taxa were summed and divided by summed prey masses to obtain total diet energy density for each herring. Diet energy densities for all herring examined were then averaged by year.

Analyses 1 and 6 - 9 (below) were restricted to juvenile herring up to 115 mm in fork length that were collected over nine years in November (2007-2015, $n = 2514$) and March (2008-2016, $n = 1889$). Nursery bay collection areas were grouped into four hydrological regions (central, north,

west, and east regions) generally following descriptions by Musgrave et al. (2013). However, the analyses presented here considered north and west regions separately, and did not include a Gulf of Alaska region, unlike Musgrave et al. (2013). All statistical analyses were performed in the R language environment (2016).

Analyses 6 and 7 – November WBED

Two separate analyses were conducted to understand spatial and temporal variation in November WBED of age-0 herring in PWS (see Table 1 for a complete description of all explanatory variables and candidate models considered in analyses). First, linear mixed-effects models, employed using the `lme` function within the `nlme` package in R (Pinheiro et al. 2017, hereafter mixed models), were used to examine continuous variation in WBED derived from stable isotope data in relation to four parameters treated as fixed main effects including (1) fork length as a measure of body size (continuous variable); (2) $\delta^{13}\text{C}$ stable isotope signature of age-0 herring (continuous variable) to assess carbon source; (3) nursery bay hydrological region in PWS (categorical variable - central, north, west, and east); and (4) year (categorical variable). Second, mixed models were again used to examine variation in November WBED in relation to three of these same parameters, fork length, nursery bay hydrological region, and year, but also $\delta^{15}\text{N}$ stable isotope signatures of age-0 herring as a continuous variable to assess trophic foraging. An *a priori* set of 10 candidate models were considered for each November analysis, including either $\delta^{13}\text{C}$ or $\delta^{15}\text{N}$ stable isotope signatures, which consisted of a null model; models for isotope, region, or year predictor variables as fixed main effects including a term for fork length to control for body size in each model (three models); a more complex multiple predictor model including fixed main effect terms for fork length, isotope, and region (one model). All models without a year term were further evaluated including a year term (three models). Additional interaction models were included: a global model with all four fixed main effects and an interaction between isotope signature and region, and a second global model with all four fixed main effects and an interaction between isotope signature and year (two models). A random effect on intercept and slope (random = $\sim 1 + \text{Fork Length} | \text{Collection Bay}$) was included in each model to control for non-independence of data given that some fish were collected from the same nursery bay, and therefore, experienced more similar local environmental conditions that might have influenced individual size and energetic status.

Analyses 8 and 9 - March WBED

Similarly, two separate analyses were conducted to understand spatial and temporal variation in March WBED derived from stable isotope data of age-0 herring in PWS. Again, mixed models included the same explanatory variables and candidate model sets describe for November analyses (Table 1).

For Analyses 6-9, the importance of including a random effect on intercept and slope was tested in preliminary analyses by comparing the fit of four models, based on Akaike's Information Criterion corrected for small sample size (AICc), for each analysis - the most parameterized fixed effect model without a random effect (using the `gls` function in R), with a random effect on intercept only (mixed model), with a random effect on slope only (mixed model), and with a

random effect on both intercept and slope (mixed model). All four models maximized the restricted log-likelihood (method = “REML”) and all models included the same fixed main effect parameters and their interaction. The most parameterized fixed effect model with a random effect on both intercept and slope received the lowest AICc value for each analysis. Therefore, a random effect on both intercept and slope was included in all candidate models for November and March analyses.

Information-theoretic methods were used to direct model selection and parameter estimation (Burnham and Anderson 2002). For each candidate model, AICc, Δ AICc and Akaike weight (w) values were calculated using the AICcmodavg package in R (Mazerolle 2017) and used to compare models (Burnham and Anderson 2002). Values for Δ AICc are scaled differences relative to the smallest AICc value in the candidate model set such that the model with the minimum AICc value has $\Delta_i = 0$ (Burnham and Anderson 2002). Values for Akaike weights are the relative likelihood of the model, given the data, normalized to sum to 1 and interpreted as probabilities (Burnham and Anderson 2002). Inference was based on the relative support for parameters across all models and weighted parameter estimates. Parameter estimation included calculation of model-averaged parameter estimates based on w values for all candidate models within a candidate model set. Standard errors (SE) and 95% confidence intervals (CI: SE*1.96) for parameter estimates were based on unconditional variances calculated across the same models. Parameter likelihood values were evaluated by summing w values across all models that included each parameter under consideration (Burnham and Anderson 2002). Ultimately, only two models were considered in comparing stable isotope and bomb calorimetry estimates of WBED, including the null model, therefore no model averaging calculations were conducted for this analysis.

Linear models were used to compare stable isotope and bomb calorimetry estimates of WBED, thus an R^2 value defined as the fraction of the total variance explained by the model, was calculated as a general measure of fit (see Crawley 2007, p. 399). For mixed models, a pseudo R^2 value was calculated following Xu (2003), which is defined as 1 - the residual variance of the full model / the residual variance of a null model. Best supported models for November and March WBED analyses were examined based on standardized residual versus fitted value plots and normal probability plots of residuals to further assess model fit.

RESULTS

Analysis 1 – Stable isotope and bomb calorimetry estimates of energy density

Models including WBED derived from bomb calorimetry were best supported (November: Δ AICc value = 0.00, March: Δ AICc value = 0.00) over null models for describing variation in both November and March WBED where values were derived from dry/wet mass and C/N atom ratios of juvenile herring. Each model received very high weight and goodness of fit values (November: $w = 1.00$, $R^2 = 0.94$; March: $w = 1.00$, $R^2 = 0.91$; Fig. 2). Estimates of WBED based on stable isotope data were considered reliable because of these strong relationships and consequently used in the analyses reported below. See also Gorman et al. (2018).

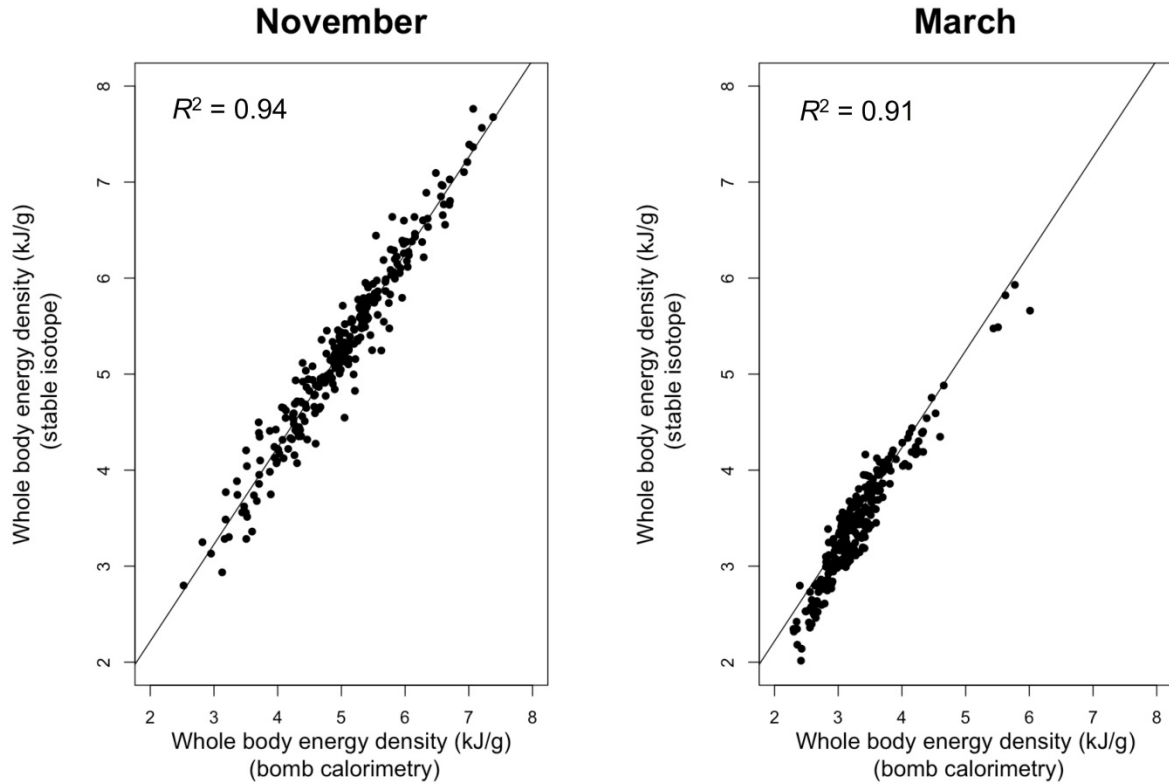


FIGURE 2. VARIATION IN NOVEMBER AND MARCH WHOLE BODY ENERGY DENSITY DERIVED FROM STABLE ISOTOPE DATA IN RELATION TO WHOLE BODY ENERGY DENSITY DERIVED FROM BOMB CALORIMETRY.

Analysis 2 – November/March WBED Time Series

Proximate analysis of juvenile herring based on the ratio of dry to wet mass and C/N atom ratio data confirmed our understanding that juvenile herring in March have a reduced energetic state in comparison with fish collected in November (Fig. 3). Spring WBED measurements are much more consistent between years than fall measurements, with the exception of 2013.

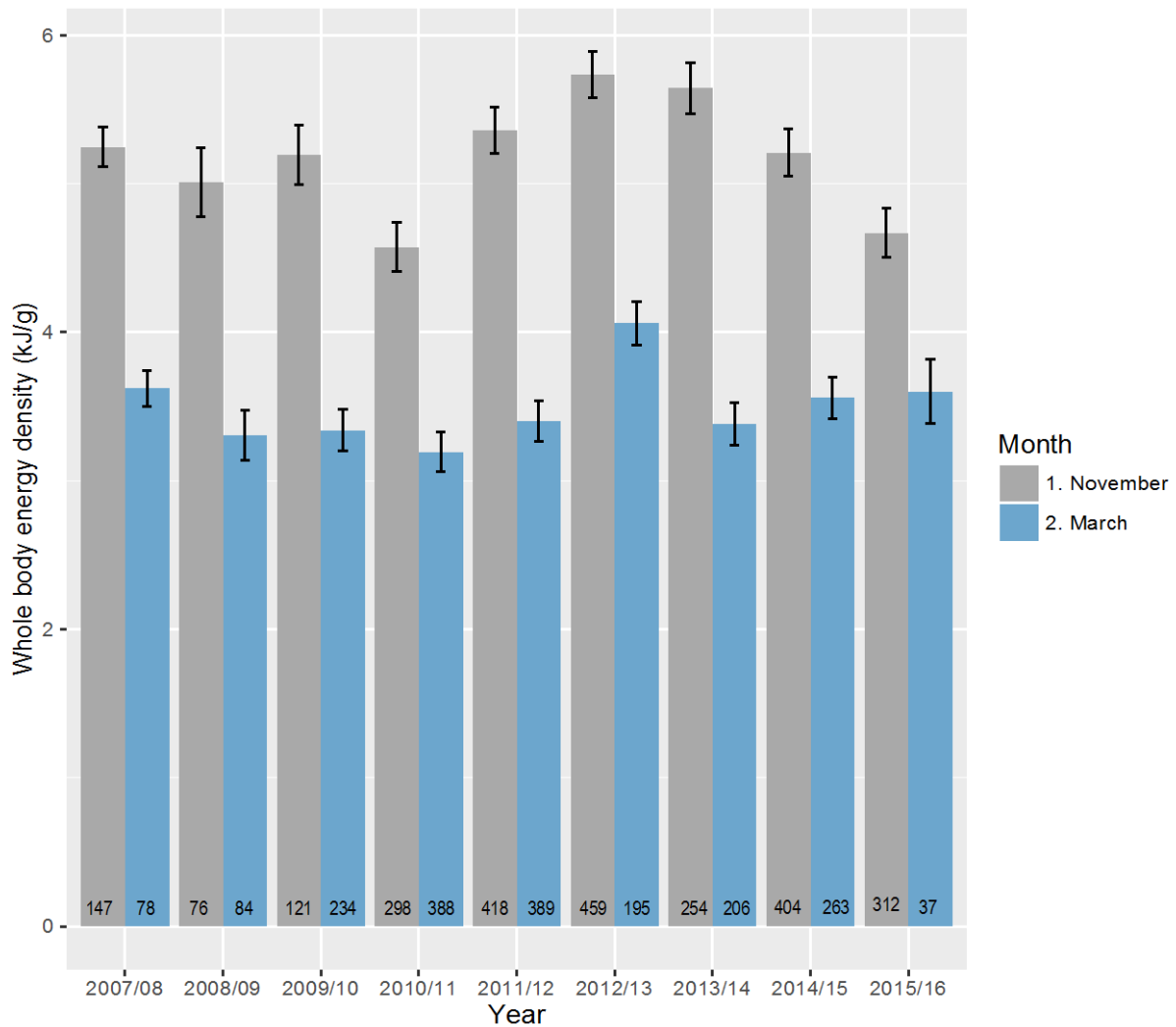


FIGURE 3. NOVEMBER AND MARCH TIME SERIES OF WBED AMONG JUVENILE HERRING COLLECTED FROM PRINCE WILLIAM SOUND. SAMPLE SIZES ARE NOTED AT THE BOTTOM OF EACH BAR. ERROR BARS ARE 95% CONFIDENCE INTERVALS.

Analysis 3 – Relationships between % lipid and RNA/DNA to fork length

Juvenile herring fat content in November increased with body size. A generalized additive model (GAM) fit to the data pooled across seven years for November 2009 - 2015 suggested % lipid increased at a faster rate for larger fish (Fig. 4). A piecewise regression model fit to the data indicated that a shift in lipid allocation rate occurs at approximately 77 mm fork length (95% CI: 67 – 87 mm, Fig. 5).

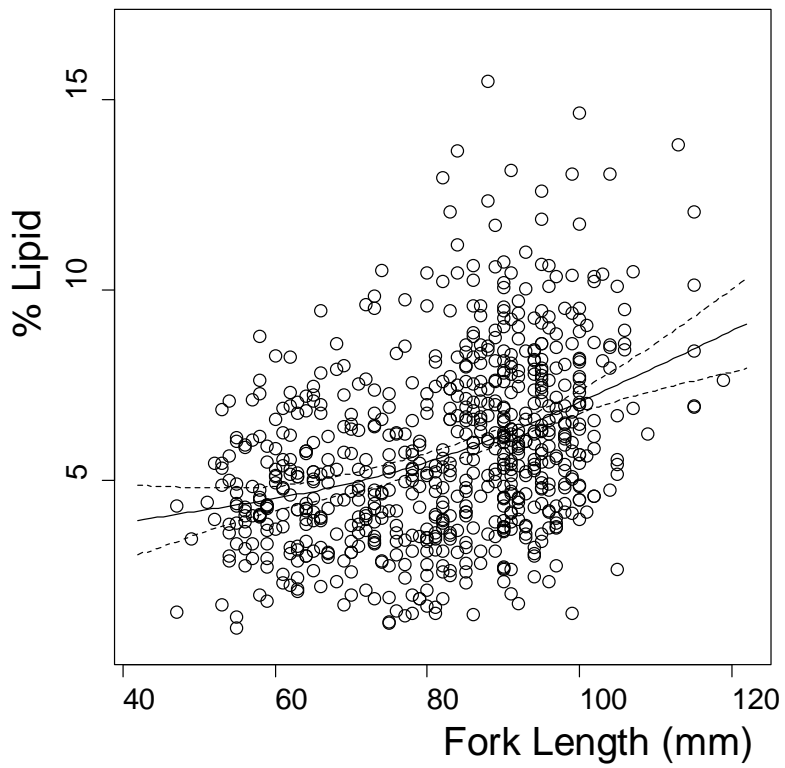


FIGURE 4. LIPID CONTENT (% WET TISSUE MASS) AS A FUNCTION OF FORK LENGTH (MM) WITH GAM FIT (DASHED LINES SHOW 95% CI) FOR JUVENILE HERRING COLLECTED IN PRINCE WILLIAM SOUND IN NOVEMBER 2009 – 2015 ($N = 708$).

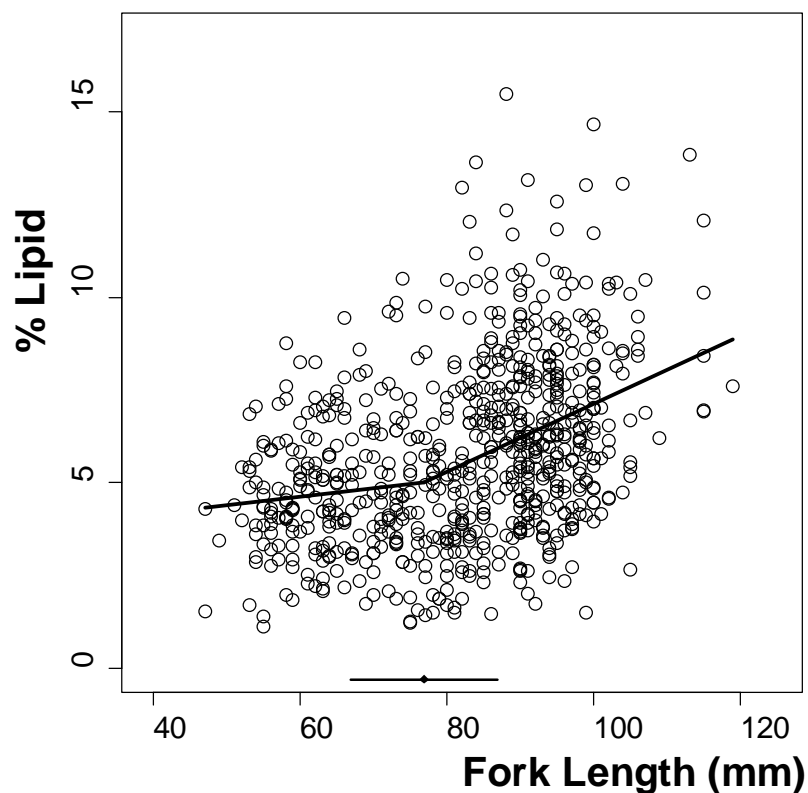


FIGURE 5. LIPID CONTENT (% WET TISSUE MASS) AS A FUNCTION OF FORK LENGTH WITH PIECEWISE REGRESSION LINE (BAR AT BOTTOM SHOWS BREAKPOINT AND 95% CI) FOR JUVENILE HERRING COLLECTED IN PRINCE WILLIAM SOUND IN NOVEMBER 2009 – 2015 ($N = 708$).

In contrast, juvenile herring growth effort (RNA/DNA ratio) decreased with body size. The GAM fit suggested a high RNA/DNA ratio for small herring, followed by a decline to minimum levels associated with no growth (Fig. 6). A piecewise regression model fit to the data indicated that a shift in growth effort occurred at approximately 74 mm fork length (95% CI: 69 – 78 mm), with minimum RNA/DNA for herring at 85 mm (95% CI: 82 – 88 mm) and larger (Fig. 7).

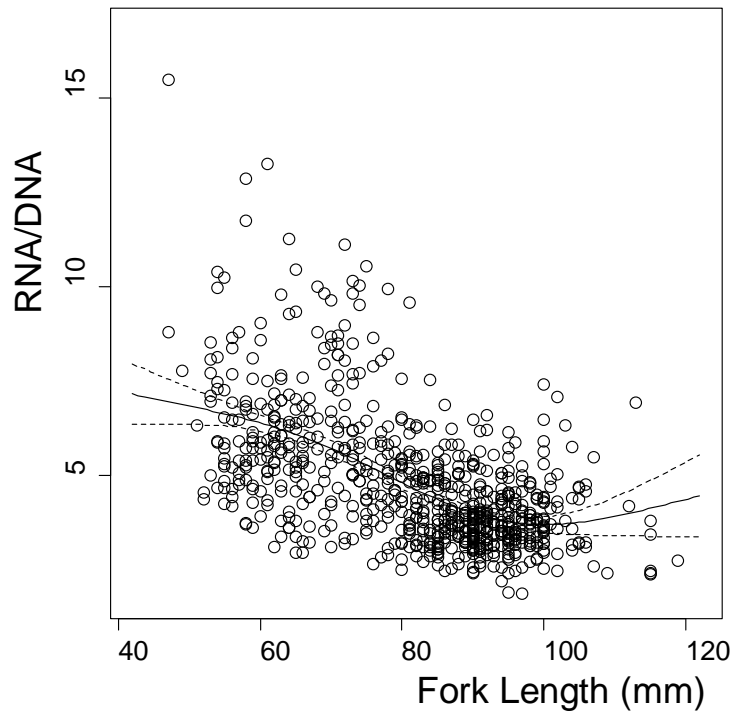


FIGURE 6. RNA/DNA AS A FUNCTION OF FORK LENGTH WITH GAM FIT (DASHED LINES SHOW 95% CI) FOR JUVENILE HERRING COLLECTED IN PRINCE WILLIAM SOUND IN NOVEMBER 2009 – 2015 ($N = 745$).

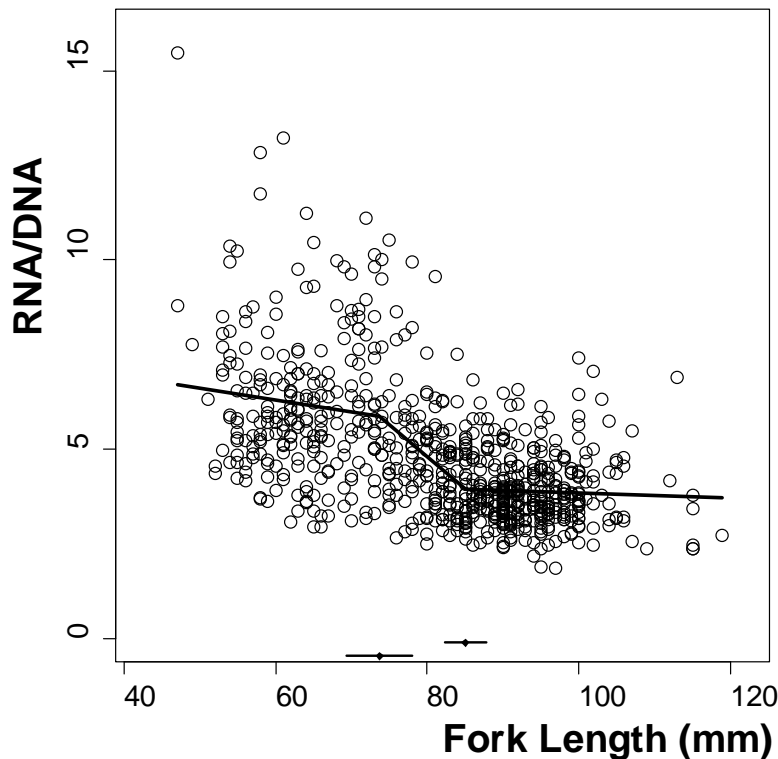


FIGURE 7. RNA/DNA AS A FUNCTION OF FORK LENGTH WITH PIECEWISE REGRESSION LINE (BARS AT BOTTOM SHOW BREAKPOINTS AND 95% CIs) FOR JUVENILE HERRING COLLECTED IN PRINCE WILLIAM SOUND IN NOVEMBER 2009 – 2015 ($N = 745$).

These size-based patterns in energy storage and growth were similar to those described for November juvenile herring from PWS as part of the Herring Survey program in 2009 – 2012 (Sewall et al. 2013).

Analysis 4 – Temporal and spatial comparisons of energy stores and growth

To compare relative condition and growth of age-0 herring across years and bays in PWS from November of 2009 to 2015, it was necessary to compare residuals from these regression models to account for the effects of different sizes of fish captured among sampling events. Comparison of lipid and RNA/DNA residuals over the 7-year period indicated juvenile herring were clearly above average in % lipid and RNA/DNA in 2012 (Fig. 8), which was the coldest year of the study (Fig. 9).

The lipid stores and growth of juvenile herring in autumn varied among bays across years, such that no specific bay consistently produced herring in the best condition. Eaglek and Simpson bays tended to be below average in lipid and growth across years, while Whale and Zaikof herring tended to be above average across years (Figs. 10 and 11).

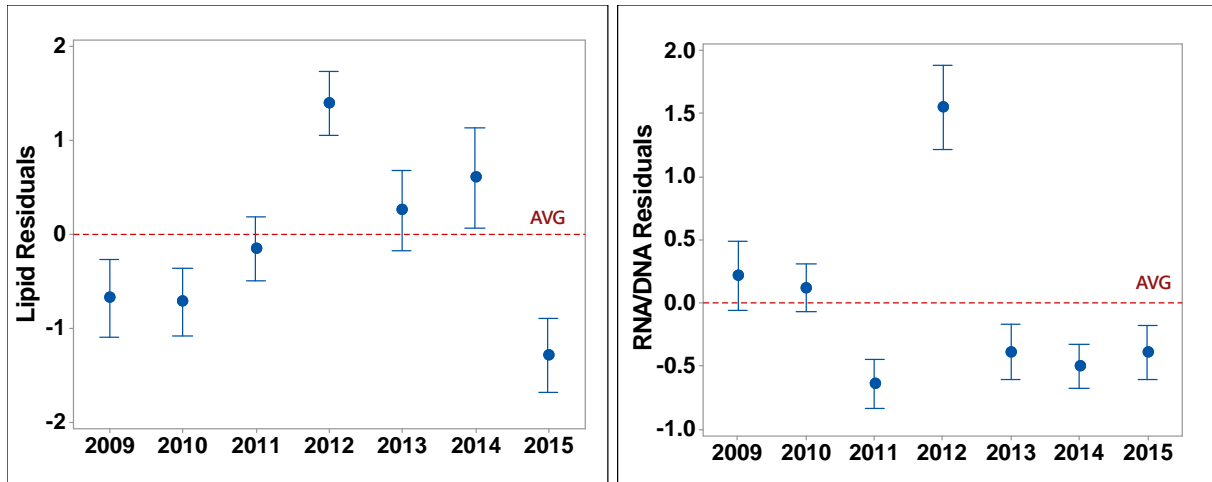


FIGURE 8. RESIDUALS FROM THE PIECEWISE REGRESSION OF LIPID (LEFT PANEL) AND RNA/DNA (RIGHT PANEL) VERSUS LENGTH OF JUVENILE HERRING COLLECTED IN PRINCE WILLIAM SOUND IN NOVEMBER 2009 – 2015. MEANS AND 95 % CONFIDENCE INTERVALS SHOWN.

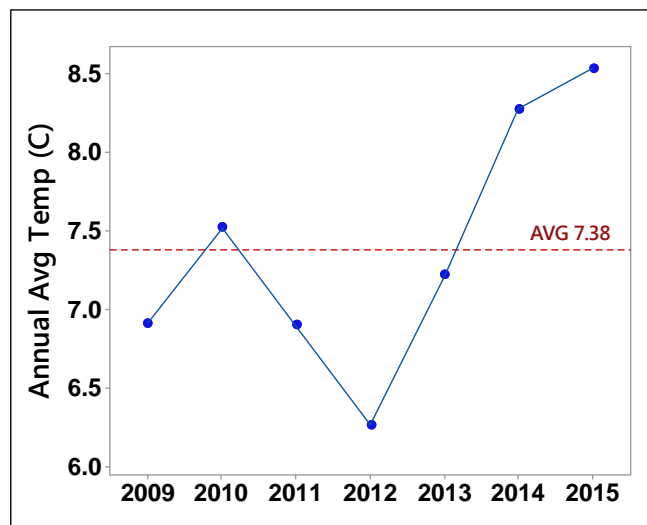


FIGURE 9. AVERAGE ANNUAL WATER TEMPERATURE IN PWS IN 2009 – 2015, AS MEASURED AT NOAA CORDOVA TIDE STATION, ~6 FT. BELOW MEAN LOWER LOW WATER. (DATA DOWNLOADED 8/8/16 FROM: [HTTPS://TIDESANDCURRENTS.NOAA.GOV/STATIONHOME.HTML?ID=9454050.](https://tidesandcurrents.noaa.gov/stationhome.html?id=9454050))

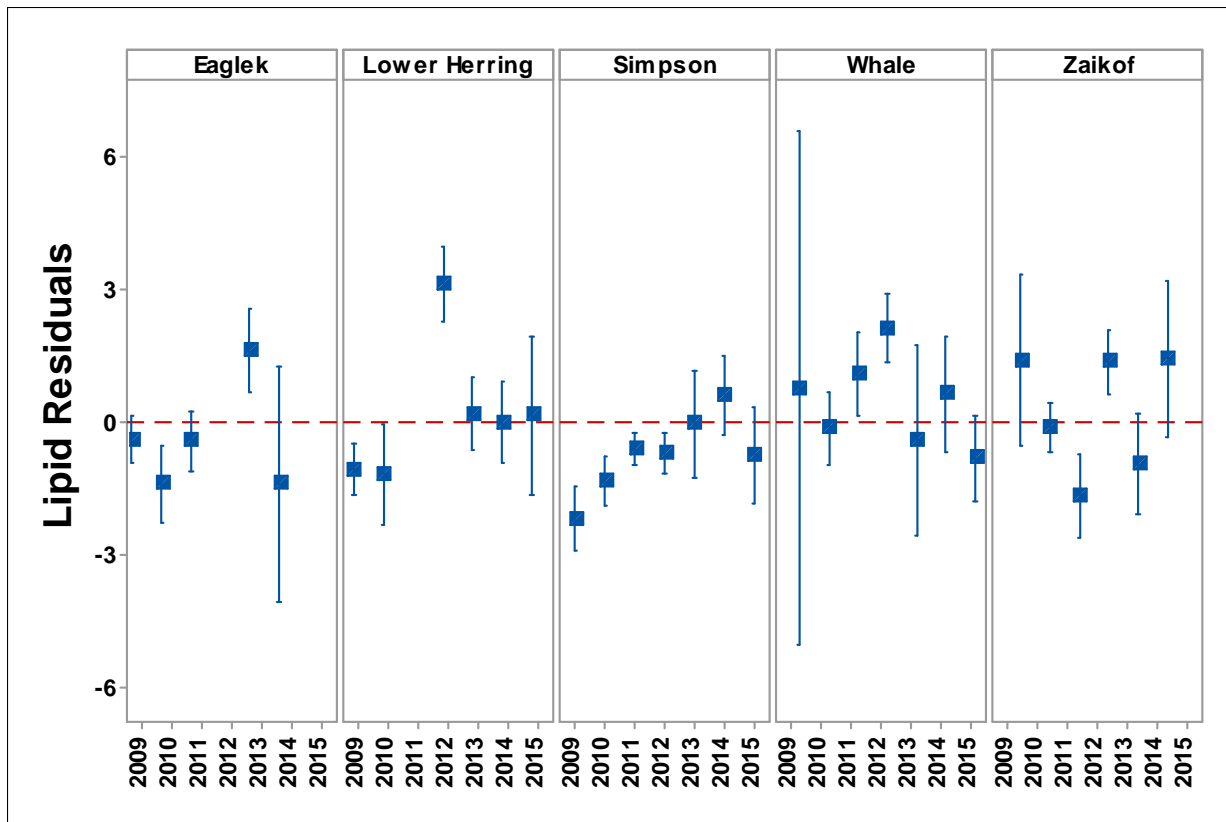


FIGURE 10. RESIDUALS FROM THE PIECEWISE REGRESSION OF LIPID VERSUS FORK LENGTH OF JUVENILE HERRING COLLECTED IN PRINCE WILLIAM SOUND IN NOVEMBER 2009 – 2015. MEANS AND 95 % CONFIDENCE INTERVALS SHOWN.

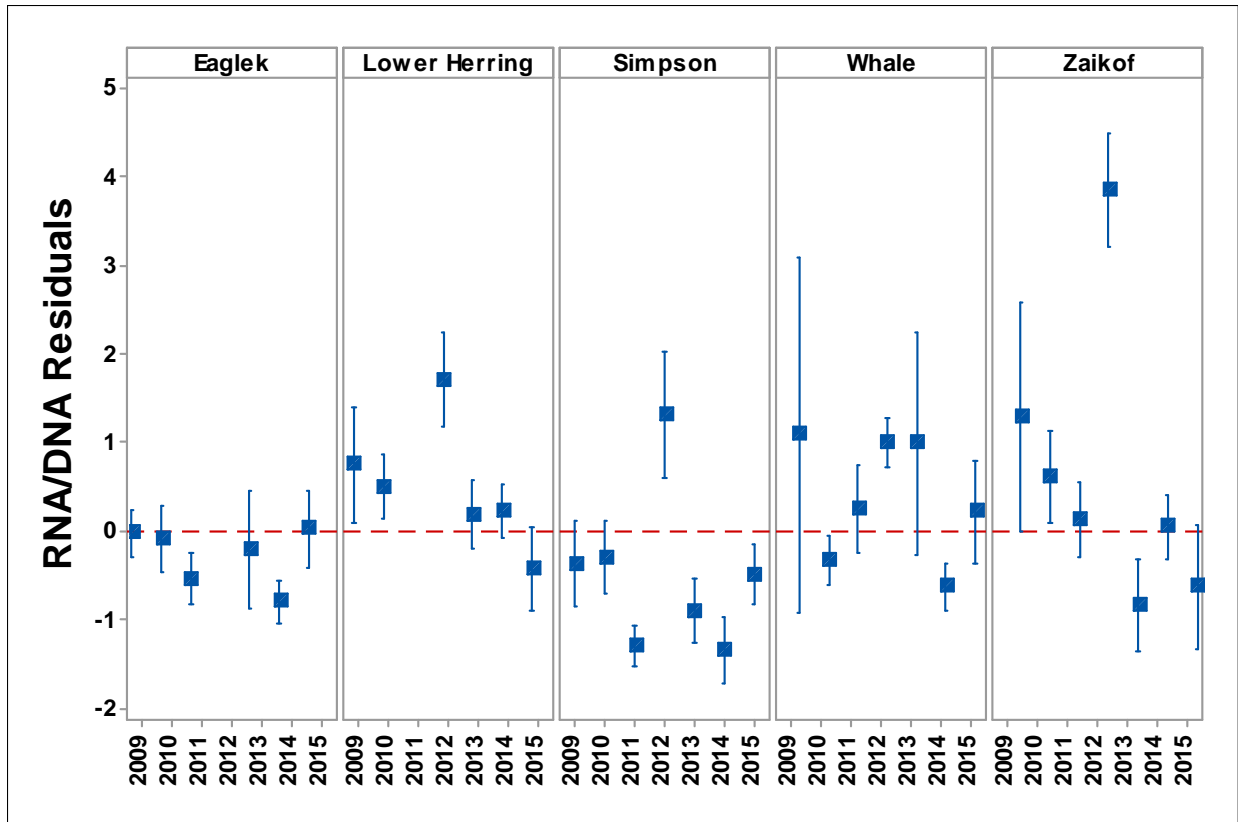


FIGURE 11. RESIDUALS FROM THE PIECEWISE REGRESSION OF RNA/DNA VERSUS FORK LENGTH OF JUVENILE HERRING COLLECTED IN PRINCE WILLIAM SOUND IN NOVEMBER 2009 – 2015. MEANS AND 95 % CONFIDENCE INTERVALS SHOWN.

Analysis 5 – Herring diet composition

By late winter (March), juvenile herring that were close to exhausting their fat stores were compelled to forage, as indicated by the higher stomach content masses (as % body weight) for herring with low % lipid (Fig. 12).

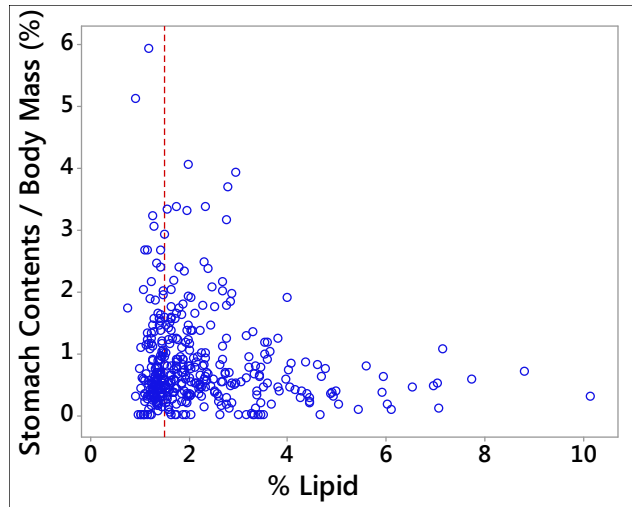


FIGURE 12. STOMACH CONTENTS MASS AS A PERCENTAGE OF BODY MASS, RELATIVE TO LIPID CONTENT (% WET TISSUE MASS) FOR JUVENILE HERRING COLLECTED FROM PRINCE WILLIAM SOUND IN MARCH OF 2010 – 2016 ($N = 393$). DASHED LINE REPRESENTS MINIMUM 1.5% LIPID REQUIRED FOR SURVIVAL IN LABORATORY CONDITIONS (J. VOLLENWEIDER UNPUBLISHED DATA).

Diet analysis across the 7 years of available data showed that juvenile herring in November 2011 had consumed the most food, as indicated by higher stomach contents masses relative to body mass (Fig. 13). Detailed prey identification and enumeration conducted since November 2011 showed that the energy density of prey in fall herring diets was highest in 2011 (Fig. 14), driven by the high proportion of euphausiids in diets that year (Fig. 15). However, the high quantity and quality of diets in fall 2011 did not appear to result in high lipid levels or growth rates for herring in fall 2011.

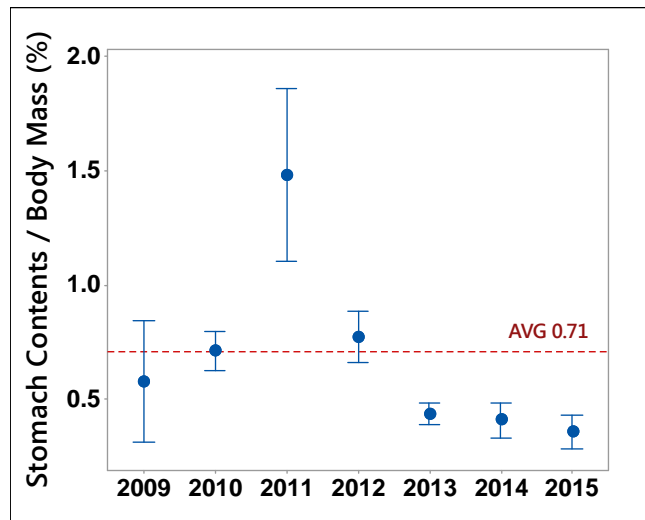


FIGURE 13. STOMACH CONTENTS MASS AS A PERCENTAGE OF BODY MASS FOR JUVENILE HERRING COLLECTED FROM PRINCE WILLIAM SOUND IN NOVEMBER OF 2009 – 2015 ($N = 745$).

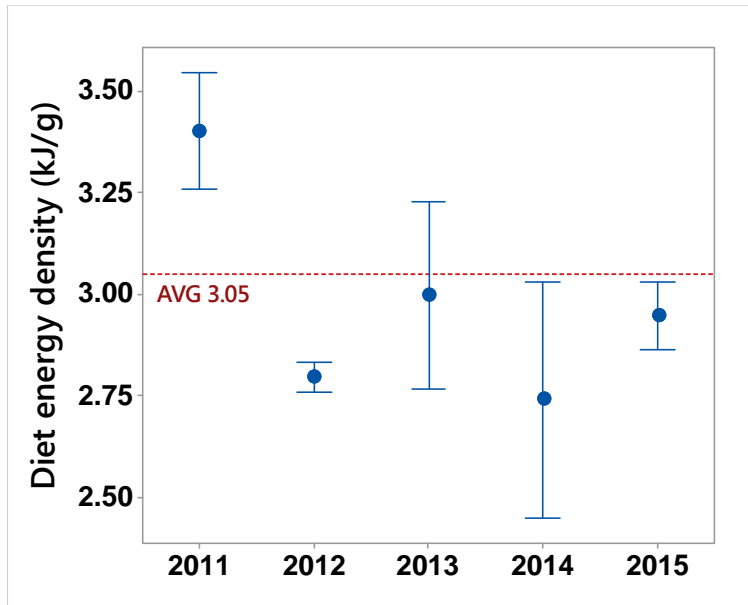


FIGURE 14. DIET ENERGY DENSITY FOR JUVENILE HERRING COLLECTED FROM PRINCE WILLIAM SOUND IN NOVEMBER OF 2011 – 2015 ($N = 303$).

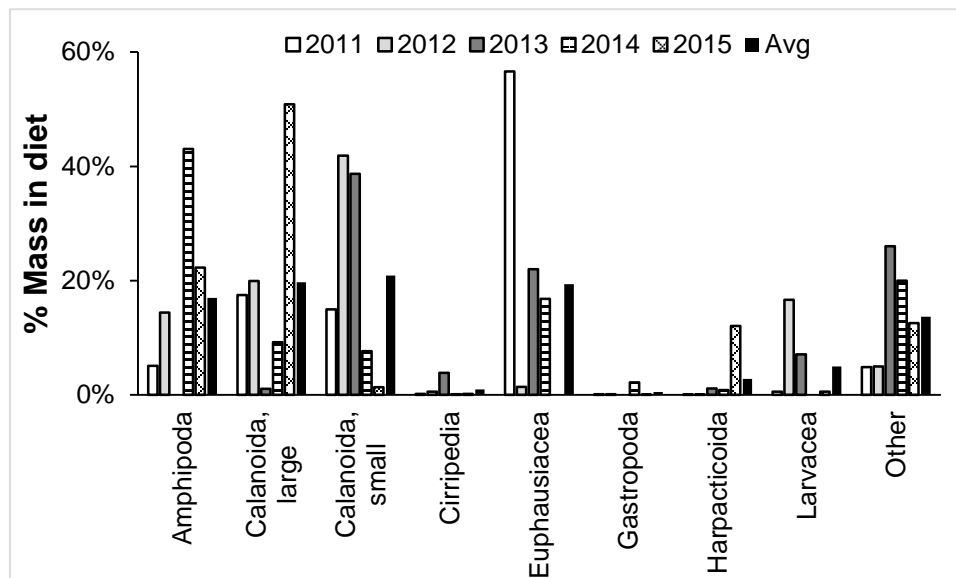


Figure 15. Diet proportion (% of total mass consumed) of prey identified in stomach contents of juvenile herring collected from Prince William Sound in November of 2011 – 2015.

Analyses 6 and 7 – November WBED

Analysis 6 – Only one model including $\delta^{13}\text{C}$ stable isotope signatures received a ΔAICc value ≤ 2.00 for describing variation in November WBED, which included all terms as fixed main effects (fork length, $\delta^{13}\text{C}$ isotope signature, hydrological region, and year), as well as an interaction between $\delta^{13}\text{C}$ isotope signature and region (Table 1: carbon stable isotope analysis for November, model 9). Plots of standardized residual versus fitted values and normal probability plots of residuals indicated model 9 was fitted adequately. This best-supported model received a

high w value (0.99), but only explained 26% of the variation in the data (Table 2). Parameter likelihoods indicated strong support for all fixed main effect parameters and the interaction between $\delta^{13}\text{C}'$ isotope signature and region (1.00, Table 3). The interaction between $\delta^{13}\text{C}'$ isotope signature and year was not supported ($3.98 \text{ E-}15$, Table 3). Fish with larger body sizes were more energy dense (0.02 ± 0.01 CI, Table 3). Fish with more depleted $\delta^{13}\text{C}'$ isotope signatures were more energy dense (-0.16 ± 0.09 CI, Table 3). The interaction between $\delta^{13}\text{C}'$ isotope signature and region was strongest in the west (-0.38 ± 0.10 CI) and north (-0.14 ± 0.12 CI) where fish with a more depleted $\delta^{13}\text{C}'$ stable isotope signature were more energy dense (Table 3, Fig. 16). Juvenile herring caught in the fall of 2013 (0.30 ± 0.16 CI) were the most energy dense, while fish caught in the fall of 2015 were the least energy dense (-1.07 ± 0.19 CI, Table 3, Fig. 16). See supplemental material Fig. 1 for plots of WBED versus $\delta^{13}\text{C}'$ stable isotope signatures for November. See also Gorman et al. (2018).

Analysis 7 – Only one model including $\delta^{15}\text{N}$ stable isotope signatures received a ΔAICc value ≤ 2.00 for describing variation in November WBED, which included all terms as fixed main effects (fork length, $\delta^{15}\text{N}$ isotope signature, hydrological region, and year), as well as an interaction between $\delta^{15}\text{N}$ isotope signature and region (Table 1: nitrogen stable isotope analysis for November, model 9). Plots of standardized residual versus fitted values and normal probability plots of residuals indicated model 9 was fitted adequately. This best-supported model received a high w value (1.00), but again only explained 23% of the variation in the data (Table 2). Parameter likelihoods indicated strong support for all fixed main effect parameters and the interaction between $\delta^{15}\text{N}$ isotope signature and region (0.99 - 1.00, Table 3). Again, the interaction between $\delta^{15}\text{N}$ isotope signature and year was not supported ($4.53 \text{ E-}07$, Table 3). Fish with larger body sizes were more energy dense (0.02 ± 0.01 CI, Table 3). Fish from northern nursery bays were more energy dense (2.88 ± 2.31 CI, Table 3). The interaction between $\delta^{15}\text{N}$ isotope signature and region was strongest in the north (-0.26 ± 0.19 CI) where fish with a more depleted $\delta^{15}\text{N}$ isotope signature were more energy dense (Fig. 17). Juvenile herring caught in the fall of 2012 were the most energy dense (0.86 ± 0.15 CI), while fish caught in the fall of 2015 were the least energy dense (-0.41 ± 0.16 CI, Table 2, Fig. 17). See supplemental material Fig. 2 for plots of WBED versus $\delta^{15}\text{N}$ stable isotope signatures for November. See also Gorman et al. (2018).

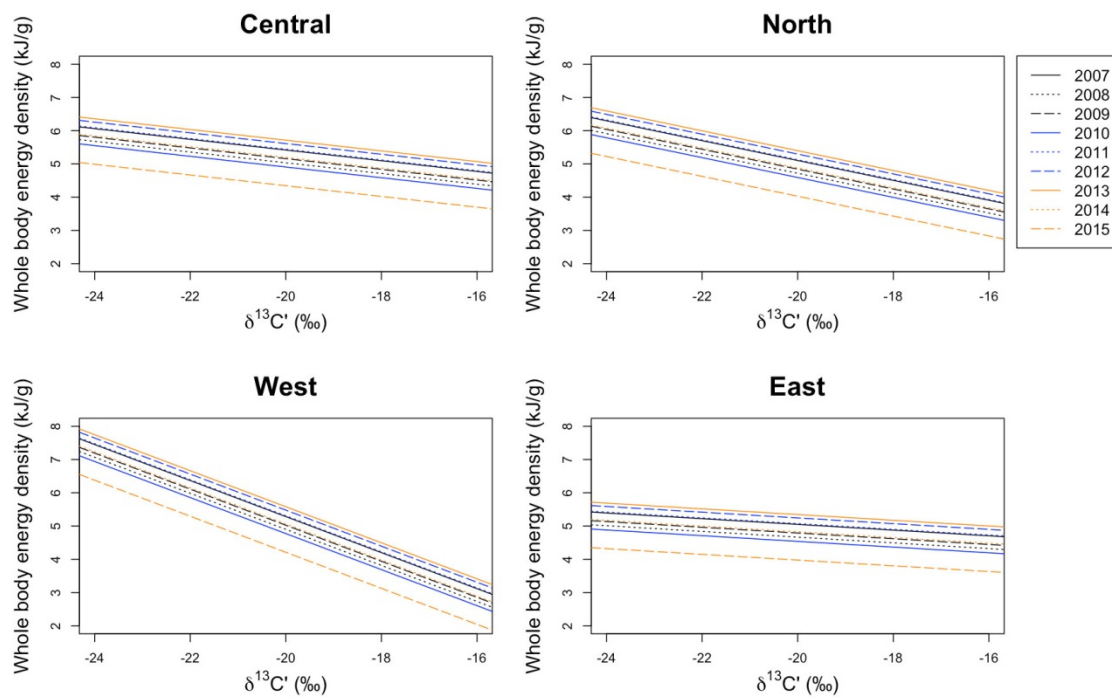


FIGURE 16. VARIATION IN NOVEMBER WHOLE BODY ENERGY DENSITY IN RELATION TO $\delta^{13}C'$, HYDROLOGIC REGION, AND YEAR. REGRESSIONS ARE BASED ON WEIGHTED PARAMETER ESTIMATES ACROSS ALL MODELS FOR THE AVERAGE SIZE HERRING AND RANGE OF $\delta^{13}C'$ VALUES IN THE NOVEMBER DATASET.

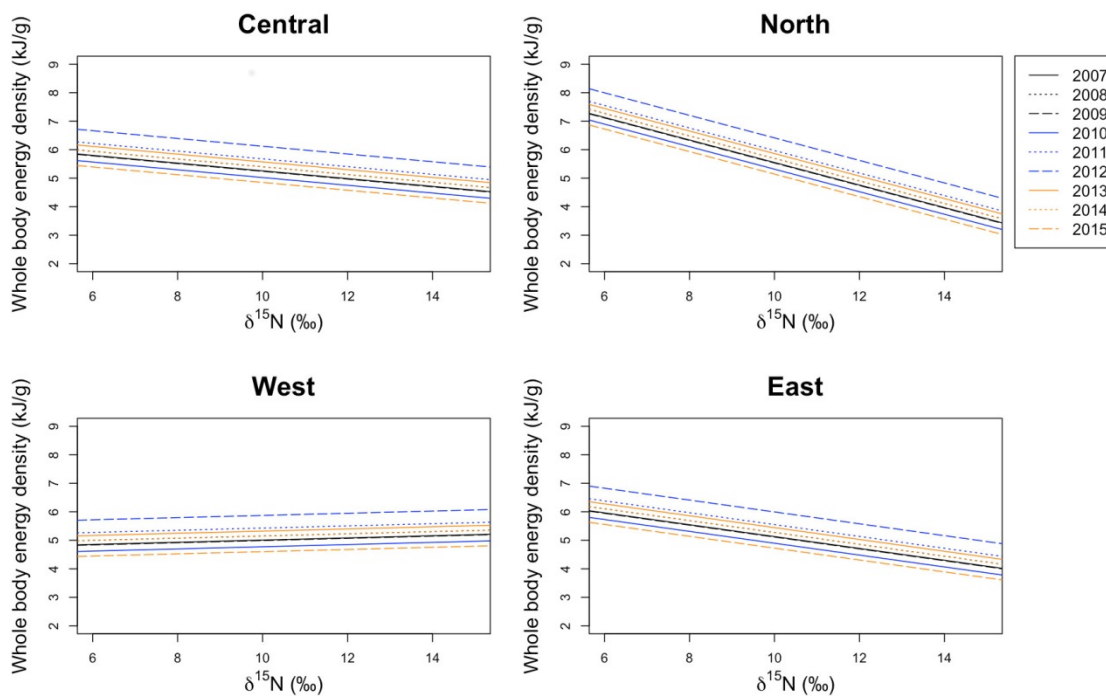


FIGURE 17. VARIATION IN NOVEMBER WHOLE BODY ENERGY DENSITY IN RELATION TO $\delta^{15}\text{N}$, HYDROLOGIC REGION, AND YEAR. REGRESSIONS ARE BASED ON WEIGHTED PARAMETER ESTIMATES ACROSS ALL MODELS FOR THE AVERAGE SIZE HERRING AND RANGE OF $\delta^{15}\text{N}$ VALUES IN THE NOVEMBER DATASET.

Analyses 8 and 9 - March WBED

Analysis 8 – Only one model including $\delta^{13}\text{C}$ stable isotope signatures received a ΔAICc value ≤ 2.00 for describing variation in March WBED, which included all terms as fixed main effects (fork length, $\delta^{13}\text{C}$ isotope signature, hydrological region, and year), as well as an interaction between $\delta^{13}\text{C}$ isotope signature and year (Table 1: carbon stable isotope analysis for March, model 10). Plots of standardized residual versus fitted values and normal probability plots of residuals indicated model 10 was fitted adequately. This best-supported model received a high w value (1.00), but only explained 22% of the variation in the data (Table 2). Parameter likelihoods indicated strong support for all fixed main effect parameters and the interaction between $\delta^{13}\text{C}$ isotope signature and year (1.00, Table 3). The interaction between $\delta^{13}\text{C}$ isotope signature and region was not supported ($8.07 \text{ E-}20$, Table 3). Again, fish with larger body sizes were more energy dense (0.02 ± 0.01 CI, Table 3). The interaction between $\delta^{13}\text{C}$ isotope signature and year was strongest for fish caught in 2016 (-1.42 ± 0.38 CI, Fig. 18) where individuals with a more depleted $\delta^{13}\text{C}$ isotope signature were more energy dense (Fig. 18). See supplemental material Fig. 3 for plots of WBED versus $\delta^{13}\text{C}$ stable isotope signatures for March. See also Gorman et al. (2018).

Analysis 9 – Similar to other analyses, only one model including $\delta^{15}\text{N}$ stable isotope signatures received a ΔAICc value ≤ 2.00 for describing variation in March WBED, which included all terms as fixed main effects (fork length, $\delta^{15}\text{N}$ isotope signature, hydrological region, and year), as well as an interaction between $\delta^{15}\text{N}$ isotope signature and year (Table 1: nitrogen stable isotope analysis for March, model 10). Plots of standardized residual versus fitted values and normal probability plots of residuals indicated model 10 was fitted adequately. This best-supported model received a high w value (1.00), but only explained 20% of the variation in the data (Table 2). Parameter likelihoods indicated strong support for all main effect parameters and the interaction between $\delta^{15}\text{N}$ isotope signature and year (1.00, Table 3). The interaction between $\delta^{15}\text{N}$ isotope signature and region was not supported ($1.83 \text{ E-}09$, Table 3). Fish with larger body sizes were more energy dense (0.02 ± 0.01 CI, Table 3). The interaction between $\delta^{15}\text{N}$ isotope signature and year was strongest for fish caught in 2016 (-0.57 ± 0.44 , Table 3) where juvenile herring with more depleted $\delta^{15}\text{N}$ isotope signatures were more energy dense (Fig. 19). See supplemental material Fig. 4 for plots of WBED versus $\delta^{15}\text{N}$ stable isotope signatures for March. See also Gorman et al. (2018).

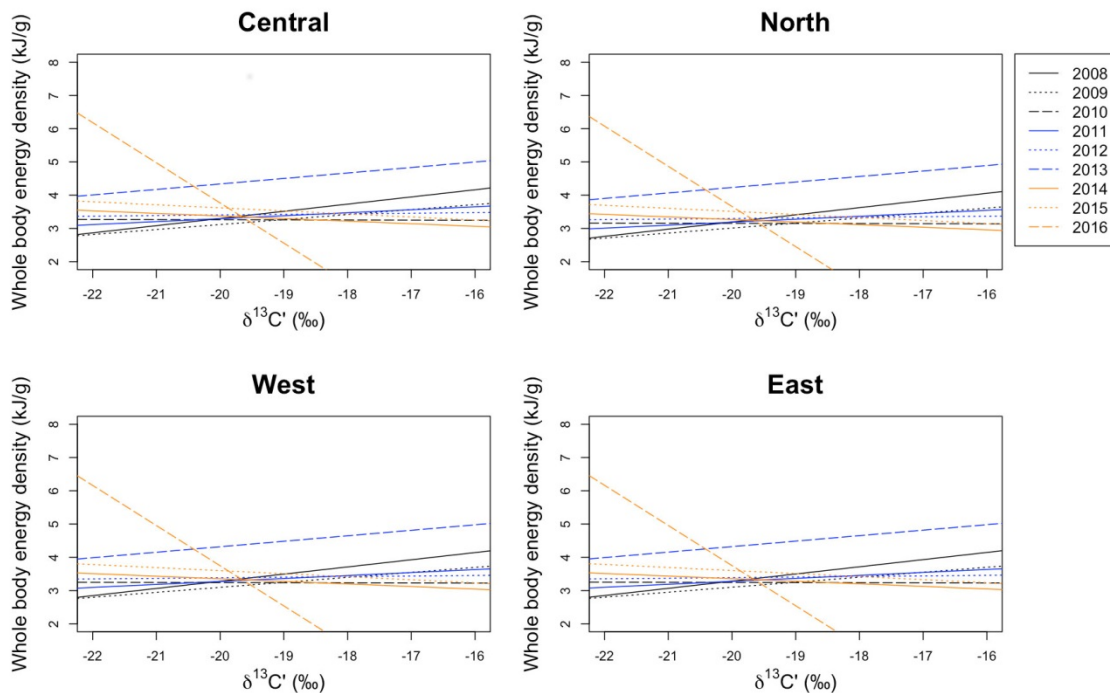


FIGURE 18. VARIATION IN MARCH WHOLE BODY ENERGY DENSITY IN RELATION TO $\delta^{13}\text{C}'$, HYDROLOGIC REGION, AND YEAR. REGRESSIONS ARE BASED ON WEIGHTED PARAMETER ESTIMATES ACROSS ALL MODELS FOR THE AVERAGE SIZE HERRING AND RANGE OF $\delta^{13}\text{C}'$ VALUES IN THE MARCH DATASET.

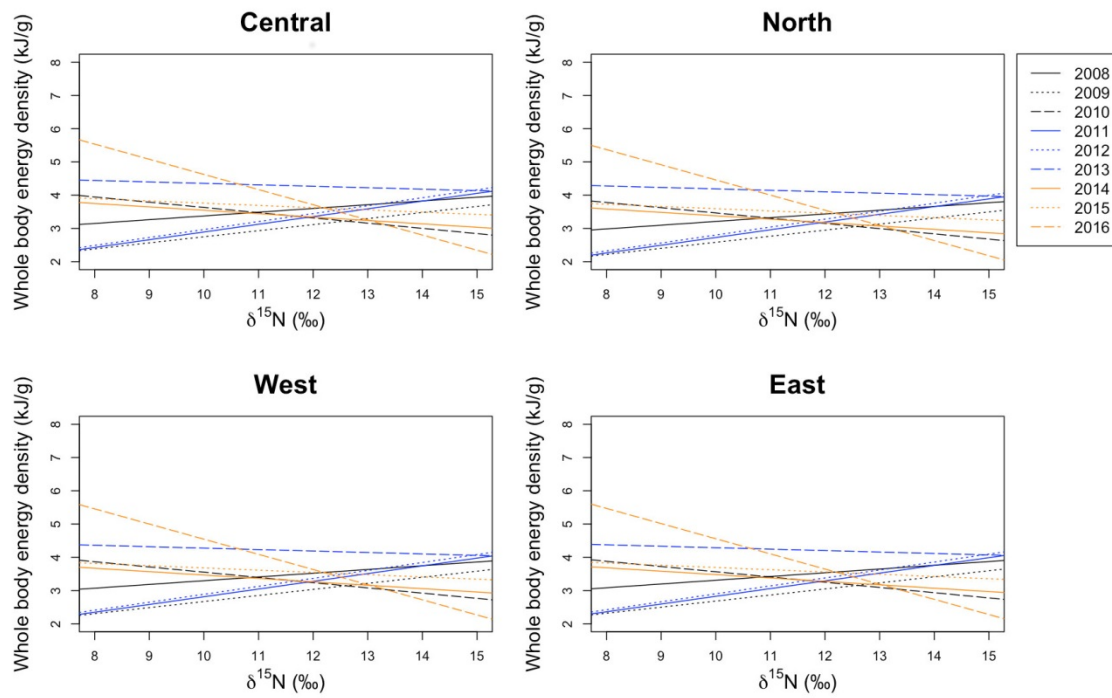


FIGURE 19. VARIATION IN MARCH WHOLE BODY ENERGY DENSITY IN RELATION TO $\delta^{15}\text{N}$, HYDROLOGIC REGION, AND YEAR. REGRESSIONS ARE BASED ON WEIGHTED PARAMETER ESTIMATES ACROSS ALL MODELS FOR THE AVERAGE SIZE HERRING AND RANGE OF $\delta^{15}\text{N}$ VALUES IN THE MARCH DATASET.

TABLE 1. CANDIDATE MODEL SETS FOR DESCRIBING VARIATION IN NOVEMBER AND MARCH WHOLE BODY ENERGY DENSITY OF JUVENILE PACIFIC HERRING IN PRINCE WILLIAM SOUND, ALASKA.

CARBON STABLE ISOTOPE ANALYSES		
MODEL NUMBER	RESPONSE VARIABLE	EXPLANATORY VARIABLES
1	NOV OR MAR WBED (KJ/G)	~1, RANDOM=~1+FL COLLECTION BAY (NULL)
2	NOV OR MAR WBED (KJ/G)	~FL + $\delta^{13}C'$, RANDOM=~1+FL COLLECTION BAY
3	NOV OR MAR WBED (KJ/G)	~FL + REGION, RANDOM=~1+FL COLLECTION BAY
4	NOV OR MAR WBED (KJ/G)	~FL + YEAR, RANDOM=~1+FL COLLECTION BAY
5	NOV OR MAR WBED (KJ/G)	~FL + $\delta^{13}C'$ + REGION, RANDOM=~1+FL COLLECTION BAY
6	NOV OR MAR WBED (KJ/G)	~FL + $\delta^{13}C'$ + YEAR, RANDOM=~1+FL COLLECTION BAY
7	NOV OR MAR WBED (KJ/G)	~FL + REGION + YEAR, RANDOM=~1+FL COLLECTION BAY
8	NOV OR MAR WBED (KJ/G)	~FL + $\delta^{13}C'$ + REGION + YEAR, RANDOM=~1+FL COLLECTION BAY
9	NOV OR MAR WBED (KJ/G)	~FL + $\delta^{13}C'$ + REGION + YEAR + $\delta^{13}C'$ *REGION, RANDOM=~1+FL COLLECTION BAY
10	NOV OR MAR WBED (KJ/G)	~FL + $\delta^{13}C'$ + REGION + YEAR + $\delta^{13}C'$ *YEAR, RANDOM=~1+FL COLLECTION BAY
NITROGEN STABLE ISOTOPE ANALYSES		
MODEL NUMBER	RESPONSE VARIABLE	EXPLANATORY VARIABLES
1	NOV OR MAR WBED (KJ/G)	~1, RANDOM=~1+FL COLLECTION BAY (NULL)
2	NOV OR MAR WBED (KJ/G)	~FL + $\delta^{15}N$, RANDOM=~1+FL COLLECTION BAY
3	NOV OR MAR WBED (KJ/G)	~FL + REGION, RANDOM=~1+FL COLLECTION BAY
4	NOV OR MAR WBED (KJ/G)	~FL + YEAR, RANDOM=~1+FL COLLECTION BAY
5	NOV OR MAR WBED (KJ/G)	~FL + $\delta^{15}N$ + REGION, RANDOM=~1+FL COLLECTION BAY
6	NOV OR MAR WBED (KJ/G)	~FL + $\delta^{15}N$ + YEAR, RANDOM=~1+FL COLLECTION BAY
7	NOV OR MAR WBED (KJ/G)	~FL + REGION + YEAR, RANDOM=~1+FL COLLECTION BAY
8	NOV OR MAR WBED (KJ/G)	~FL + $\delta^{15}N$ + REGION + YEAR, RANDOM=~1+FL COLLECTION BAY
9	NOV OR MAR WBED (KJ/G)	~FL + $\delta^{15}N$ + REGION + YEAR + $\delta^{15}N$ *REGION, RANDOM=~1+FL COLLECTION BAY
10	NOV OR MAR WBED (KJ/G)	~FL + $\delta^{15}N$ + REGION + YEAR + $\delta^{15}N$ *YEAR, RANDOM=~1+FL COLLECTION BAY

ABBREVIATIONS: WBED = WHOLE BODY ENERGY DENSITY, FL = FORK LENGTH, $\delta^{13}C'$ = LIPID CORRECTED CARBON STABLE ISOTOPE SIGNATURE, $\delta^{15}N$ = NITROGEN STABLE ISOTOPE SIGNATURE.

TABLE 2. CANDIDATE MODELS DESCRIBING VARIATION IN WHOLE BODY ENERGY DENSITY OF JUVENILE HERRING IN PRINCE WILLIAM SOUND, ALASKA. MODELS PRESENTED ARE THOSE DETERMINED TO BE MOST PARSIMONIOUS, AS WELL ALL MODELS RECEIVING $\Delta AICc$ VALUES ≤ 2 .

Month and isotope	Response variable	Model number	Explanatory variables	Number of parameters	$\Delta AICc$	w	<i>Pseudo R</i> ²
November, $\delta^{13}C'$	WBED (kJ/g)	9	FL + $\delta^{13}C'$ + Region + Year + $\delta^{13}C' * \text{Region}$, random= $\sim 1 + \text{FL} \text{Collection Bay}$	21	0.00	0.99	0.26
November, $\delta^{15}N$	WBED (kJ/g)	9	FL + $\delta^{15}N$ + Region + Year + $\delta^{15}N * \text{Region}$, random= $\sim 1 + \text{FL} \text{Collection Bay}$	21	0.00	1.00	0.23
March, $\delta^{13}C'$	WBED (kJ/g)	10	FL + $\delta^{13}C'$ + Region + Year + $\delta^{13}C' * \text{Year}$, random= $\sim 1 + \text{FL} \text{Collection Bay}$	26	0.00	1.00	0.22
March, $\delta^{15}N$	WBED (kJ/g)	10	FL + $\delta^{15}N$ + Region + Year + $\delta^{15}N * \text{Year}$, random= $\sim 1 + \text{FL} \text{Collection Bay}$	26	0.00	1.00	0.20

Abbreviations: $\Delta AICc$ = Akaike's Information Criterion corrected for small sample size, w = Akaike weight, WBED = whole body energy density, FL = fork length, $\delta^{13}C'$ = lipid corrected carbon stable isotope signature, $\delta^{15}N$ = nitrogen stable isotope signature.

TABLE 3. PARAMETER ESTIMATES AND LIKELIHOODS FROM CANDIDATE MODELS FOR DESCRIBING VARIATION IN WHOLE BODY ENERGY DENSITY OF JUVENILE HERRING IN PRINCE WILLIAM SOUND, ALASKA. PARAMETER ESTIMATES (\pm 95% CI) ARE WEIGHTED AVERAGES, AND CIs WERE CALCULATED AS 1.96*STANDARD ERRORS THAT ARE BASED ON UNCONDITIONAL VARIANCES. PARAMETER LIKELIHOODS ARE AKAIKE WEIGHT (w) VALUES SUMMED ACROSS ALL MODELS THAT INCLUDE THE VARIABLE.

A) Parameters from candidate models including $\delta^{13}\text{C}'$					
Response variable	Explanatory variables	Parameter likelihoods		Parameter estimates \pm CI	
		November	March	November	March
WBED (kJ/g)	Intercept	1.00	1.00	0.38 ± 2.14	5.73 ± 5.49
	FL	1.00	1.00	0.02 ± 0.01	0.02 ± 0.01
	$\delta^{13}\text{C}'$	1.00	1.00	-0.16 ± 0.09	0.22 ± 0.29
	Location-East	1.00	1.00	1.13 ± 2.00	-0.02 ± 0.14
	Location-North	1.00	1.00	-3.07 ± 2.44	-0.11 ± 0.15
	Location-West	1.00	1.00	-7.75 ± 2.17	-0.02 ± 0.15
	Year2008/09 ^a	1.00	1.00	-0.38 ± 0.23	-1.50 ± 6.80
	Year2009/10 ^a	1.00	1.00	-0.26 ± 0.20	-4.43 ± 5.86
	Year2010/11 ^a	1.00	1.00	-0.51 ± 0.17	-2.54 ± 5.79
	Year2011/12 ^a	1.00	1.00	0.02 ± 0.16	-3.87 ± 5.67
	Year2012/13 ^a	1.00	1.00	0.19 ± 0.20	0.02 ± 6.48
	Year2013/14 ^a	1.00	1.00	0.30 ± 0.16	-5.80 ± 5.81
	Year2014/15 ^a	1.00	1.00	-0.22 ± 0.17	-5.83 ± 6.16
	Year2015/16 ^a	1.00	1.00	-1.07 ± 0.19	-28.01 ± 7.29
	$\delta^{13}\text{C}'$ *LocationEast	1.00	8.07 E-20	0.08 ± 0.10	$-5.71 \text{ E-}21 \pm 2.49 \text{ E-}20$
	$\delta^{13}\text{C}'$ *LocationNorth	1.00	8.07 E-20	-0.14 ± 0.12	$-6.98 \text{ E-}21 \pm 3.02 \text{ E-}20$
	$\delta^{13}\text{C}'$ *LocationWest	1.00	8.07 E-20	-0.38 ± 0.10	$-1.04 \text{ E-}20 \pm 4.25 \text{ E-}20$
	$\delta^{13}\text{C}'$ *Year2008/09 ^a	3.89 E-15	1.00	$-1.16 \text{ E-}15 \pm 5.06 \text{ E-}15$	-0.07 ± 0.36
	$\delta^{13}\text{C}'$ *Year2009/10 ^a	3.89 E-15	1.00	$-1.50 \text{ E-}15 \pm 6.17 \text{ E-}15$	-0.22 ± 0.31
	$\delta^{13}\text{C}'$ *Year2010/11 ^a	3.89 E-15	1.00	$5.95 \text{ E-}18 \pm 1.10 \text{ E-}15$	-0.13 ± 0.31
	$\delta^{13}\text{C}'$ *Year2011/12 ^a	3.89 E-15	1.00	$6.15 \text{ E-}17 \pm 1.08 \text{ E-}15$	-0.20 ± 0.30
	$\delta^{13}\text{C}'$ *Year2012/13 ^a	3.89 E-15	1.00	$-3.83 \text{ E-}16 \pm 2.04 \text{ E-}15$	-0.05 ± 0.34

	$\delta^{13}\text{C}'*\text{Year}2013/14^a$	3.89 E-15	1.00	$-3.16 \text{ E-}16 \pm 1.85 \text{ E-}15$	-0.29 ± 0.31
	$\delta^{13}\text{C}'*\text{Year}2014/15^a$	3.89 E-15	1.00	$-2.43 \text{ E-}16 \pm 1.58 \text{ E-}15$	-0.31 ± 0.33
	$\delta^{13}\text{C}'*\text{Year}2015/16^a$	3.89 E-15	1.000	$-1.78 \text{ E-}15 \pm 7.15 \text{ E-}15$	-1.42 ± 0.38
B) Parameters from candidate models including $\delta^{15}\text{N}$					
Response variable	Explanatory variables	Parameter likelihoods		Parameter estimates \pm CI	
		November	March	November	March
WBED (kJ/g)	Intercept	1.00	1.00	5.09 ± 2.18	0.40 ± 4.40
	FL	1.00	1.00	0.02 ± 0.01	0.02 ± 0.01
	$\delta^{15}\text{N}$	1.00	1.00	-0.14 ± 0.16	0.11 ± 0.36
	Location-East	0.99	1.00	0.59 ± 2.28	-0.07 ± 0.10
	Location-North	0.99	1.00	2.88 ± 2.31	-0.17 ± 0.11
	Location-West	0.99	1.00	-1.99 ± 2.58	-0.08 ± 0.11
	Year2008/09 ^a	1.00	1.00	0.14 ± 0.22	-1.33 ± 6.79
	Year2009/10 ^a	1.00	1.00	-0.02 ± 0.19	2.96 ± 4.57
	Year2010/11 ^a	1.00	1.00	-0.23 ± 0.16	-1.68 ± 4.52
	Year2011/12 ^a	1.00	1.00	0.42 ± 0.15	-1.67 ± 4.64
	Year2012/13 ^a	1.00	1.00	0.86 ± 0.15	2.54 ± 4.82
	Year2013/14 ^a	1.00	1.00	0.32 ± 0.17	2.32 ± 4.42
	Year2014/15 ^a	1.00	1.00	0.14 ± 0.15	2.19 ± 4.58
	Year2015/16 ^a	1.00	1.00	-0.41 ± 0.16	6.93 ± 5.32
	$\delta^{15}\text{N}*\text{LocationEast}$	0.99	1.83 E-09	-0.07 ± 0.18	$3.64 \text{ E-}10 \pm 1.46 \text{ E-}09$
	$\delta^{15}\text{N}*\text{LocationNorth}$	0.99	1.83 E-09	-0.26 ± 0.19	$5.20 \text{ E-}11 \pm 3.45 \text{ E-}10$
	$\delta^{15}\text{N}*\text{LocationWest}$	0.99	1.83 E-09	0.17 ± 0.21	$1.45 \text{ E-}11 \pm 2.72 \text{ E-}10$
	$\delta^{15}\text{N}*\text{Year}2008/09^a$	4.53 E-07	1.00	$1.71 \text{ E-}08 \pm 1.99 \text{ E-}07$	0.07 ± 0.54
	$\delta^{15}\text{N}*\text{Year}2009/10^a$	4.53 E-07	1.00	$1.06 \text{ E-}07 \pm 4.92 \text{ E-}07$	-0.27 ± 0.37
	$\delta^{15}\text{N}*\text{Year}2010/11^a$	4.53 E-07	1.00	$-1.42 \text{ E-}08 \pm 1.86 \text{ E-}07$	0.12 ± 0.37
	$\delta^{15}\text{N}*\text{Year}2011/12^a$	4.53 E-07	1.00	$1.71 \text{ E-}09 \pm 1.55 \text{ E-}07$	0.13 ± 0.38
	$\delta^{15}\text{N}*\text{Year}2012/13^a$	4.53 E-07	1.00	$1.16 \text{ E-}07 \pm 4.98 \text{ E-}07$	-0.16 ± 0.40

	$\delta^{15}\text{N}*\text{Year}2013/14^a$	4.53 E-07	1.00	$2.50 \text{ E-}08 \pm 1.87 \text{ E-}07$	-0.22 ± 0.36
	$\delta^{15}\text{N}*\text{Year}2014/15^a$	4.53 E-07	1.00	$3.12 \text{ E-}08 \pm 2.25 \text{ E-}07$	-0.18 ± 0.38
	$\delta^{15}\text{N}*\text{Year}2015/16^a$	4.53 E-07	1.00	$-1.77 \text{ E-}08 \pm 1.95 \text{ E-}07$	-0.57 ± 0.44

Abbreviations: \pm CI = plus or minus 95% confidence interval, WBED = whole body energy density, FL = fork length, $\delta^{13}\text{C}'$ = lipid corrected carbon stable isotope signature, $\delta^{15}\text{N}$ = nitrogen stable isotope signature.

DISCUSSION

This study has shown several energetic techniques to be reliably measured in juvenile herring including WBED calculated from dry/wet and C/N stable isotope data, in addition to WBED calculated from bomb calorimetry, % lipid, RNA/DNA ratios, and diet composition. We found a very strong relationship between WBED energy density derived from calorimetry and isotope techniques. This result is important, because it indicates that stable isotopes, which provide additional data on trophic foraging, can be used as a reliable, and accurate metric of WBED. Percent lipid and RNA/DNA ratios are interesting metrics when coupled together because they provide information on storage of energy versus investment in growth. Lastly, our diet data help reveal how feeding influences juvenile herring condition, and how herring condition influences winter feeding.

The November and March time series of WBED, based on dry/wet and C/N ratios confirmed the general understanding that juvenile herring in PWS build nutrient reserves ahead of winter that are the primary energy source for maintenance metabolism throughout the winter. Temporal and spatial differences in this time series is further discussed below concerning $\delta^{13}\text{C}$ and $\delta^{15}\text{N}$ as predictors of age-0 herring energy density and physical oceanography related to spatial and temporal variation in GoA derived deep-water transport throughout PWS.

Our study identified important factors influencing the WBED of juvenile Pacific herring in PWS for fish sampled in both the fall and spring. First, for both seasons, larger fish were more energy dense and our data suggest that in the fall juvenile herring must attain a critical size threshold in order to transition from growth to energy storage. Juvenile herring are thought to build nutrient reserves through their first fall that are used during overwinter while fasting when food availability is low (Norcross et al. 2001). Kline et al. (2016) confirmed this dynamic in high temporal resolution studies where fish maximized their energy levels in November, which were then rapidly lost over the next one to two months with energy maintained at minimum levels required for survival through March. Growth during winter appeared minimal, yet fish sampled in the spring were larger than those sampled in the fall suggestive of size dependent mortality (see also Norcross et al. 2001, Kline et al. 2016). In addition, our data suggest that small, lean herring depleted their energy stores in late winter, subsequently taking on greater predation risk by foraging to avert starvation. Our observation regarding the positive relationship between size and energy density provides a plausible mechanism underlying observations regarding overwinter size dependent mortality among PWS juvenile Pacific herring.

For the November dataset, a strong negative relationship between WBED and the $\delta^{13}\text{C}'$ isotope signature of individual fish, particularly those collected from the northern and western regions of PWS, indicated that fish with a more depleted $\delta^{13}\text{C}'$ isotope signature were more energy dense. Previous work on isotopic gradients between the GoA and PWS indicated that the mode $\delta^{13}\text{C}'$ value of *N. cristatus* collected from the GoA was -23‰, while the mode value for this zooplankton species collected in PWS was -19‰ (e.g., Kline 2009). Our data ranged approximately from -22‰ to -18‰. Thus, in comparison with established isotopic gradients, we conclude that carbon derived from the GoA directly enhances the fall quality of juvenile herring in PWS, particularly in the north and western regions of PWS. This result is important, as earlier work did not consider carbon source as a potential correlate of juvenile herring quality that might play a role in survival. Results regarding this interaction between $\delta^{13}\text{C}'$ value and hydrological

region of PWS further indicate a role for teleconnections with the GoA operating on the quality of juvenile herring. In November, fish collected from the eastern region were less energy dense than fish collected from other regions (central, northern and western). This spatial trend in the quality of fish was also true for energy storage and growth metrics. The central, northern and western regions of PWS all are areas characterized by deep bathymetry associated with a marine canyon that extends from the continental shelf into PWS that follows a cyclonic east to west trajectory. Water from the GoA flows into PWS through this marine canyon and its distribution in the region is determined by bathymetry, particularly in the summer and early fall when downwelling is relaxed and deep water more easily transits into PWS through the bottom layer (Cooney et al. 2001b, Halverson et al. 2013). Thus, it is not surprising that the regions in PWS associated with deep bathymetry and an expected influx of water from the GoA also produce juvenile herring that hold a GoA carbon signature that are more energy dense, particularly in early winter.

During the fall, a negative relationship between WBED and $\delta^{15}\text{N}$ isotope signature was observed in the northern region of PWS indicating that fish feeding on relatively lower trophic level prey were more energy dense. Isotopic studies of zooplankton in PWS have indicated that prey such as copepods are depleted in $\delta^{15}\text{N}$ relative to other dominant prey such as amphipods and euphausiids (Kline 1999). The diets of juvenile herring in the northern region of PWS might have primarily consisted of copepods, which would explain feeding at relatively lower trophic levels. However, juvenile herring diets can be highly variable and further research is needed to investigate this explanation.

Results for both $\delta^{13}\text{C}$ and $\delta^{15}\text{N}$ isotopes clearly indicate that carbon source and trophic foraging are more strongly related to WBED in the fall than in the spring, which likely reflects the fact that fish are foraging more aggressively in the summer and fall in order to accumulate energy reserves for overwinter maintenance metabolism. Oceanographic exchange with GoA carbon suggests that ocean-climate conditions that enhance the intrusion of GoA water into PWS should have a positive effect on the quality of juvenile herring, particularly ocean-climate conditions that operate in the late summer and fall. The lack of a relationship in spring between WBED and the $\delta^{13}\text{C}'$ isotope signature of individual fish suggests that some amount of local PWS feeding might be occurring during winter such that isotope signatures of fish become slightly enriched. Our diet composition data suggest that fish do in fact forage in the winter, particularly smaller fish. In fact, Kline et al. (2016) discuss the possibility of winter-feeding in juvenile herring, particularly given observations of more enriched $\delta^{13}\text{C}'$ isotope signatures reflective of local PWS production. Only in 2016 did the negative relationship between WBED and the $\delta^{13}\text{C}'$ isotope signature persist. Environmental conditions were extremely warm in 2016 and it is possible that the spring bloom occurred earlier in 2016 providing fish with food resources typically found outside the late winter season.

Year was an important factor in both fall and spring analyses. In the fall, fish were most energy dense in 2012 and 2013, and least energy dense in 2015. In the spring, fish were the most energy dense in 2013 with all other years being rather similar in terms of energy density. The winter of 2012/13 was one of the coldest in the nine-year time series; November and December 2012 were the coldest November and December months since 2007, while January through March 2013 was relatively average for temperature. Cold temperatures reduce the metabolism of fish possibly making it easier to survive the winter. Accordingly, fish captured in the spring of 2013 were

among the highest quality in the time series. The fall of 2015 occurred during a marked warming period in the GoA, i.e., “the blob” (Bond et al. 2015). Temperatures leading into the fall of 2015 were anomalously warm and associated with reduced quality of juvenile herring. Thus, even in the relatively short time series presented here, there appears to be conspicuous links to water temperature regimes in PWS where cold environmental conditions enhance the energy density of fish, while warm environmental conditions reduce juvenile herring quality.

It is notable that the interaction between $\delta^{13}\text{C}'$ isotope signature and region was only supported in fall analyses, while the interaction between $\delta^{13}\text{C}'$ isotope signature and year was supported in spring analyses. This result leads us to highlight the important seasonal differences driving intrusion of water from the GoA into PWS that shapes energy density of juvenile herring in the fall, and the likely scenario that winter-feeding by juvenile herring might enrich their tissues without considerable energy gain, removing any relationship between WBED and $\delta^{13}\text{C}'$ isotope signature in the spring.

In summary, the quality of juvenile herring in PWS appears to be influenced by oceanographic exchange with the GoA that is facilitated by PWS bathymetry and circulation, in addition to local temperature regimes. Zooplankton community structure and abundance presumably act as important transport mechanisms for GoA carbon to PWS juvenile herring. The energetic condition of young herring is enhanced in the northern and western regions of PWS and during colder temperature regimes. Best-supported models for both November and March had relatively low pseudo R^2 values (0.20 – 0.26), highlighting that other factors must be important predictors of WBED for young herring. For this reason, it remains dubious whether oceanographic exchange with the GoA is driving energetic variability that influences juvenile herring production and recruitment to the spawning population. Links between GoA and PWS oceanographic exchange and juvenile herring recruitment would be better established by long-term coupled oceanographic (zooplankton community structure and abundance, as well as $\delta^{13}\text{C}$ and $\delta^{15}\text{N}$ stable isotopes) sampling in the GoA and PWS much like the work reported by Kline (2009), as well as modeling of these connections (Coyle et al. 2013). Other possible approaches include using isotope methods to compare the geochemical signature of otoliths between juvenile herring in the eastern and western/northern regions of PWS during their first summer growth phase and those of older, recruited herring (e.g., Walther et al. 2008). If a large proportion of the spawning population had otolith geochemical signatures from the first summer growth phase that are more similar to juveniles from a specific region of PWS, greater links between GoA/PWS oceanographic exchange and herring recruitment would be established.

CONCLUSIONS

Juvenile (age-0) Pacific herring of PWS, Alaska are seasonally energetically variable with greater energy stores in fall as compared with spring. This dynamic allows fish to sustain themselves over-winter when food resources are scarce. Our data suggest that larger fish are more energy dense and there appears to be a size-related dynamic whereby larger fish in the fall can store more energy as opposed to investing in growth. Over-winter, there appears to be size-dependent mortality as fish caught in spring tended to be larger than fish caught in the fall with minimal over-winter growth apparent. The quality of juvenile herring in PWS appears to be importantly influenced by teleconnections with the GoA that are facilitated by PWS bathymetry and circulation, in addition to temperature regimes. It is likely that the northern and western

regions of PWS are hotspots for juvenile Pacific herring production, while colder temperatures likely ensure greater overwinter survival via effects on metabolism. Impacts of age-0 herring over-winter energetics on survival and recruitment to the spawning population remain an important outstanding question. Survival-modeling of the data presented here is forthcoming and should help address the gap concerning relationships between energetics and survival/recruitment.

ACKNOWLEDGEMENTS

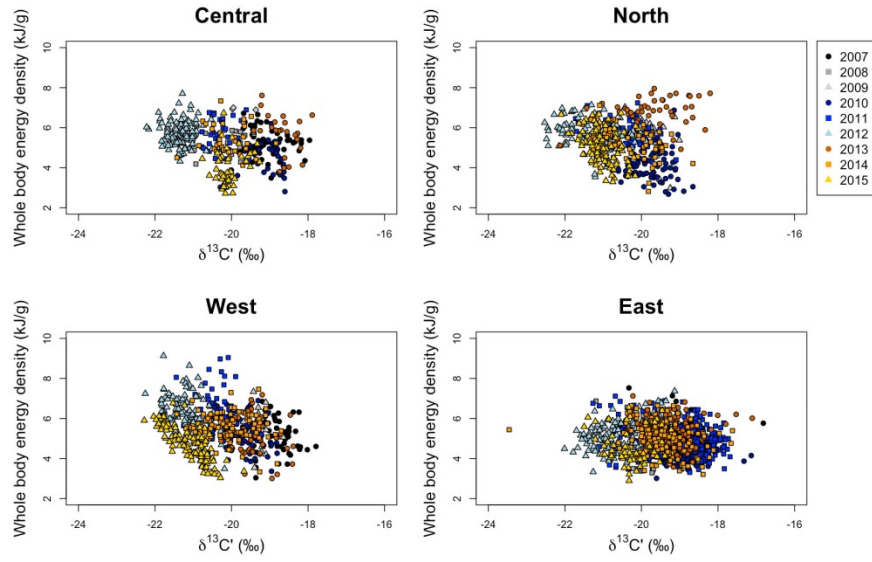
We are especially grateful to the *Exxon Valdez* Oil Spill Trustee Council (EVOSTC) for long-term support of research on the energetics of juvenile herring in PWS. The findings and conclusions presented by the authors are their own and do not necessarily reflect the views or position of the EVOSTC. Captain Dave Beam and crew of the F/V *Montague* assisted with fall collections of herring, while Cordova District Fishermen United assisted with spring collections. Several excellent field and lab technicians including K. Siwicke, J. Todd, D. Roberts, J. McMahon, A. Potter and V. Gonzalez assisted with field collections and sample processing for stable isotopes and bomb calorimetry at Prince William Sound Science Center. N. Haubenstock and T. Howe at the Alaska Stable Isotope Facility, University of Alaska Fairbanks, analyzed samples for carbon and nitrogen stable isotopes. We thank A. Schaefer for assistance with mapping. The Prince William Sound Science Center provided administrative and logistical support. Auke Bay Labs thanks R. Bare, S. Ballard, R. Bradshaw, S. Christiansen, E. Conheady, K. Cox, A. Eller, E. Fergusson, H. Findlay, C. Fugate, M. Garrison, K. Heffern, L. Heifetz, T. Jarvis, J. Moran, S. Mosher, B. Nelson, T. Parker, C. Pihl, E. Pihl, A. Robertson, L. Schaufler, A. Sreenivasan, and W. Strasburger for assistance with this project.

LITERATURE CITED

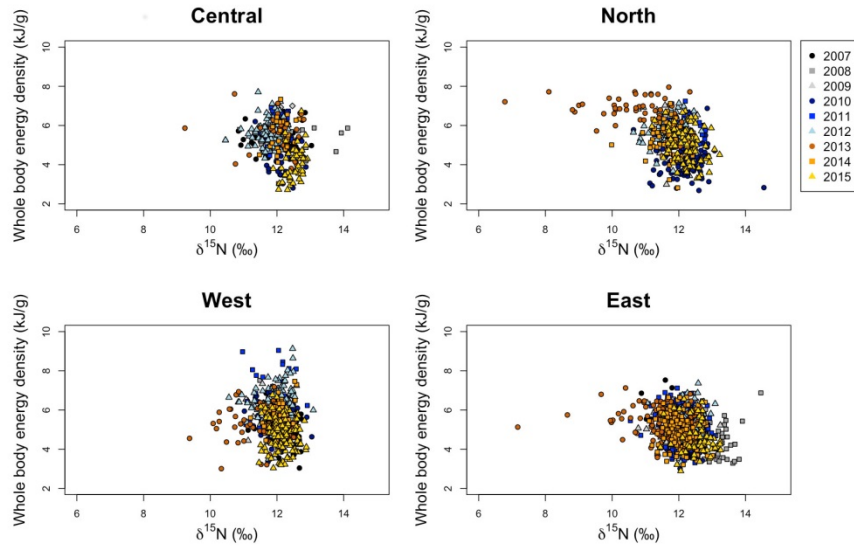
- Bernreuther, M., J. P. Herrmann, M. A. Peck, and A. Temming. 2013. Growth energetics of juvenile herring, *Clupea harengus* L.: food conversion efficiency and temperature dependency of metabolic rate. *Journal of Applied Ichthyology* 29:331-340.
- Bond, N. A., M. F. Cronin, H. Freeland, and N. Mantua. 2015. Causes and impacts of the 2014 warm anomaly in the NE Pacific. *Geophysical Research Letters* 42:3414-3420.
- Buckley, L. J. 1984. RNA-DNA ratio: an index of larval fish growth in the sea. *Marine Biology* 80:291-298.
- Burnham, K. P., and D. R. Anderson. 2002. *Model Selection and Multi-Model Inference: A Practical Information Theoretic Approach*. Springer-Verlag, New York, NY.
- Caldarone, E. M., M. Wagner, J. St. Onge-Burns, and L. J. Buckley. 2001. Protocol and guide for estimating nucleic acids in larval fish using a fluorescence microplate reader.
- Cooney, R. T., J. R. Allen, M. A. Bishop, D. L. Eslinger, T. Kline, B. L. Norcross, C. P. McRoy, J. Milton, J. Olsen, V. Patrick, A. J. Paul, D. Salmon, D. Scheel, G. L. Thomas, S. L. Vaughan, and T. M. Willette. 2001a. Ecosystem control of pink salmon (*Oncorhynchus gorbuscha*) and Pacific herring (*Clupea pallasii*) populations in Prince William Sound, Alaska. *Fisheries Oceanography* 10:1-13.
- Cooney, R. T., K. O. Coyle, E. Stockmar, and C. Stark. 2001b. Seasonality in surface-layer net zooplankton communities in Prince William Sound, Alaska. *Fisheries Oceanography* 10:97-109.
- Coyle, K. O., G. A. Gibson, K. Hedstrom, A. J. Hermann, and R. R. Hopcroft. 2013. Zooplankton biomass, advection and production on the northern Gulf of Alaska shelf from simulations and field observations. *Journal of Marine Systems* 128:185-207.
- Coyle, K. O., A. J. Paul, and D. A. Ziemann. 1990. Copepod populations during the spring bloom in an Alaskan subarctic embayment. *Journal of Plankton Research* 12:759-797.
- Crawley, M. J. 2007. *The R Book*. John Wiley & Sons, Ltd, West Sussex, UK.
- Folch, J., M. Lees, and G. H. Sloane Stanley. 1957. A simple method for the isolation and purification of total lipids from animal tissues. *Journal of Biological Chemistry* 226:497-509.
- Foy, R. J., and B. L. Norcross. 1999. Spatial and temporal variability in the diet of juvenile Pacific herring (*Clupea pallasii*) in Prince William Sound, Alaska. *Canadian Journal of Zoology-Revue Canadienne De Zoologie* 77:697-706.
- Gorman, K. B., T. C. Kline Jr., M. E. Roberts, F. F. Sewall, R. A. Heintz, and W. S. Pegau. 2018. Spatial and temporal variation in winter condition of juvenile Pacific herring (*Clupea pallasii*) in Prince William Sound, Alaska: oceanographic exchange with the Gulf of Alaska. *Deep-Sea Research II* 147:116-126.
- Halverson, M. J., C. Belanger, and S. M. Gay. 2013. Seasonal transport variations in the straits connecting Prince William Sound to the Gulf of Alaska. *Continental Shelf Research* 63:S63-S78.
- Jodice, P. G. R., D. D. Roby, K. R. Turco, R. M. Suryan, D. B. Irons, J. F. Piatt, M. T. Shultz, D. G. Roseneau, A. B. Kettle, and J. A. Anthony. 2006. Assessing the nutritional stress hypothesis: relative influence of diet quantity and quality on seabird productivity. *Marine Ecology Progress Series* 325:267-279.
- Kline, T. C. 1999. Temporal and spatial variability of C-13/C-12 and N-15/N-14 in pelagic biota of Prince William Sound, Alaska. *Canadian Journal of Fisheries and Aquatic Sciences* 56:94-117.

- _____. 2009. Characterization of carbon and nitrogen stable isotope gradients in the northern Gulf of Alaska using terminal feed stage copepodite-V *Neocalanus cristatus*. *Deep-Sea Research Part II-Topical Studies in Oceanography* 56:2537-2552.
- _____. 2013. PWS Herring Survey: Pacific Herring Energetic Recruitment Factors. Exxon Valdez Oil Spill Restoration Project Final Report (Project 10100132-C).
- Kline, T. C., and R. W. Campbell. 2010. Prince William Sound Herring Forage Contingency. Exxon Valdez Oil Spill Restoration Project Final Report (Project 070811).
- Kline, T. C., K. B. Gorman, F. S. Sewall, R. A. Heintz, and W. S. Pegau. 2016. Changes in condition of Pacific Herring (*Clupea pallasii*) during their first autumn to spring period. EVOS Final Report.
- Mazerolle, M. J. 2017.
- McConnaughey, T., and C. P. McRoy. 1979. Food-web structure and the fractionation of carbon isotopes in the Bering Sea. *Marine Biology* 53:257-262.
- Muggeo, V. M. R. 2015.
- Muradian, M. 2015. Modeling the population dynamics of herring in the Prince William Sound, Alaska. University of Washington, Seattle, Washington.
- Musgrave, D. L., M. J. Halverson, and W. S. Pegau. 2013. Seasonal surface circulation, temperature, and salinity in Prince William Sound, Alaska. *Continental Shelf Research* 53:20-29.
- Norcross, B. L., E. D. Brown, R. J. Foy, M. Frandsen, S. M. Gay, T. C. Kline, D. M. Mason, E. V. Patrick, A. J. Paul, and K. D. E. Stokesbury. 2001. A synthesis of the life history and ecology of juvenile Pacific herring in Prince William Sound, Alaska. *Fisheries Oceanography* 10:42-57.
- Paul, A. J., and J. M. Paul. 1998. Comparisons of whole body energy content of captive fasting age zero Alaskan Pacific Herring (*Clupea pallasii* Valenciennes) and cohorts overwintering in nature. *Journal of Experimental Marine Biology and Ecology* 226:75-86.
- Paul, A. J., J. M. Paul, and T. C. Kline Jr. 2001. Estimating whole body energy content for juvenile Pacific herring from condition factor, dry weight, and carbon/nitrogen ratio. Pages 121-133 in F. Funk, J. Blackburn, D. Hay, A. J. Paul, R. Stephenson, R. Toresen, and D. Witherell, editors. *Herring: Expectations for a New Millennium*. University of Alaska Sea Grant, AK-SG-01-04, Fairbanks.
- Pinheiro, J., D. Bates, S. DebRoy, D. Sarkar, and R Core Team. 2017.
- Post, J. R., and E. A. Parkinson. 2001. Energy allocation strategy in young fish: Allometry and survival. *Ecology* 82:1040-1051.
- R Core Team. 2016.
- Sewall, F. F., R. A. Heintz, and J. J. Vollenweider. 2013. Prince William Sound Herring Survey: Value of Growth and Energy Storage as Predictors of Winter Performance in Young-of-the-year Herring from Prince William Sound, Exxon Valdez Oil Spill Trustee Council Final Report (Project 10100132-D), National Marine Fisheries Service, Juneau, Alaska.
- Sreenivasan, A. 2011. Nucleic acid ratios as an index of growth and nutritional ecology in Pacific cod (*Gadus macrocephalus*), walleye pollock (*Theragra chalcogramma*), and Pacific herring (*Clupea pallasii*). University of Alaska Fairbanks.
- Stallings, C. D., F. C. Coleman, C. C. Koenig, and D. A. Markiewicz. 2010. Energy allocation in juveniles of a warm-temperate reef fish. *Environmental Biology of Fishes* 88:389-398.

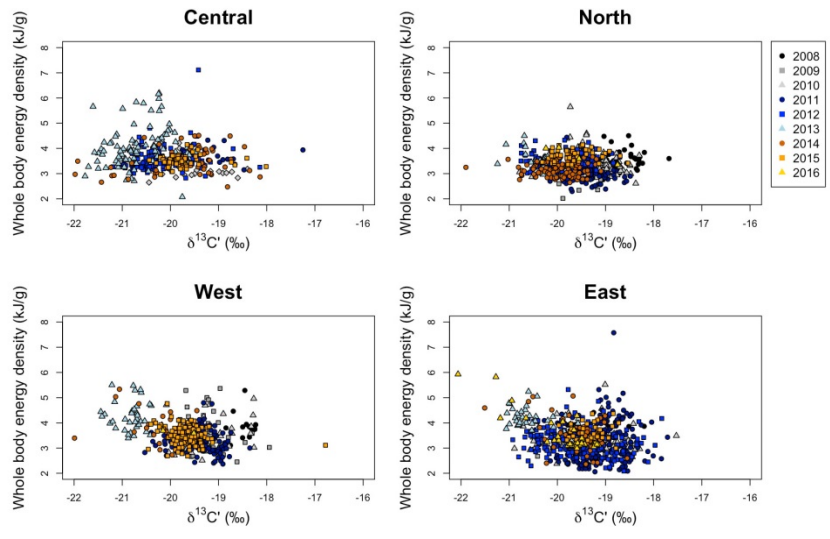
- Sturdevant, M. V., J. A. Orsi, and E. A. Fergusson. 2012. Diets and Trophic Linkages of Epipelagic Fish Predators in Coastal Southeast Alaska during a Period of Warm and Cold Climate Years, 1997-2011. *Marine and Coastal Fisheries* 4:526-545.
- Thorne, R. E., and G. L. Thomas. 2008. Herring and the “Exxon Valdez” oil spill: an investigation into historical data conflicts. *ICES Journal of Marine Science: Journal du Conseil* 65:44-50.
- Vollenweider, J. J., R. A. Heintz, L. Schaufler, and R. Bradshaw. 2011. Seasonal cycles in whole-body proximate composition and energy content of forage fish vary with water depth. *Marine Biology* 158:413-427.
- Walther, B. D., S. R. Thorrold, and J. E. Olney. 2008. Geochemical signatures in otoliths record natal origins of American shad. *Transactions of the American Fisheries Society* 137:57-69.
- Womble, J. N., and M. F. Sigler. 2006. Seasonal availability of abundant, energy-rich prey influences the abundance and diet of a marine predator, the Steller sea lion *Eumetopias jubatus*. *Marine Ecology Progress Series* 325:281-293.
- Xu, R. 2003. Measuring explained variation in linear mixed effects models. *Statistics in Medicine* 22:3527-3541.



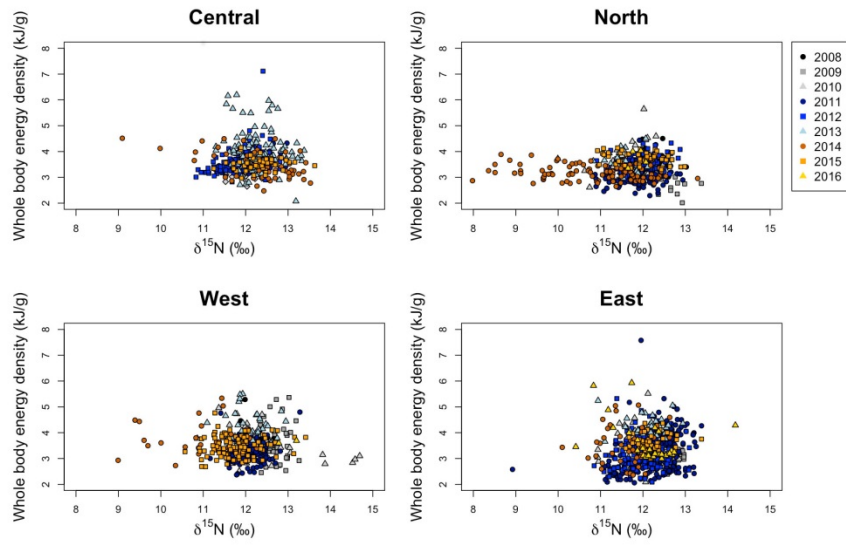
SUPPLEMENTAL MATERIAL FIGURE 1.



SUPPLEMENTAL MATERIAL FIGURE 2.



SUPPLEMENTAL MATERIAL FIGURE 3.



SUPPLEMENTAL MATERIAL FIGURE 4.



Contents lists available at ScienceDirect

Deep-Sea Research Part II

journal homepage: www.elsevier.com/locate/dsr2

Spatial and temporal variation in winter condition of juvenile Pacific herring (*Clupea pallasii*) in Prince William Sound, Alaska: Oceanographic exchange with the Gulf of Alaska



Kristen B. Gorman^{a,*}, Thomas C. Kline Jr^a, Megan E. Roberts^a, Fletcher F. Sewall^b,
Ron A. Heintz^b, W. Scott Pegau^a

^a Prince William Sound Science Center, 300 Breakwater Ave., PO Box 705, Cordova, AK 99574, United States

^b NOAA Alaska Fisheries Science Center, Atke Bay Laboratories, Ted Stevens Marine Research Institute, 17109 Pt. Lena Loop Road, Juneau, AK 99801, United States

ARTICLE INFO

Keywords:

Clupea pallasii
Energetics
Gulf of Alaska
Oceanographic exchange
Overwinter
Pacific herring
Prince William Sound
Stable isotope

ABSTRACT

Spatial variability in early and late winter measures of whole body energy density of juvenile (age-0) Pacific herring (*Clupea pallasii*) of Prince William Sound (PWS), Alaska was examined over nine years of study. Pacific herring in this region remain considered as an injured resource over the 25 years following the *Exxon Valdez* oil spill, however factors responsible for the lack of recovery by herring in PWS are a source of ongoing debate. Given the species' key ecological role in energy transfer to higher predators, and its economic role in a historical commercial fishery within the region, significant research effort has focused on understanding environmental factors that shape nutritional processes and the quality of these young forage fish. During November (early winter), factors such as juvenile herring body size, hydrological region of PWS, year, and the interaction between carbon ($\delta^{13}\text{C}$) or nitrogen ($\delta^{15}\text{N}$) stable isotope signature and hydrological region were all important predictors of juvenile herring energy density. In particular, analyses indicated that in the northern and western regions of PWS, juvenile herring with more depleted $\delta^{13}\text{C}$ values (which reflect a Gulf of Alaska carbon source) were more energy dense. Results suggest that intrusion of water derived from the Gulf of Alaska enhances the condition of age-0 herring possibly through alterations in zooplankton community structure and abundance, particularly in the northern and western regions of PWS in the fall, which is consistent with regional circulation. During March (late winter), factors such as juvenile herring body size, year, and the interaction between $\delta^{13}\text{C}$ or $\delta^{15}\text{N}$ isotope signature and year were all important predictors of juvenile herring energy density. Results differed for early and late winter regarding the interaction between stable isotope signatures and region or year, suggesting important seasonal aspects of circulation contribute to variation in PWS juvenile herring energy density. In addition, winter-feeding may enrich herring without considerable energy gain, removing any relationship between energy density and $\delta^{13}\text{C}$ isotope signature in late winter.

1. Introduction

Important oceanographic exchange has been described between the Gulf of Alaska (GoA) and Prince William Sound (PWS), a complex fjord-estuary located at the GoA's northernmost boundary (Fig. 1). For example, Kline (1997, 1999a, 1999b, 2001, 2009) relied on naturally occurring ratios of stable carbon ($^{13}\text{C}/^{12}\text{C}$, $\delta^{13}\text{C}$) and nitrogen ($^{15}\text{N}/^{14}\text{N}$, $\delta^{15}\text{N}$) isotope signatures of zooplankton and forage fishes to demonstrate isotopic gradients between the GoA and PWS, and subsequent oceanographic exchange between the regions driven by circulation. A strong gradient in $\delta^{13}\text{C}$ was confirmed as *Neocalanus cristatus* copepods collected from the GoA were depleted in $\delta^{13}\text{C}$ relative to those collected

from within PWS, which contrasts with a weak gradient based on $\delta^{15}\text{N}$ of *N. cristatus* (Kline, 2009). Stable isotope techniques are a particularly robust method for discerning oceanographic exchange as the ratio of heavy to light isotopes of carbon and nitrogen in tissues can provide both *source* and *process* information due to isotopic fractionation (Peterson and Fry, 1987). For example, variation in the fractionation of carbon during photosynthesis can distinguish sources of primary productivity such as between nearshore and pelagic phytoplankton (Kelly, 2000). Thus, $\delta^{13}\text{C}$ values provide *source* information due to the origins of the carbon signature and the fact that $\delta^{13}\text{C}$ tends not to vary greatly across trophic levels (Peterson and Fry, 1987). However, $\delta^{15}\text{N}$ values capture a distinct signature of trophic position due to the differential

* Corresponding author.

E-mail address: kgorman@pwssc.org (K.B. Gorman).

<http://dx.doi.org/10.1016/j.dsr2.2017.10.010>

Available online 12 October 2017

0967-0645/ © 2017 The Authors. Published by Elsevier Ltd. This is an open access article under the CC BY-NC-ND license (<http://creativecommons.org/licenses/by-nc-nd/4.0/>).

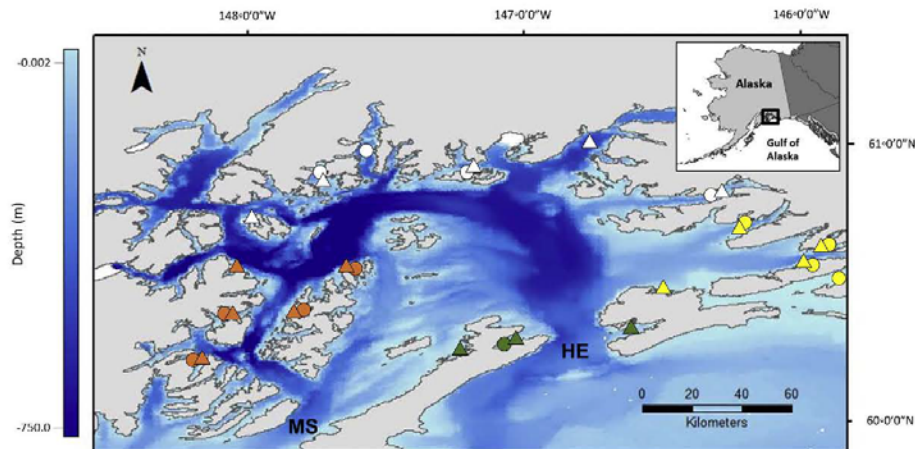


Fig. 1. Bathymetry and location of Prince William Sound nursery bays sampled for juvenile Pacific herring. Bathymetry is noted by the blue gradient, November sampling locations are noted by circles, and March sampling locations are noted by triangles. Hydrological regions included Central (green), North (white), West (orange), and East (yellow). Hinchinbrook Entrance and Montague Strait are noted as HE and MS, respectively.

excretion of the lighter isotope by consumers (Peterson and Fry, 1987). Thus, as elements such as carbon and nitrogen are produced and consumed throughout a food-web, they fractionate and are reflected in plant and animal tissues at varying time scales due to isotopic turnover rates related to metabolic activity, and for these reasons provide excellent information on the origin and distribution, or trophic position, of consumers (Deniro and Epstein, 1978, 1981).

Oceanographic exchange between the GoA and PWS, and relationships between general circulation and trophic linkages among PWS biota became increasingly important topics following the grounding of the Exxon Valdez oil tanker on Bligh Reef in March 1989, which reportedly released ~11 million gallons of crude oil into the coastal marine environment damaging apex predators, fish populations and other species, as well as valuable commercial fisheries such as Pink Salmon (*Oncorhynchus gorbuscha*) and Pacific Herring (*Clupea pallasii*, hereafter herring) (Brown et al., 1996; Cooney et al., 2001a; Norcross et al., 2001). Factors responsible for the ongoing lack of recovery by herring in Prince William Sound are a source of ongoing debate (Ward et al., 2017). Early studies following the spill, as part of the Sound Ecosystem Assessment (SEA) program, took an integrated ecosystem approach to better understand how environmental factors might additionally be influencing the recovery of injured populations (Cooney et al., 2001a). The SEA program outlined key hypotheses that have continued to shape current research and particularly the work described here. In the context of the current study, the SEA program's "river-lake" hypothesis provides a framework for testing ideas regarding trophic linkages between the GoA and PWS that are driven by seasonal circulation. The "river-lake" hypothesis states that during periods of strong downwelling in the GoA, the influence of the Alaska Coastal Current, which flows westerly along the GoA continental margin (Weingartner et al., 2005), on PWS is stronger and more "river-like" with enhanced flushing, conversely during periods of weak downwelling, the ACC's influence on PWS is weaker and more "lake-like" with greater retention of water (Cooney et al., 2001a; Kline, 1999b).

To date, the herring population of PWS remains an injured resource from the Exxon Valdez oil spill, as the population biomass has remained at or below ~20,000 mt since 1998 and continues below this level that would allow a commercial catch (Muradian et al., 2017). Survival of juvenile (age-0) herring through their first winter is considered a

potential factor limiting strong recruitment to the spawning population, and has therefore been the focus of past and ongoing research. Herring build energy reserves through the fall to fuel their metabolism during winter's low food abundance (Norcross et al., 2001), making environmental drivers of fall energy levels of particular interest. Here, we examine spatial and temporal variability in early and late winter measures of energy density among juvenile herring collected since 2007 as part of the PWS Herring Survey (pilot work 2007–2008, 2009–2011) and the PWS Herring Research and Monitoring Program (2012–2016) supported by long-term funding through the Exxon Valdez Oil Spill Trustee Council.

Following the SEA program's "river-lake" hypothesis, we tested the idea that oceanographic exchange between the northern GoA and PWS control juvenile herring nutritional processes and therefore the quality of these young forage fish. Similar to previous studies, our work relies on stable isotope gradients previously established between the GoA and PWS (e.g., Kline, 1999a, 1999b; Kline, 2009). Our work takes a relatively simple multi-model approach to understanding spatial and temporal variability in early (November) and late (March) winter measures of energy density by considering factors such as distinct hydrological regions of PWS related to circulation (space), year (time), either $\delta^{13}\text{C}$ or $\delta^{15}\text{N}$ signatures of fish tissues (trophic linkages) to assess either carbon source or relative trophic position, as well as interactions among these variables. We evaluate the same candidate models for both early and late winter measures of energy density to reveal seasonal differences in important explanatory variables.

2. Materials and methods

2.1. Study area

Prince William Sound, Alaska is a hydrographically complex, fjord-estuary located at the northern extent of the GoA (Fig. 1) that ranges in depth to nearly 800 m in the northwestern passage (Fig. 1; Halverson et al., 2013b; Niebauer et al., 1994). The Chugach National Forest, a mountainous temperate rainforest including numerous ice fields and tidewater glaciers, surrounds the region. Given the coastal rainforest climate, freshwater input from precipitation and glacial runoff is significant and varies seasonally with major contributions occurring in late summer and early fall (Beamer et al., 2016; Royer, 1979). To the south,

several large islands define the primary oceanographic conduits through which local PWS waters interact with the GoA, namely Hinchbrook Entrance (HE) and Montague Strait (MS; Fig. 1). The Alaska Coastal Current (ACC), which flows westerly along the GoA continental margin, and the Alaskan Stream (AS), which extends from the northern Gulf of Alaska to the western Aleutians just beyond the shelf break (Johnson et al., 1988; Royer, 1979; Stabeno and Reed, 1991; Weingartner et al., 2005) are the primary external oceanographic forces that influence PWS circulation and regional marine ecology (Cooney et al., 2001a; Eslinger et al., 2001; Kline, 1999b; Niebauer et al., 1994). General circulation of PWS, which flows cyclonically east to west, is highly seasonally influenced by interactions between the ACC and AS, freshwater input, and wind intensity. For example, during winter, strong easterly winds associated with the Aleutian low drive coastal downwelling over the continental shelf resulting in greater forcing of surface waters into PWS through HE that circulate cyclonically east to west and exit through MS (Cooney et al., 2001a; Halverson et al., 2013a; Niebauer et al., 1994). Conversely, during summer, the high pressure in the North Pacific causes a relaxation or even reversal of the downwelling allowing subsurface dense water to rise and transit into PWS through the bottom layer (Cooney et al., 2001a; Halverson et al., 2013a; Niebauer et al., 1994). Summertime surface flow in PWS becomes complex due to the addition of freshwater, which can result in eddies and current reversals (Vaughan et al., 2001; Wang et al., 2001).

2.2. Field sampling

Juvenile herring (age-0) were collected from a total of 19 nursery bays in PWS during research cruises in November, and by contracted commercial herring fisherman in March, of each year between 2007 and 2016 using cast and gill nets, or trawl gear. In November, fish were caught at night with field operations generally occurring around the new moon. Samples were collected using a midwater trawl where groups of fish were targeted during acoustic surveys of each bay. At times, deck lights were used to attract herring that were collected by cast and gill net along-side the research vessel as these gear types do not sample effectively at depth. Cast and gill net samples were taken to primarily compare with trawl caught samples. Although the use of deck lights might have imposed a bias by attracting more poor condition fish eager to feed, the spread of juvenile herring energy values collected by cast and gill nets spanned that of fish collected by trawl. Thus, capture methods are not expected to impose any bias on the energetic quality of the fish sampled during this study. In March, fish were caught using fisherman gill nets only. Nursery bays sampled during the SEA program were again sampled (i.e. Simpson, Eaglek, Whale and Zaikof Bays), in addition to many others including Cordova Harbor, Windy Bay, Double Bay, Port Gravina, Port Fidalgo, Valdez Arm, Jackson Hole (Glacier Island), Unakwik, West Twin Bay (Perry Island), Northwest Bay (Knight Island), Main Bay, Paddy Bay, Lower Herring Bay, Port Chalmers, and Port Etches (Fig. 1). Not all bays were sampled each year. Upon capture, fish were frozen in groups of 25–50 per sampling location and saved for laboratory processing at Prince William Sound Science Center in Cordova, Alaska.

2.3. Stable isotope and bomb calorimetry methods

In the laboratory, frozen juvenile herring were thawed and wet mass (mg) obtained using an analytical balance (Mettler). Length of each fish was measured to the nearest mm. Otoliths were excised and saved for other analyses. Fish were oven-dried (60 °C) and the final whole body dry mass recorded. Dried herring were ground to a fine powder using a ball mill (Retsch). Approximately 0.1–0.2 mg from each powdered herring was loaded into a tin capsule. Loaded capsules were sent to the University of Alaska Fairbanks Stable Isotope Facility where carbon (C) and nitrogen (N) mass spectrometric analyses were performed. Resultant data for juvenile herring included %C, %N, $^{13}\text{C}/^{12}\text{C}$, and

$^{15}\text{N}/^{14}\text{N}$ with the heavy to light isotope ratios reported using delta notation, $\delta^{13}\text{C}$ and $\delta^{15}\text{N}$, respectively, calculated using the following equation: $\delta^{13}\text{C}$ or $\delta^{15}\text{N} = ((R_{\text{sample}}/R_{\text{standard}}) - 1) \times 1000$, where R_{sample} is the ratio of the heavy to light isotope for either $^{13}\text{C}/^{12}\text{C}$ or $^{15}\text{N}/^{14}\text{N}$, and R_{standard} is the heavy to light isotope ratios for international standards – Vienna PeeDee Belemnite for carbon and atmospheric N_2 (Air) for nitrogen. Percent C and N data were used to ascertain C/N atom ratios. The ratios of dry to wet mass and C to N atoms were used to determine whole body energy density (WBED) based on relationships derived from (Paul et al., 2001) and refined by (Kline, 2013) using the following equation: WBED (kJ/g wet mass) = $-2.90242 + 32.585 \times (\text{dry/wet mass ratio}) + 0.103514 \times \text{C/N atom ratio}$ (see also Kline and Campbell, 2010). Raw $\delta^{13}\text{C}$ data were mathematically corrected for lipid content using the method of McConnaughey and McRoy (1979); see also Kline and Campbell (2010). Lipid-corrected values of $\delta^{13}\text{C}$ are hereafter reported as $\delta^{13}\text{C}$.

A semi-micro calorimeter (Parr Instruments, model 6725) was used to perform bomb calorimetry (Parr Instrument Company, 2009) on a subset (~10%) of dried herring samples analyzed for $\delta^{13}\text{C}$ and $\delta^{15}\text{N}$ stable isotopes to ground-truth energy density estimates from dry/wet and C/N ratios. Although it was expected that estimates of WBED derived from dry/wet and C/N ratios would tightly correlate with energy density estimates derived from bomb calorimetry (e.g., Kline and Campbell, 2010), we explored these relationships for both November and March.

2.4. Statistical analyses

All analyses were restricted to juvenile herring up to 115 mm in fork length that were collected over nine years in November (2007–2015, $n = 2514$) and March (2008–2016, $n = 1889$). Nursery bay collection areas were grouped into four hydrological regions (central, north, west, and east regions, Fig. 1) following descriptions by Musgrave et al. (2013). However, the analyses presented here considered north and west regions separately, and did not include a Gulf of Alaska region, unlike Musgrave et al. (2013). All statistical analyses were performed in the R language environment version 3.4.1 (2017).

Least-squares linear models (lm function in R, hereafter linear models) were used to account for variation in WBED derived from stable isotope data for both November ($n = 258$) and March ($n = 253$). Two candidate models were considered for both November and March including an equal-means (null) model and a model with WBED derived from bomb calorimetry.

Two separate analyses were conducted to understand spatial and temporal variation in November WBED of age-0 herring in PWS (see Appendix A for a complete description of all explanatory variables and candidate models considered in analyses). First, linear mixed-effects models, employed using the lme function within the nlme package in R (Pinheiro et al., 2017, hereafter mixed models), were used to examine continuous variation in WBED derived from stable isotope data in relation to four parameters treated as fixed main effects including (1) fork length as a measure of body size (continuous variable); (2) $\delta^{13}\text{C}$ stable isotope signature of age-0 herring (continuous variable) to assess carbon source; (3) nursery bay hydrological region in PWS (categorical variable – central, north, west, and east); and (4) year (categorical variable). Second, mixed models were again used to examine variation in November WBED in relation to three of these same parameters, fork length, nursery bay hydrological region, and year, but also $\delta^{15}\text{N}$ stable isotope signatures of age-0 herring as a continuous variable to assess trophic foraging. An *a priori* set of 10 candidate models were considered for each November analysis, including either $\delta^{13}\text{C}$ or $\delta^{15}\text{N}$ stable isotope signatures, which consisted of a null model; models for isotope, region, or year predictor variables as fixed main effects including a term for fork length to control for body size in each model (three models); a more complex multiple predictor model including fixed main effect terms for fork length, isotope, and region (one model). All models

Appendix A

Open Access manuscript available at <https://doi.org/10.1016/j.dsr2.2017.10.010>

K.B. Gorman et al.

Deep-Sea Research Part II 147 (2018) 116–126

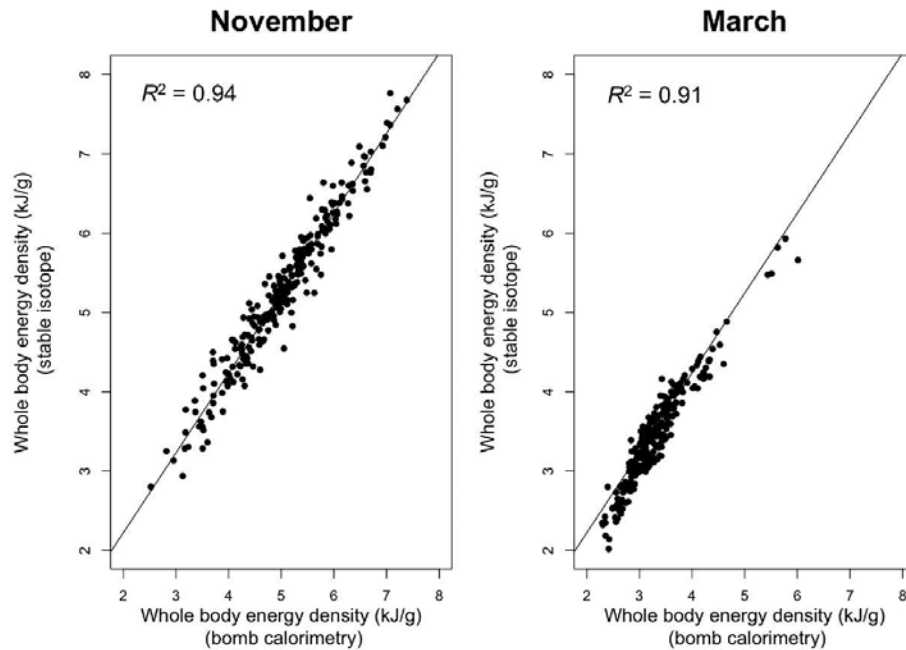


Fig. 2. Variation in November and March whole body energy density of juvenile Pacific herring derived from stable isotope data in relation to whole body energy density derived from bomb calorimetry.

without a year term were further evaluated including a year term (three models). Additional interaction models were included: a global model with all four fixed main effects and an interaction between isotope signature and region, and a second global model with all four fixed main effects and an interaction between isotope signature and year (two models). A random effect on intercept and slope (random = $\sim 1 + \text{Fork Length}[\text{Collection Bay}]$) was included in each model to control for non-independence of data given that some fish were collected from the same nursery bay, and therefore, experienced more similar local environmental conditions that might have influenced individual size and energetic status.

Similarly, two separate analyses were conducted to understand spatial and temporal variation in March WBED derived from stable isotope data of age-0 herring in PWS. Again, mixed models included the same explanatory variables and candidate model sets describe for November analyses (Appendix A).

For November and March WBED analyses, the importance of including a random effect on intercept and slope was tested in preliminary analyses by comparing the fit of four models, based on Akaike's Information Criterion corrected for small sample size (AICc), for each analysis - the most parameterized fixed effect model without a random effect (using the `glm` function in R), with a random effect on intercept only (mixed model), with a random effect on slope only (mixed model), and with a random effect on both intercept and slope (mixed model). All four models maximized the restricted log-likelihood (method = "REML") and all models included the same fixed main effect parameters and their interaction. The most parameterized fixed effect model with a random effect on both intercept and slope received the lowest AICc value for each analysis. Therefore, a random effect on both intercept and slope was included in all candidate models for November and March analyses.

Information-theoretic methods were used to direct model selection and parameter estimation (Burnham and Anderson, 2002). For each

candidate model, AICc, ΔAICc and Akaike weight (w) values were calculated using the `AICcmodavg` package in R (Mazerolle, 2017) and used to compare models (Burnham and Anderson, 2002). Values for ΔAICc are scaled differences relative to the smallest AICc value in the candidate model set such that the model with the minimum AICc value has $\Delta_i = 0$ (Burnham and Anderson, 2002). Values for Akaike weights are the relative likelihood of the model, given the data, normalized to sum to 1 and interpreted as probabilities (Burnham and Anderson, 2002). Inference was based on the relative support for parameters across all models and weighted parameter estimates. Parameter estimation included calculation of model-averaged parameter estimates based on w values for all candidate models within a candidate model set. Standard errors (SE) and 95% confidence intervals (CI: $\text{SE} \times 1.96$) for parameter estimates were based on unconditional variances calculated across the same models. Parameter likelihood values were evaluated by summing w values across all models that included each parameter under consideration (Burnham and Anderson, 2002). Ultimately, only two models were considered in comparing stable isotope and bomb calorimetry estimates of WBED, including the null model, therefore no model averaging calculations were conducted for this analysis.

Linear models were used to compare stable isotope and bomb calorimetry estimates of WBED, thus an R^2 value defined as the fraction of the total variance explained by the model, was calculated as a general measure of fit (see Crawley, 2007, p. 399). For mixed models, a pseudo R^2 value was calculated following Xu (2003), which is defined as $1 - \frac{\text{residual variance of the full model}}{\text{residual variance of a null model}}$. Best supported models for November and March WBED analyses were examined based on standardized residual versus fitted value plots and normal probability plots of residuals to further assess model fit.

3. Results

Models including WBED derived from bomb calorimetry were best

Table 1

Candidate models describing variation in whole body energy density of juvenile Pacific herring in Prince William Sound, Alaska. Models presented are those determined to be most parsimonious, as well as all models receiving ΔAICc values ≤ 2 .

Month and isotope	Response variable	Model number	Explanatory variables	Number of parameters	ΔAICc	w	Pseudo R^2
November, $\delta^{13}\text{C}$	WBED (kJ/g)	9	FL + $\delta^{13}\text{C}$ + Region + Year + $\delta^{13}\text{C}$ *Region, random = $-1 + \text{FL} \text{Collection Bay}$	21	0.00	0.99	0.26
November, $\delta^{15}\text{N}$	WBED (kJ/g)	9	FL + $\delta^{15}\text{N}$ + Region + Year + $\delta^{15}\text{N}$ *Region, random = $-1 + \text{FL} \text{Collection Bay}$	21	0.00	1.00	0.23
March, $\delta^{13}\text{C}$	WBED (kJ/g)	10	FL + $\delta^{13}\text{C}$ + Region + Year + $\delta^{13}\text{C}$ *Year, random = $-1 + \text{FL} \text{Collection Bay}$	26	0.00	1.00	0.22
March, $\delta^{15}\text{N}$	WBED (kJ/g)	10	FL + $\delta^{15}\text{N}$ + Region + Year + $\delta^{15}\text{N}$ *Year, random = $-1 + \text{FL} \text{Collection Bay}$	26	0.00	1.00	0.20

Abbreviations: ΔAICc = Akaike's Information Criterion corrected for small sample size, w = Akaike weight, WBED = whole body energy density, FL = fork length, $\delta^{13}\text{C}$ = lipid corrected carbon stable isotope signature, $\delta^{15}\text{N}$ = nitrogen stable isotope signature.

supported (November: ΔAICc value = 0.00, March: ΔAICc value = 0.00) over null models for describing variation in both November and March WBED where values were derived from dry/wet mass and C/N atom ratios of juvenile herring. Each model received very high weight and goodness of fit values (November: $w = 1.00$, $R^2 = 0.94$; March: $w = 1.00$, $R^2 = 0.91$; Fig. 2). Estimates of WBED based on stable isotope data were considered reliable because of these strong relationships and consequently used in the analyses reported below.

3.1. November

Only one model including $\delta^{13}\text{C}$ stable isotope signatures received a ΔAICc value ≤ 2.00 for describing variation in November WBED, which included all terms as fixed main effects (fork length, $\delta^{13}\text{C}$ isotope signature, hydrological region, and year), as well as an interaction between $\delta^{13}\text{C}$ isotope signature and region (Appendix A: carbon stable isotope analysis for November, model 9). Plots of standardized residual versus fitted values and normal probability plots of residuals indicated model 9 was fitted adequately. This best-supported model received a high w value (0.99), but only explained 26% of the variation in the data (Table 1). Parameter likelihoods indicated strong support for all fixed main effect parameters and the interaction between $\delta^{13}\text{C}$ isotope signature and region (1.00, Table 2). The interaction between $\delta^{13}\text{C}$ isotope signature and year was not supported (3.98 E-15, Table 2). Fish with larger body sizes were more energy dense (0.02 ± 0.01 CI, Table 2). Fish with more depleted $\delta^{13}\text{C}$ isotope signatures were more energy dense (-0.16 ± 0.09 CI, Table 2). The interaction between $\delta^{13}\text{C}$ isotope signature and region was strongest in the west (-0.38 ± 0.10 CI) and north (-0.14 ± 0.12 CI) where fish with a more depleted $\delta^{13}\text{C}$ stable isotope signature were more energy dense (Table 2, Fig. 3). Juvenile herring caught in the fall of 2013 (0.30 ± 0.16 CI) were the most energy dense, while fish caught in the fall of 2015 were the least energy dense (-1.07 ± 0.19 CI, Table 2, Fig. 3). See Supplemental material Fig. 1 for plots of WBED versus $\delta^{13}\text{C}$ stable isotope signatures for November.

Only one model including $\delta^{15}\text{N}$ stable isotope signatures received a ΔAICc value ≤ 2.00 for describing variation in November WBED, which included all terms as fixed main effects (fork length, $\delta^{15}\text{N}$ isotope signature, hydrological region, and year), as well as an interaction between $\delta^{15}\text{N}$ isotope signature and region (Appendix A: nitrogen stable isotope analysis for November, model 9). Plots of standardized residual versus fitted values and normal probability plots of residuals indicated model 9 was fitted adequately. This best-supported model received a high w value (1.00), but again only explained 23% of the variation in the data (Table 1). Parameter likelihoods indicated strong support for all fixed main effect parameters and the interaction between $\delta^{15}\text{N}$ isotope signature and region (0.99–1.00, Table 2). Again, the interaction between $\delta^{15}\text{N}$ isotope signature and year was not supported (4.53 E-07, Table 2). Fish with larger body sizes were more energy dense (0.02 ± 0.01 CI, Table 2). Fish from northern nursery bays were more

energy dense (2.88 ± 2.31 CI, Table 2). The interaction between $\delta^{15}\text{N}$ isotope signature and region was strongest in the north (-0.26 ± 0.19 CI) where fish with a more depleted $\delta^{15}\text{N}$ isotope signature were more energy dense (Fig. 4). Juvenile herring caught in the fall of 2012 were the most energy dense (0.86 ± 0.15 CI), while fish caught in the fall of 2015 were the least energy dense (-0.41 ± 0.16 CI, Table 2, Fig. 4). See Supplemental material Fig. 2 for plots of WBED versus $\delta^{15}\text{N}$ stable isotope signatures for November.

3.2. March

Only one model including $\delta^{13}\text{C}$ stable isotope signatures received a ΔAICc value ≤ 2.00 for describing variation in March WBED, which included all terms as fixed main effects (fork length, $\delta^{13}\text{C}$ isotope signature, hydrological region, and year), as well as an interaction between $\delta^{13}\text{C}$ isotope signature and year (Appendix A: carbon stable isotope analysis for March, model 10). Plots of standardized residual versus fitted values and normal probability plots of residuals indicated model 10 was fitted adequately. This best-supported model received a high w value (1.00), but only explained 22% of the variation in the data (Table 1). Parameter likelihoods indicated strong support for all fixed main effect parameters and the interaction between $\delta^{13}\text{C}$ isotope signature and year (1.00, Table 2). The interaction between $\delta^{13}\text{C}$ isotope signature and region was not supported (8.07 E-20, Table 2). Again, fish with larger body sizes were more energy dense (0.02 ± 0.01 CI, Table 2). The interaction between $\delta^{13}\text{C}$ isotope signature and year was strongest for fish caught in 2016 (-1.42 ± 0.38 CI, Fig. 5) where individuals with a more depleted $\delta^{13}\text{C}$ isotope signature were more energy dense (Fig. 5). See Supplemental material Fig. 3 for plots of WBED versus $\delta^{13}\text{C}$ stable isotope signatures for March.

Similar to other analyses, only one model including $\delta^{15}\text{N}$ stable isotope signatures received a ΔAICc value ≤ 2.00 for describing variation in March WBED, which included all terms as fixed main effects (fork length, $\delta^{15}\text{N}$ isotope signature, hydrological region, and year), as well as an interaction between $\delta^{15}\text{N}$ isotope signature and year (Appendix A: nitrogen stable isotope analysis for March, model 10). Plots of standardized residual versus fitted values and normal probability plots of residuals indicated model 10 was fitted adequately. This best-supported model received a high w value (1.00), but only explained 20% of the variation in the data (Table 1). Parameter likelihoods indicated strong support for all main effect parameters and the interaction between $\delta^{15}\text{N}$ isotope signature and year (1.00, Table 2). The interaction between $\delta^{15}\text{N}$ isotope signature and region was not supported (1.83 E-09, Table 2). Fish with larger body sizes were more energy dense (0.02 ± 0.01 CI, Table 2). The interaction between $\delta^{15}\text{N}$ isotope signature and year was strongest for fish caught in 2016 (-0.57 ± 0.44 , Table 2) where juvenile herring with more depleted $\delta^{15}\text{N}$ isotope signatures were more energy dense (Fig. 5). See Supplemental material Fig. 4 for plots of WBED versus $\delta^{15}\text{N}$ stable isotope signatures for March.

Table 2

Parameter estimates and likelihoods from candidate models for describing variation in November and March whole body energy density of juvenile Pacific herring in Prince William Sound, Alaska. Parameter estimates (\pm 95% confidence intervals) are weighted averages. Parameter likelihoods are Akaike weight (w) values summed across all models that include the variable. Results are presented for A) candidate models including $\delta^{13}C'$ and B) candidate models including $\delta^{15}N$.

A) Parameters from candidate models including $\delta^{13}C'$					
Response variable	Explanatory variables	Parameter likelihoods		Parameter estimates \pm CI	
		November	March	November	March
WBED (kJ/g)	Intercept	1.00	1.00	0.38 \pm 2.14	5.73 \pm 5.49
	FL	1.00	1.00	0.02 \pm 0.01	0.02 \pm 0.01
	$\delta^{13}C'$	1.00	1.00	-0.16 \pm 0.09	0.22 \pm 0.29
	Location-East	1.00	1.00	1.13 \pm 2.00	-0.02 \pm 0.14
	Location-North	1.00	1.00	-3.07 \pm 2.44	-0.11 \pm 0.15
	Location-West	1.00	1.00	-7.75 \pm 2.17	-0.02 \pm 0.15
	Year2008/09 ^a	1.00	1.00	-0.38 \pm 0.23	-1.50 \pm 6.80
	Year2009/10 ^a	1.00	1.00	-0.26 \pm 0.20	-4.43 \pm 5.86
	Year2010/11 ^a	1.00	1.00	-0.51 \pm 0.17	-2.54 \pm 5.79
	Year2011/12 ^a	1.00	1.00	0.02 \pm 0.16	-3.87 \pm 5.67
	Year2012/13 ^a	1.00	1.00	0.19 \pm 0.20	0.02 \pm 6.48
	Year2013/14 ^a	1.00	1.00	0.30 \pm 0.16	-5.80 \pm 5.81
	Year2014/15 ^a	1.00	1.00	-0.22 \pm 0.17	-5.83 \pm 6.16
	Year2015/16 ^a	1.00	1.00	-1.07 \pm 0.19	-28.01 \pm 7.29
	$\delta^{13}C'$ *LocationEast	1.00	8.07 E-20	0.08 \pm 0.10	-5.71 E-21 \pm 2.49 E-20
	$\delta^{13}C'$ *LocationNorth	1.00	8.07 E-20	-0.14 \pm 0.12	-6.98 E-21 \pm 3.02 E-20
	$\delta^{13}C'$ *LocationWest	1.00	8.07 E-20	-0.38 \pm 0.10	-1.04 E-20 \pm 4.25 E-20
	$\delta^{13}C'$ *Year2008/09 ^a	3.89 E-15	1.00	-1.16 E-15 \pm 5.06 E-15	-0.07 \pm 0.36
	$\delta^{13}C'$ *Year2009/10 ^a	3.89 E-15	1.00	-1.50 E-15 \pm 6.17 E-15	-0.22 \pm 0.31
	$\delta^{13}C'$ *Year2010/11 ^a	3.89 E-15	1.00	5.95 E-18 \pm 1.10 E-15	-0.13 \pm 0.31
	$\delta^{13}C'$ *Year2011/12 ^a	3.89 E-15	1.00	6.15 E-17 \pm 1.08 E-15	-0.20 \pm 0.30
	$\delta^{13}C'$ *Year2012/13 ^a	3.89 E-15	1.00	-3.83 E-16 \pm 2.04 E-15	-0.05 \pm 0.34
	$\delta^{13}C'$ *Year2013/14 ^a	3.89 E-15	1.00	-3.16 E-16 \pm 1.85 E-15	-0.29 \pm 0.31
$\delta^{13}C'$ *Year2014/15 ^a	3.89 E-15	1.00	-2.43 E-16 \pm 1.58 E-15	-0.31 \pm 0.33	
$\delta^{13}C'$ *Year2015/16 ^a	3.89 E-15	1.000	-1.78 E-15 \pm 7.15 E-15	-1.42 \pm 0.38	
B) Parameters from candidate models including $\delta^{15}N$					
Response variable	Explanatory variables	Parameter likelihoods		Parameter estimates \pm CI	
		November	March	November	March
WBED (kJ/g)	Intercept	1.00	1.00	5.09 \pm 2.18	0.40 \pm 4.40
	FL	1.00	1.00	0.02 \pm 0.01	0.02 \pm 0.01
	$\delta^{15}N$	1.00	1.00	-0.14 \pm 0.16	0.11 \pm 0.36
	Location-East	0.99	1.00	0.59 \pm 2.28	-0.07 \pm 0.10
	Location-North	0.99	1.00	2.88 \pm 2.31	-0.17 \pm 0.11
	Location-West	0.99	1.00	-1.99 \pm 2.58	-0.08 \pm 0.11
	Year2008/09 ^a	1.00	1.00	0.14 \pm 0.22	-1.33 \pm 6.79
	Year2009/10 ^a	1.00	1.00	-0.02 \pm 0.19	2.96 \pm 4.57
	Year2010/11 ^a	1.00	1.00	-0.23 \pm 0.16	-1.68 \pm 4.52
	Year2011/12 ^a	1.00	1.00	0.42 \pm 0.15	-1.67 \pm 4.64
	Year2012/13 ^a	1.00	1.00	0.86 \pm 0.15	2.54 \pm 4.82
	Year2013/14 ^a	1.00	1.00	0.32 \pm 0.17	2.32 \pm 4.42
	Year2014/15 ^a	1.00	1.00	0.14 \pm 0.15	2.19 \pm 4.58
	Year2015/16 ^a	1.00	1.00	-0.41 \pm 0.16	6.93 \pm 5.32
	$\delta^{15}N$ *LocationEast	0.99	1.83 E-09	-0.07 \pm 0.18	3.64 E-10 \pm 1.46 E-09
	$\delta^{15}N$ *LocationNorth	0.99	1.83 E-09	-0.26 \pm 0.19	5.20 E-11 \pm 3.45 E-10
	$\delta^{15}N$ *LocationWest	0.99	1.83 E-09	0.17 \pm 0.21	1.45 E-11 \pm 2.72 E-10
	$\delta^{15}N$ *Year2008/09 ^a	4.53 E-07	1.00	1.71 E-08 \pm 1.99 E-07	0.07 \pm 0.54
	$\delta^{15}N$ *Year2009/10 ^a	4.53 E-07	1.00	1.06 E-07 \pm 4.92 E-07	-0.27 \pm 0.37
	$\delta^{15}N$ *Year2010/11 ^a	4.53 E-07	1.00	-1.42 E-08 \pm 1.86 E-07	0.12 \pm 0.37
	$\delta^{15}N$ *Year2011/12 ^a	4.53 E-07	1.00	1.71 E-09 \pm 1.55 E-07	0.13 \pm 0.38
	$\delta^{15}N$ *Year2012/13 ^a	4.53 E-07	1.00	1.16 E-07 \pm 4.98 E-07	-0.16 \pm 0.40
	$\delta^{15}N$ *Year2013/14 ^a	4.53 E-07	1.00	2.50 E-08 \pm 1.87 E-07	-0.22 \pm 0.36
$\delta^{15}N$ *Year2014/15 ^a	4.53 E-07	1.00	3.12 E-08 \pm 2.25 E-07	-0.18 \pm 0.38	
$\delta^{15}N$ *Year2015/16 ^a	4.53 E-07	1.00	-1.77 E-08 \pm 1.95 E-07	-0.57 \pm 0.44	

Abbreviations: \pm CI = plus or minus 95% confidence interval, WBED = whole body energy density, FL = fork length, $\delta^{13}C'$ = lipid corrected carbon stable isotope signature, $\delta^{15}N$ = nitrogen stable isotope signature.

^a Signifies a parameter including Year, or an interaction with Year, where the first year noted is for November and the second year for March, i.e., parameters estimates for Year 2008/09 would be for November 2008 and March 2009, respectively.

4. Discussion

Our study identified important factors influencing the WBED of juvenile Pacific herring in PWS, Alaska for fish sampled in early and late winter. For November analyses, a strong negative relationship between WBED and the $\delta^{13}C'$ isotope signature of fish, particularly those collected from the northern and western regions of PWS, indicated that fish with a more depleted $\delta^{13}C'$ isotope signature were more energy dense (Fig. 3, Supplemental material Fig. 1). This is an interesting result

given previous work on isotopic gradients between the GoA and PWS, which indicated that while there is some overlap, $\delta^{13}C'$ values of *N. cristatus* collected from the GoA ranged from -27‰ to -17‰, while $\delta^{13}C'$ values for *N. cristatus* collected from PWS ranged from -23‰ to -17‰ with $\delta^{13}C'$ values of -21‰ to 20‰ representing an approximate demarcation between carbon derived from the GoA and PWS, respectively (see Kline, 2009 Figure 7). Our $\delta^{13}C'$ isotope data for November ranged approximately from -24‰ to -17‰ across all regions of PWS (Supplemental material Fig. 1). However, in both the northern

Appendix A

Open Access manuscript available at <https://doi.org/10.1016/j.dsr2.2017.10.010>

K.B. Gorman et al.

Deep-Sea Research Part II 147 (2018) 116–126

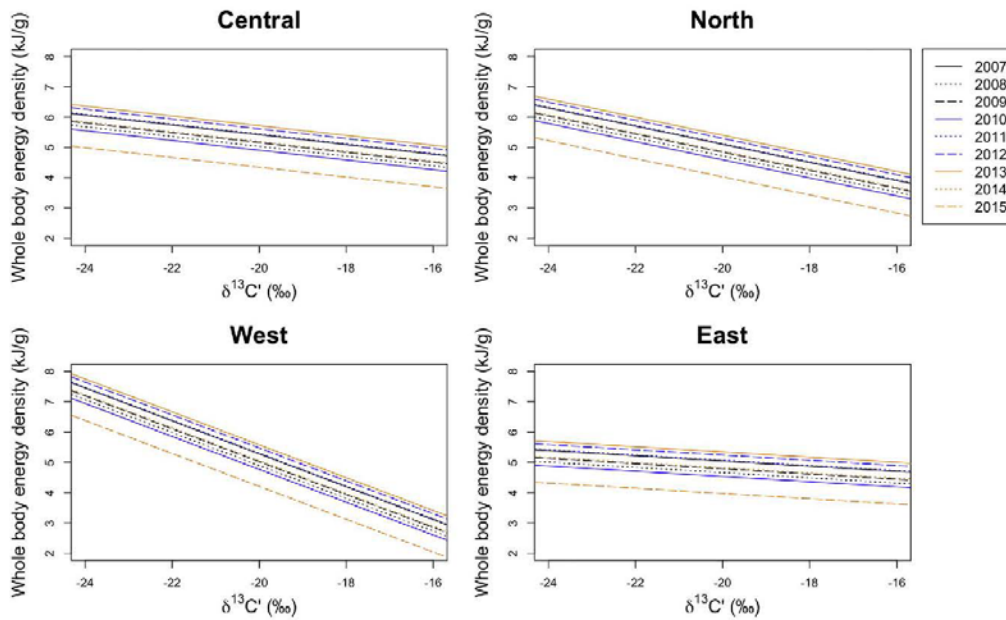


Fig. 3. Modeled variation in November whole body energy density of juvenile Pacific herring of Prince William Sound, Alaska in relation to $\delta^{13}\text{C}'$, hydrological region, and year. Regressions are based on weighted parameter estimates across all models for the average size herring and range of $\delta^{13}\text{C}'$ values (-23.46 to -16.82) for samples collected in November.

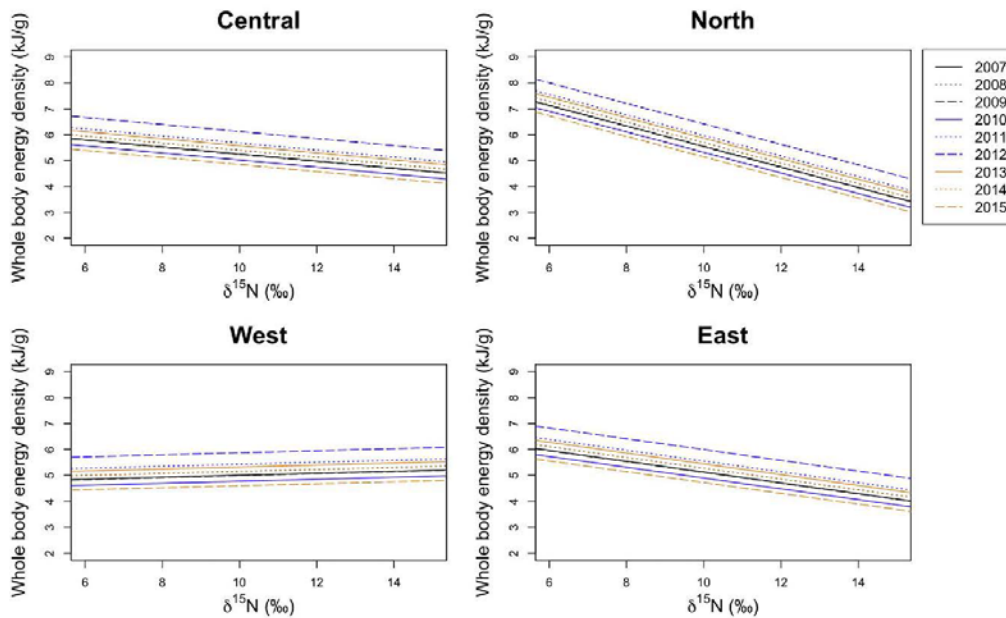


Fig. 4. Modeled variation in November whole body energy density of juvenile Pacific herring of Prince William Sound, Alaska in relation to $\delta^{15}\text{N}$, hydrological region, and year. Regressions are based on weighted parameter estimates across all models for the average size herring and range of $\delta^{15}\text{N}$ values (6.79 – 14.55) for samples collected in November.

and western regions of PWS, $\delta^{13}\text{C}'$ data appear to be marginally skewed towards more depleted $\delta^{13}\text{C}'$ values, particularly in comparison with data from the eastern region (Supplemental material Fig. 1). We

interpret these findings as evidence that carbon derived from the GoA ($\delta^{13}\text{C}' < -20.5\text{‰}$) enhances the early winter quality of juvenile herring in PWS, particularly in the northern and western regions of PWS.

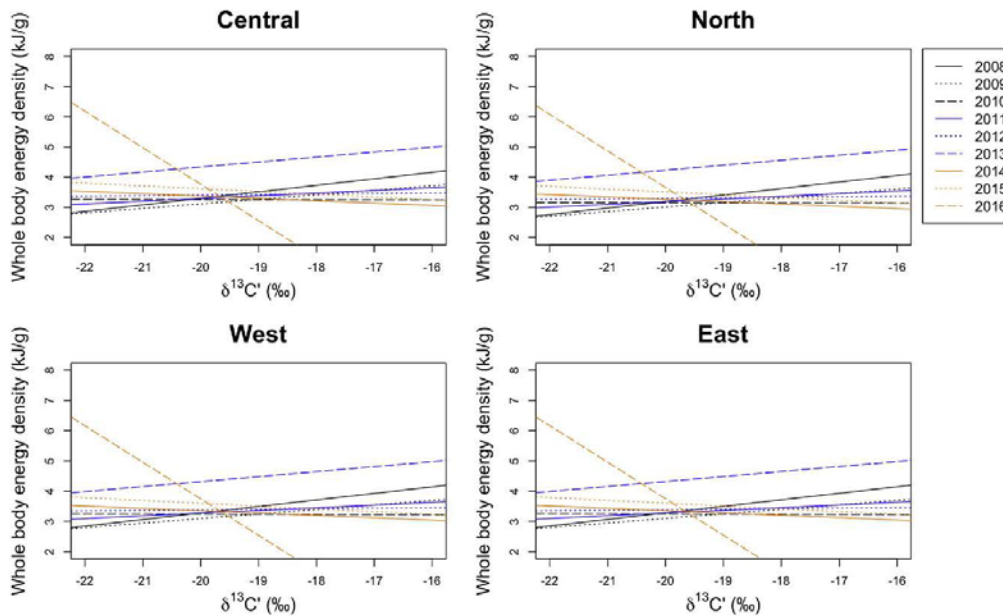


Fig. 5. Modeled variation in March whole body energy density of juvenile Pacific herring of Prince William Sound, Alaska in relation to $\delta^{13}\text{C}'$, hydrological region, and year. Regressions are based on weighted parameter estimates across all models for the average size herring and range of $\delta^{13}\text{C}'$ values (-22.06 to -16.78) for samples collected in March.

Earlier studies did not consider carbon source as a potential correlate of juvenile herring quality (Kline, 1997, 1999a, 1999b, 2000, 2001; Paul and Paul, 1999). Our demonstration of the interaction between $\delta^{13}\text{C}'$ value and hydrological region of PWS indicates a role for oceanographic exchange with the GoA operating on the quality of juvenile herring. In November, fish collected from the eastern region were less energy dense than fish collected from other regions (central, northern and western, Table 2). The central, northern and western regions of PWS are all areas characterized by deep bathymetry associated with a marine canyon that extends from the continental shelf into PWS that follows a cyclonic east to west trajectory (Fig. 1). Water from the GoA flows into PWS through this marine canyon and its distribution in the region is determined by bathymetry, particularly in the summer and early fall when downwelling is relaxed and deep water more easily transits into PWS through the bottom layer (Cooney et al., 2001b; Halverson et al., 2013a). Thus, it is not surprising that the regions in PWS associated with deep bathymetry and an expected influx of water from the GoA also produce juvenile herring that hold a GoA carbon signature that are more energy dense, particularly in early winter (Figs. 1 and 3). Interestingly, earlier studies by Paul and Paul (1999) demonstrated that WBED of juvenile herring collected from areas such as Eaglek, Whale and Zaikof Bays in the northern, western and central regions of PWS, respectively, were not different from each other, however, juvenile herring collected from Simpson Bay in the eastern region had lower WBED values than fish from these other areas. Their study was conducted across only three years (1995–1997), however, coupled with our results it appears that these regional dynamics in herring WBED are mainly consistent.

We are intrigued by the finding that although $\delta^{13}\text{C}'$ data appear to be marginally skewed towards more depleted $\delta^{13}\text{C}'$ values in the northern and western regions of PWS, the range of $\delta^{13}\text{C}'$ values across all regions is not that dramatically different. However, there is clearly a stronger relationship between $\delta^{13}\text{C}'$ and WBED in the northern and western regions of PWS (Fig. 3; Supplemental material Fig. 1). This

suggests to us that there may be different transport mechanisms driving relationships between $\delta^{13}\text{C}'$ and WBED of PWS juvenile herring possibly in the context of different zooplankton communities and abundance associated with different hydrological regions of PWS. Early studies identified *Neocalanus*, *Calanus*, and *Pseudocalanus* copepods overwintering (October and November) in areas deeper than ~ 400 m in PWS in preparation for reproduction in January and February (Damkaer, 1977; Eslinger et al., 2001). These deep areas of PWS therefore provide excellent reproductive habitat for these species elevating their densities relative to other areas of the GoA shelf (Cooney, 1986). Research conducted during the years of the current study confirmed that in some years large calanoids can comprise up to 50% of the diet of juvenile herring in early winter (Gorman et al., 2017). Thus, we suggest the relationship between $\delta^{13}\text{C}'$ and WBED of PWS juvenile herring might be driven by differing zooplankton communities with variable energetic qualities and/or abundances dominating the various hydrological regions of PWS, providing a transport mechanism for GoA carbon to influence juvenile herring quality.

During the fall, a negative relationship between WBED and $\delta^{15}\text{N}$ isotope signature was observed in the northern region of PWS (Fig. 4) indicating that fish feeding on relatively lower trophic level prey were more energy dense. Isotopic studies of zooplankton in PWS have additionally indicated that prey such as copepods are depleted in $\delta^{15}\text{N}$ relative to other dominant prey such as amphipods and euphausiids (Kline, 1999b). The diets of juvenile herring in the northern region of PWS might have primarily consisted of copepods, which corroborates our thinking in terms of $\delta^{13}\text{C}'$ variability and would explain feeding at relatively lower trophic levels.

Results for $\delta^{13}\text{C}'$ stable isotopes indicate that carbon source is more strongly related to WBED in the fall than in the spring (Figs. 3 and 5), which likely reflects fish foraging more aggressively in the summer and fall to accumulate energy reserves for overwintering. Oceanographic exchange with GoA carbon suggests that ocean-climate conditions enhancing the intrusion of GoA water into PWS should have a positive

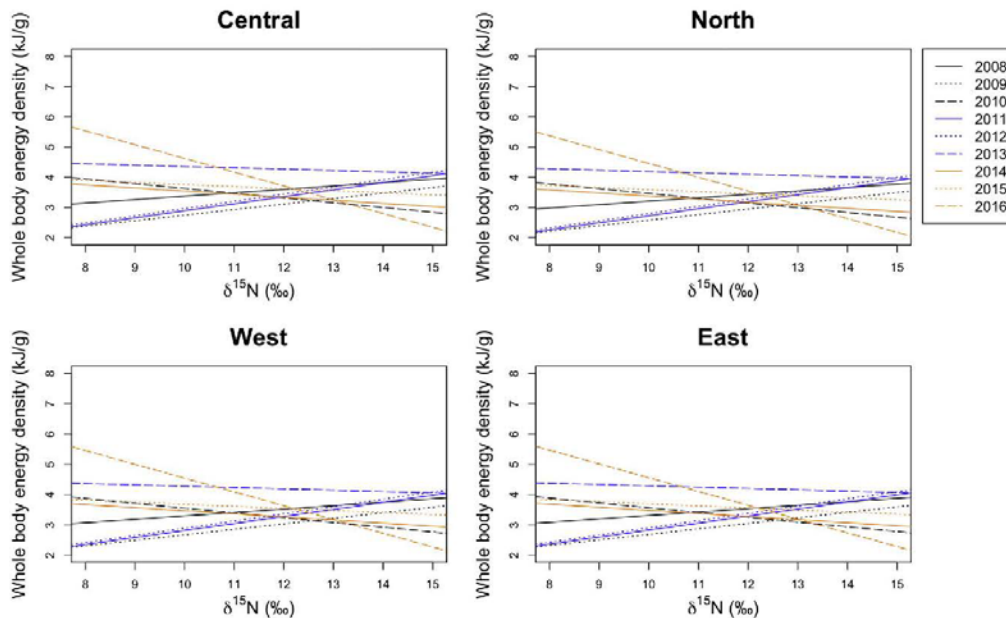


Fig. 6. Modeled variation in March whole body energy density of juvenile Pacific herring of Prince William Sound, Alaska in relation to $\delta^{15}\text{N}$, hydrological region, and year. Regressions are based on weighted parameter estimates across all models for the average size herring and range of $\delta^{15}\text{N}$ values (7.98–14.69) for samples collected in March.

effect on the quality of juvenile herring, particularly those intrusions that operate in the late summer and fall. The lack of a relationship in spring between WBED and the $\delta^{13}\text{C}$ isotope signature of individual fish (Table 2, Fig. 5) suggests that some amount of local PWS feeding might be occurring during winter leading to isotope signatures of fish becoming slightly enriched. Winter-feeding by juvenile herring in Simpson Bay, PWS, has been suggested given observations of more enriched $\delta^{13}\text{C}$ isotope signatures reflective of local PWS production (Gorman, Sewall and Heintz unpubl. data; see also Foy and Norcross, 1999; Kline and Campbell, 2010). Only in one year (2016) did the negative relationship between WBED and $\delta^{13}\text{C}$ isotope signatures persist (Fig. 5). Environmental conditions were extremely warm in 2016 and it is possible that the spring bloom occurred earlier in 2016 providing fish with food resources typically found outside the late winter season.

Year was an important factor in both early and late winter analyses. In November, fish were most energy dense in 2012 and 2013, and least energy dense in 2015 (Figs. 3 and 4). In March, fish were the most energy dense in 2013 with all other years being rather similar in terms of energy density (Figs. 5 and 6). Interestingly, in early winter 2012 and 2015 fish were also the most depleted in $\delta^{13}\text{C}$ of the nine-year time series (Supplemental material Fig. 1). Herring were also most depleted in March in 2013, but not in 2016 (Supplemental material Fig. 3). The opposing annual results between WBED and $\delta^{13}\text{C}$ further suggests the possibility that yearly variation in WBED is ultimately driven by variation in zooplankton community structure and abundance influenced by GoA intrusion. One environmental factor that stands out between early and late winter 2012/13 and 2015/16 is temperature. The winter of 2012/13 was one of the coldest in the nine-year time series - November and December 2012 were the coldest November and December months since 2007, while January through March 2013 was relatively average for temperature (Cordova NOAA tide station data). Cold temperatures reduce the metabolism of fish, possibly making it easier to survive the winter. Accordingly, fish captured in the spring of 2013

were among the highest quality in the time series. The fall of 2015 occurred during a marked warming period in the GoA (Bond et al., 2015). Temperatures leading into the fall of 2015 were anomalously warm and associated with reduced quality of juvenile herring. Thus, even in the relatively short time series presented here, there appears to be links to water temperature regimes in PWS and the GoA, where cold environmental conditions enhance the energy density of fish, while warm environmental conditions reduce juvenile herring quality. We note, however, that temperature is one of many environmental factors that shape yearly conditions for juvenile herring. A recent study by Ward et al. (2017) noted freshwater discharge as an important factor influencing herring productivity in PWS before, during and after the Exxon Valdez oil spill. Further, the intensity of downwelling on the shelf is known to play a role in GoA intrusions into PWS with seasonal variability important to “river-lake” dynamics (Cooney et al., 2001a). However, we note that downwelling intensity has not consistently correlated with annual measures of spring zooplankton stocks (Eslinger et al., 2001).

It is interesting that the interaction between $\delta^{13}\text{C}$ isotope signature and region was only supported for November analyses, while the interaction between $\delta^{13}\text{C}$ isotope signature and year was supported for March analyses. This result leads us to highlight the important seasonal differences driving intrusion of water from the GoA into PWS that then shapes energy density of juvenile herring in the fall, and the likely scenario that winter-feeding by juvenile herring might enrich their tissues without considerable energy gain, thereby removing any relationship between WBED and $\delta^{13}\text{C}$ isotope signature in the spring. Enhanced winter downwelling is predicted to make PWS more “river-like” flushing zooplankton out of the PWS system. Thus, it may not be surprising that juvenile herring foraging during winter may be relying more on local production than that from the GoA.

Lastly, larger fish were more energy dense during both early and late winter seasons. Our results generally follow those from early studies by Paul and Paul (1998) that showed larger fish, from older age

classes, are more energy dense. However, age-0 herring are thought to build nutrient reserves through their first fall that are used during overwinter while fasting when food availability is low (Blaxter and Holiday, 1963; Norcross et al., 2001; Paul et al., 1998). High temporal resolution studies have indicated that fish maximized their energy levels in November and energy is rapidly lost over the next one to two months, with energy maintained at minimum levels through March (Gorman, Sewall and Heintz, unpubl. data). Growth during winter appeared minimal, yet fish sampled in the spring were larger than those sampled in the fall (Gorman, Sewall and Heintz, unpubl. data), suggestive of size-dependent mortality (see also Foy and Norcross, 1999; Norcross et al., 2001; Paul et al., 1998). Our observation regarding the positive relationship between size and energy density of juvenile herring provides a plausible mechanism underlying overwinter size dependent mortality. Through experimental studies, Paul and Paul (1998) determined that captive juvenile herring that died from starvation had WBED values < 3.2 – 3.6 kJ/g wet weight. Our results show WBED of juvenile herring in March to range between 3 – 4 kJ/g wet mass (Figs. 5 and 6, Supplemental material Figs. 3 and 4), which is generally in the range detected by Paul and Paul (1998), and further supports the idea that juvenile herring in the spring appear to exist near the energetic limits that support life.

In summary, the quality of juvenile herring in PWS appears to be influenced by oceanographic exchange with the GoA that is facilitated by PWS bathymetry and circulation, in addition to local temperature regimes. Zooplankton community structure and abundance presumably act as important transport mechanisms for GoA carbon to PWS juvenile herring. The energetic condition of young herring is enhanced in the northern and western regions of PWS and during colder temperature regimes. Best-supported models for both November and March had relatively low pseudo R^2 values (0.20–0.26), highlighting that other factors must be important predictors of WBED for young herring. For this reason, it remains dubious whether oceanographic exchange with the GoA is driving energetic variability that influences juvenile herring production and recruitment to the spawning population. Links between

GoA and PWS oceanographic exchange and juvenile herring recruitment would be better established by long-term coupled oceanographic (zooplankton community structure and abundance, as well as $\delta^{13}\text{C}$ and $\delta^{15}\text{N}$ stable isotopes) sampling in the GoA and PWS much like the work reported by Kline (2009), as well as modeling of these connections (Coyle et al., 2013). Other possible approaches include using isotope methods to compare the geochemical signature of otoliths between juvenile herring in the eastern and western/northern regions of PWS during their first summer growth phase and those of older, recruited herring (e.g., Walther et al., 2008). If a large proportion of the spawning population had otolith geochemical signatures from the first summer growth phase that are more similar to juveniles from a specific region of PWS, greater links between GoA/PWS oceanographic exchange and herring recruitment would be established.

Acknowledgements

We thank three anonymous reviewers, R. Hopcroft (guest editor), and K. Drinkwater (editor) for comments that greatly improved the manuscript. Captain D. Beam and crew of the F/V *Montague* assisted with fall collections of herring, while members of Cordova District Fishermen United assisted with spring collections. Several excellent field and lab technicians including K. Siwicke, J. Todd, K. Jurica, D. Roberts, J. McMahon, A. Potter, and V. Gonzalez assisted with field collections and sample processing for stable isotopes and bomb calorimetry. N. Haubenstock and T. Howe at the Alaska Stable Isotope Facility, University of Alaska Fairbanks, analyzed samples for carbon and nitrogen stable isotopes. We thank J. Maselko and T. Morgan for statistical advice, and A. Schaefer for assistance with mapping. Prince William Sound Science Center provided administrative and logistical support. We are especially grateful to the Exxon Valdez Oil Spill Trustee Council for long-term support of research on the energetics of juvenile herring in PWS. The findings and conclusions presented by the authors are their own and do not necessarily reflect the views or position of the Trustee Council.

Appendix A. Candidate model sets for describing variation in November and March whole body energy density of juvenile Pacific herring in Prince William Sound, Alaska

Carbon Stable Isotope Analyses		
Model number	Response variable	Explanatory variables
1	Nov or Mar WBED (kJ/g)	~1, random = ~1 + FL Collection Bay (null)
2	Nov or Mar WBED (kJ/g)	~FL + $\delta^{13}\text{C}$, random = ~1 + FL Collection Bay
3	Nov or Mar WBED (kJ/g)	~FL + Region, random = ~1 + FL Collection Bay
4	Nov or Mar WBED (kJ/g)	~FL + Year, random = ~1 + FL Collection Bay
5	Nov or Mar WBED (kJ/g)	~FL + $\delta^{13}\text{C}$ + Region, random = ~1 + FL Collection Bay
6	Nov or Mar WBED (kJ/g)	~FL + $\delta^{13}\text{C}$ + Year, random = ~1 + FL Collection Bay
7	Nov or Mar WBED (kJ/g)	~FL + Region + Year, random = ~1 + FL Collection Bay
8	Nov or Mar WBED (kJ/g)	~FL + $\delta^{13}\text{C}$ + Region + Year, random = ~1 + FL Collection Bay
9	Nov or Mar WBED (kJ/g)	~FL + $\delta^{13}\text{C}$ + Region + Year + $\delta^{13}\text{C} \times \text{Region}$, random = ~1 + FL Collection Bay
10	Nov or Mar WBED (kJ/g)	~FL + $\delta^{13}\text{C}$ + Region + Year + $\delta^{13}\text{C} \times \text{Year}$, random = ~1 + FL Collection Bay
Nitrogen Stable Isotope Analyses		
Model number	Response variable	Explanatory variables
1	Nov or Mar WBED (kJ/g)	~1, random = ~1 + FL Collection Bay (null)
2	Nov or Mar WBED (kJ/g)	~FL + $\delta^{15}\text{N}$, random = ~1 + FL Collection Bay
3	Nov or Mar WBED (kJ/g)	~FL + Region, random = ~1 + FL Collection Bay
4	Nov or Mar WBED (kJ/g)	~FL + Year, random = ~1 + FL Collection Bay
5	Nov or Mar WBED (kJ/g)	~FL + $\delta^{15}\text{N}$ + Region, random = ~1 + FL Collection Bay
6	Nov or Mar WBED (kJ/g)	~FL + $\delta^{15}\text{N}$ + Year, random = ~1 + FL Collection Bay
7	Nov or Mar WBED (kJ/g)	~FL + Region + Year, random = ~1 + FL Collection Bay
8	Nov or Mar WBED (kJ/g)	~FL + $\delta^{15}\text{N}$ + Region + Year, random = ~1 + FL Collection Bay
9	Nov or Mar WBED (kJ/g)	~FL + $\delta^{15}\text{N}$ + Region + Year + $\delta^{15}\text{N} \times \text{Region}$, random = ~1 + FL Collection Bay

10 Nov or Mar WBED (kJ/g) \sim FL + $\delta^{15}\text{N}$ + Region + Year + $\delta^{15}\text{N}$ *Year, random = \sim 1 + FL|Collection Bay

Abbreviations: WBED = whole body energy density, FL = fork length, $\delta^{15}\text{N}$ = lipid corrected carbon stable isotope signature.
 $\delta^{15}\text{N}$ = nitrogen stable isotope signature.

Appendix B. Supporting information

Supplementary data associated with this article can be found in the online version at <http://dx.doi.org/10.1016/j.dsr2.2017.10.010>.

References

- Beamer, J.P., Hill, D.F., Arendt, A., Liston, G.E., 2016. High-resolution modeling of coastal freshwater discharge and glacier mass balance in the Gulf of Alaska watershed. *Water Resour. Res.* 52, 3888–3909.
- Blaxter, J.H., Holdiday, P.G., 1963. The behavior and physiology of herring and other clupeids. *Adv. Mar. Biol.* 1, 261–393.
- Bond, N.A., Cronin, M.F., Freeland, H., Mantua, N., 2015. Causes and impacts of the 2014 warm anomaly in the NE Pacific. *Geophys. Res. Lett.* 42, 3414–3420.
- Brown, E.D., Norcross, B.L., Short, J.W., 1996. An introduction to studies on the effects of the Exxon Valdez oil spill on early life history stages of Pacific herring, *Clupea pallasii*, in Prince William Sound, Alaska. *Can. J. Fish. Aquat. Sci.* 53, 2337–2342.
- Burnham, K.P., Anderson, D.R., 2002. Model Selection and Multi-Model Inference: A Practical Information Theoretic Approach. Springer-Verlag, New York, NY.
- Cooney, R.T., 1986. The seasonal occurrence of *Neocalanus cristatus*, *Neocalanus plumchrus*, and *Eucalanus bungii* over the shelf of the northern Gulf of Alaska. *Cont. Shelf Res.* 5, 541–553.
- Cooney, R.T., Allen, J.R., Bishop, M.A., Esslinger, D.L., Kline, T., Norcross, B.L., McRoy, C.P., Milton, J., Olsen, J., Patrick, V., Paul, A.J., Salmon, D., Scheel, D., Thomas, G.L., Vaughan, S.L., Willette, T.M., 2001a. Ecosystem control of pink salmon (*Oncorhynchus gorbuscha*) and Pacific herring (*Clupea pallasii*) populations in Prince William Sound, Alaska. *Fish. Oceanogr.* 10, 1–13.
- Cooney, R.T., Coyle, K.O., Stockmar, E., Stark, C., 2001b. Seasonality in surface-layer net zooplankton communities in Prince William Sound, Alaska. *Fish. Oceanogr.* 10, 97–109.
- Core Team, R., 2017. R: A Language and Environment for Statistical Computing. R Foundation for Statistical Computing, Vienna, Austria. <https://www.r-project.org/>.
- Coyle, K.O., Gibson, G.A., Hedstrom, K., Hermann, A.J., Hopcroft, R.R., 2013. Zooplankton biomass, advection and production on the northern Gulf of Alaska shelf from simulations and field observations. *J. Mar. Syst.* 128, 185–207.
- Crawley, M.J., 2007. The R Book. John Wiley & Sons, Ltd, West Sussex, UK.
- Damkaer, D.M., 1977. Initial Zooplankton Investigations in Prince William Sound, Gulf of Alaska, and lower Cook Inlet. Environmental Assessment of the Alaska Continental Shelf. Annual Reports of the Principal Investigators, for the Year Ending 1997 (Receptors – Fish, Littoral, Benthos). U.S. Dept. of Commerce, Washington D.C. pp. 137–274.
- Deniro, M.J., Epstein, S., 1978. Influence of diet on distribution of carbon isotopes in animals. *Geochim. Cosmochim. Acta* 42, 495–506.
- Deniro, M.J., Epstein, S., 1981. Influence of diet on the distribution of nitrogen isotopes in animals. *Geochim. Cosmochim. Acta* 45, 341–351.
- Esslinger, D.L., Cooney, R.T., McRoy, C.P., Ward, A., Kline, T.C., Simpson, E.P., Wang, J., Allen, J.R., 2001. Plankton dynamics: observed and modeled responses to physical conditions in Prince William Sound, Alaska. *Fish. Oceanogr.* 10 (Suppl. 1), S81–S96.
- Foy, R.J., Norcross, B.L., 1999. Feeding Behavior of Herring (*Clupea pallasii*) Associated with Zooplankton Availability in Prince William Sound, Alaska., Ecosystem Approaches for Fisheries Management (AK-SG-99-01). University of Alaska Sea Grant, Fairbanks, pp. 129–135.
- Gorman, K.B., Kline Jr., T.C., Roberts, M.E., Sewall, F.S., Heintz, R.A., Pegau, W.S., 2017. Herring Condition Monitoring. Exxon Valdez Long-Term Herring Research and Monitoring Final Report (Restoration Project 16120111-L). Prince William Sound Science Center, Cordova, Alaska and NOAA Alaska Fisheries Science Center, Juneau, Alaska.
- Halverson, M.J., Belanger, C., Gay, S.M., 2013a. Seasonal transport variations in the straits connecting Prince William Sound to the Gulf of Alaska. *Cont. Shelf Res.* 63, S63–S78.
- Halverson, M.J., Ohlmann, J.C., Johnson, M.A., Pegau, W.S., 2013b. Disruption of a cyclonic eddy circulation by wind stress in Prince William Sound, Alaska. *Cont. Shelf Res.* 63, S13–S25.
- Johnson, W.R., Royer, T.C., Luick, J.L., 1988. On the seasonal variability of the Alaska Coastal Current. *J. Geophys. Res. Oceans* 93, 12423–12437.
- Kelly, J.F., 2000. Stable isotopes of carbon and nitrogen in the study of avian and mammalian trophic ecology. *Can. J. Zool.* 78, 1–27.
- Kline, T.C., 1997. Confirming forage fish food web dependencies in Prince William Sound using natural stable isotope tracers, Forage Fishes in Marine Ecosystems. In: *Proceedings of the International Symposium on the Role of Forage Fishes in Marine Ecosystems*. University of Alaska Sea Grant College Program, pp. 257–269.
- Kline, T.C., 1999a. Monitoring Changes in Oceanographic Forcing using the Carbon and Nitrogen Isotopic Composition of Prince William Sound pelagic biota, Ecosystem Approaches for Fisheries Management (AK-SG-99-01). University of Alaska Sea Grant, Fairbanks, pp. 87–95.
- Kline, T.C., 1999b. Temporal and spatial variability of C-13/C-12 and N-15/N-14 in pelagic biota of Prince William Sound, Alaska. *Can. J. Fish. Aquat. Sci.* 56, 94–117.
- Kline, T.C., 2009. Characterization of carbon and nitrogen stable isotope gradients in the northern Gulf of Alaska using terminal feed stage copepodite-V *Neocalanus cristatus*. *Deep-Sea Res. II* 56, 2537–2552.
- Kline, T.C., 2013. PWS Herring Survey: Pacific Herring Energetic Recruitment Factors. Exxon Valdez Oil Spill Restoration Project Final Report (Project 10100132-C).
- Kline, T.C., Campbell, R.W., 2010. Prince William Sound Herring Forage Contingency. Exxon Valdez Oil Spill Restoration Project Final Report (Project 070811).
- Kline, T.C., 2000. Trophic position of Pacific herring in Prince William Sound, Alaska, based on their stable isotope abundance. In: Funk, F., Blackburn, J., Hay, D., Paul, A.J., Stephenson, R., Toresen, R., Witherell, D. (Eds.), *Herring: Expectations for a New Millennium*, pp. 69–80.
- Kline, T.C., 2001. Evidence of biophysical coupling from shifts in abundance of natural stable carbon and nitrogen isotopes in Prince William Sound, Alaska. In: Kruse, G.H., Bez, N., Booth, A., Dorn, M.W., Hills, S., Lipcius, R.N., Pelletier, D., Roy, C., Smith, S.J., Witherell, D. (Eds.), *Spatial Processes and Management of Marine Populations*, pp. 363–376.
- Mazerolle, M.J., 2017. AICcmodavg: model selection and multimodel inference based on QAIC(c). R. Package Version 2 (1-1). <https://cran.r-project.org/package=AICcmodavg>.
- McConnaughey, T., McRoy, C.P., 1979. Food-web structure and the fractionation of carbon isotopes in the Bering Sea. *Mar. Biol.* 53, 257–262.
- Muradian, M.L., Branch, T.A., Moffitt, S.D., Hulson, P.J.F., 2017. Bayesian stock assessment of Pacific herring in Prince William Sound, Alaska. *PLoS ONE* 12, 29.
- Musgrave, D.L., Halverson, M.J., Pegau, W.S., 2013. Seasonal surface circulation, temperature, and salinity in Prince William Sound, Alaska. *Cont. Shelf Res.* 53, 20–29.
- Niebauer, H.J., Royer, T.C., Weingartner, T.J., 1994. Circulation of Prince William Sound, Alaska. *J. Geophys. Res. Oceans* 99, 14113–14126.
- Norcross, B.L., Brown, E.D., Foy, R.J., Frandsen, M., Gay, S.M., Kline, T.C., Mason, D.M., Patrick, E.V., Paul, A.J., Stokesbury, K.D.E., 2001. A synthesis of the life history and ecology of juvenile Pacific herring in Prince William Sound, Alaska. *Fish. Oceanogr.* 10, 42–57.
- Parr Instrument Company, 2009. Introduction to Bomb Calorimetry, Moline, Illinois.
- Paul, A.J., Paul, J.M., 1998. Comparisons of whole body energy content of captive fasting age zero Alaskan Pacific herring (*Clupea pallasii Valenciennes*) and cohorts over-wintering in nature. *J. Exp. Mar. Biol. Ecol.* 226, 75–86.
- Paul, A.J., Paul, J.M., 1999. Interannual and regional variations in body length, weight and energy content of age-0 Pacific herring from Prince William Sound, Alaska. *J. Fish. Biol.* 54, 996–1001.
- Paul, A.J., Paul, J.M., Brown, E.D., 1998. Fall and spring somatic energy content for Alaskan Pacific herring (*Clupea pallasii Valenciennes* 1847) relative to age, size and sex. *J. Exp. Mar. Biol. Ecol.* 223, 133–142.
- Paul, A.J., Paul, J.M., Kline Jr., T.C., 2001. Estimating whole body energy content for juvenile Pacific herring from condition factor, dry weight, and carbon/nitrogen ratio (AK-SG-01-04). In: Funk, F., Blackburn, J., Hay, D., Paul, A.J., Stephenson, R., Toresen, R., Witherell, D. (Eds.), *Herring: Expectations for a New Millennium*. University of Alaska Sea Grant, Fairbanks, pp. 121–133.
- Peterson, B.J., Fry, B., 1987. Stable isotopes in ecosystem studies. *Annu. Rev. Ecol. Syst.* 18, 293–320.
- Pinheiro, J., Bates, D., DebRoy, S., Sarkar, D., Core Team, R., 2017. nlme: linear and nonlinear mixed effects models. R. Package Version 3, 1–131. <https://cran.r-project.org/package=nlme>.
- Royer, T.C., 1979. Effect of precipitation and runoff on coastal circulation in the Gulf of Alaska. *J. Phys. Oceanogr.* 9, 555–563.
- Stabeno, P.J., Reed, R.K., 1991. Recent Lagrangian measurements along the Alaskan Stream. *Deep-Sea Res.* 38, 289–296.
- Vaughan, S.L., Mooers, C.N.K., Gay, S.M., 2001. Physical variability in Prince William Sound during the SEA study (1994-98). *Fish. Oceanogr.* 10, 58–80.
- Walcher, B.D., Thorrold, S.R., Olney, J.E., 2008. Geochemical signatures in otoliths record natal origins of American shad. *T. Am. Fish. Soc.* 137, 57–69.
- Wang, J., Jin, M.B., Patrick, E.V., Allen, J.R., Esslinger, D.L., Mooers, C.N.K., Cooney, R.T., 2001. Numerical simulations of the seasonal circulation patterns and thermohaline structures of Prince William Sound, Alaska. *Fish. Oceanogr.* 10, 132–148.
- Ward, E.J., Adkison, M., Couture, J., Dressel, S.C., Litzow, M.A., Moffitt, S., Neher, T.H., Trochta, J., Brenner, R., 2017. Evaluating signals of oil spill impacts, climate, and species interactions in Pacific herring and Pacific salmon populations in Prince William Sound and Copper River, Alaska. *PLoS ONE* 12, e0172898.
- Weingartner, T.J., Danielson, S.L., Royer, T.C., 2005. Freshwater variability and predictability in the Alaska Coastal Current. *Deep-Sea Res. II* 52, 169–191.
- Xu, R., 2003. Measuring explained variation in linear mixed effects models. *Stat. Med.* 22, 3527–3541.